

UNIVERSIDAD SAN FRANCISCO DE QUITO USFQ

Colegio de Posgrados



**The Use of Molecular Tools to Study Outbreaks of Tropical
Febrile Diseases with Emphasis in Arbovirosis**

Sully Estefanía Márquez Aguilar

Gabriel Trueba Piedrahita, Ph.D.

Manuscript style thesis submitted in partial fulfillment of the requirements for the Degree of Doctor
of Philosophy (Ph.D.) in Microbiology

Tesis presentada en cumplimiento parcial de los requisitos para el Grado de Doctor (Ph.D.)
en Microbiología

Quito, 12 de enero del 2024

Universidad San Francisco de Quito USFQ**Colegio de posgrados**

We recommended acceptance of this thesis in partial fulfillment of the candidate's requirements for the Degree of Doctor of Philosophy in Microbiology

Sully Estefanía Márquez Aguilar

Firmas

Gabriel Antonio Trueba Piedrahita Ph.D.

Director del Trabajo de Titulación

Gabriel Antonio Trueba Piedrahita Ph.D.

Director del Programa de Doctorado en
Microbiología

Carlos Valle Ph.D.

Decano del Colegio de Ciencias Biológicas y
Ambientales COCIBA

Hugo Burgos Ph.D.

Decano del Colegio de Posgrados

Miembros del comité de tesis

Paul Cárdenas Ph.D.

Josefina Coloma Ph.D.

Jesse Waggoner Ph.D.

Quito, 12 de enero del 2024

© Derechos de Autor

Por medio del presente documento certifico que he leído todas las Políticas y Manuales de la Universidad San Francisco de Quito USFQ, incluyendo la Política de Propiedad Intelectual USFQ, y estoy de acuerdo con su contenido, por lo que los derechos de propiedad intelectual del presente trabajo quedan sujetos a lo dispuesto en esas Políticas.

Asimismo, autorizo a la USFQ para que realice la digitalización y publicación de este trabajo en el repositorio virtual, de conformidad a lo dispuesto en el Art. 144 de la Ley Orgánica de Educación Superior.

Nombre del estudiante: Sully Estefanía Márquez Aguilar

Código de estudiante: 00209755

C. I.: 1718171919

Quito, 12 de enero del 2024

ACLARACIÓN PARA PUBLICACIÓN

Nota: El presente trabajo, en su totalidad o cualquiera de sus partes, no debe ser considerado como una publicación, incluso a pesar de estar disponible sin restricciones a través de un repositorio institucional. Esta declaración se alinea con las prácticas y recomendaciones presentadas por el Committee on Publication Ethics COPE descritas por Barbour et al. (2017) Discussion document on best practice for issues around theses publishing, disponible en <http://bit.ly/COPETheses>.

UNPUBLISHED DOCUMENT

Note: The following graduation thesis is available through Universidad San Francisco de Quito USFQ institutional repository. Nonetheless, this thesis – in whole or in part – should not be considered a publication. This statement follows the recommendations presented by the Committee on Publication Ethics COPE described by Barbour et al. (2017) Discussion document on best practice for issues around theses publishing available on <http://bit.ly/COPETheses>.

DEDICATORIA

To my family, for their unconditional support, for being my inspiration and strength to not give up during this journey.

AGRADECIMIENTOS

Firstly, I would like to thank my supervisor Gabriel Trueba for his unconditional support, for his patience, for listening to me, for being my mentor, for being the light during this journey, to teach me that everything is possible when you fight for your goal and also for your trust in my work and for your valuable advice.

I want to thank Josefina Coloma and Joseph Eisenberg for accepting me as a PhD student in the dengue project and to trust in me for processing the febrile samples of the active surveillance. I also wanted to thank for their financial support so I could perform my PhD thesis during these 5 years and for their support so I could participate in several important meetings as PANDENGUE. Moreover, many thanks for their valuable contributions for each one of the publications.

I want to thank Paul Cardenas, for believing in me, for include me as part of the genomic surveillance of SARS-CoV-2, for connecting me with the Paraguayan colleagues, for listening to me, for his unconditional friendship, for his valuable advice, for being a model as a leader and for supporting me during this journey.

I want to thank Jesse Waggoner for accepting being an ad-hoc committee member and it was a privilege to have in person the researcher that established the ZCD real-time PCR assay that I used during my thesis.

I want to thank Gwen for her valuable contributions as a coauthor, for always being there when I needed, for guiding me during manuscript preparation.

I want to thank Shannon Bennett and Bernardo Gutierrez for teaching me how to perform and interpret phylogenetic analysis and also for their guidance during this process.

I want to thank Fabián Sáenz for providing us the PCR protocol for malaria detection and for helping me to perform the assay, it was a very valuable contribution.

I want to thank Patricio Rojas, for not letting me quit, for always giving me the best advice and for being in the goods and the bads.

I want to thank Veronica Barragan and her group for helping us with the Leptospira analysis of the serum samples and also for her valuable support and advice.

I want to thank the A2CARES consortium for including me and for being amazing colleagues, I learned a lot in each one of the meetings.

I want to thank the people in the field (auxiliaries, brigadistas, Mauricio) for their hard work during these years, also to Jessica Uruchima and William Cevallos for the logistics, without them this project would no be possible.

I want to thank the Microbiology Institute staff for their support in the different stages of my PhD, specially to David, Erika and Lis who were a great team and were always there when I needed help.

I want to thank Liz Salazar for her hard work in the virology lab. She arrives in the right moment and without her the cell culture would not be possible, she was the light in the lab, looking forward working with you.

I want to thank Belen Prado for support me in the very first extraction and sequencing of SARS-CoV-2, for her friendship, for being an incredible colleague and also for providing the pipeline for

dengue genome assembly, obtaining the final consensus sequences, and submitted sequences to GenBank.

I want to thank Elsa, don Leonel, Cristhiam, Gerald and Yuri from SSI Nicaragua for this great collaboration in capacity building, for sharing with me their knowledge in different topics as sequencing, biorepository management, cell culture and for their incredible friendship.

I want to thank Mateo, Carlita, Dey, Barbarita, Maritza, Andrea, Sole, Tere, Nicole and Sarita for being such amazing friends, for not letting me alone, for their patience, for their good vibes, for their valuable advice and support during my PhD.

Finally, I want to thank my family and God for everything, for being the friends that will always be there, for being the angels of my life, my PhD was only possible thanks to them. We did it as an amazing team!! Thanks a lot!

RESUMEN

En los últimos 20 años, se ha observado en todo el mundo la aparición y resurgimiento de patógenos nuevos y conocidos (virus, bacterias, parásitos). La incidencia y prevalencia de diferentes patógenos, valores que miden niveles de transmisión e infección, puede variar según varios factores como la ubicación (altitud, latitud, área urbana o rural, las condiciones ambientales (estación, temperatura, precipitación, humedad), grupo etario, la inmunidad previa, acceso a educación, factores culturales, comportamientos sociales, etc. La mayoría de estas enfermedades se reportan comúnmente en países tropicales y subtropicales y se caracterizan por su diversidad, sintomatología no específica (fiebre, dolor de cabeza, mialgia, artralgia, escalofríos y sarpullido) de los cuales, la fiebre es el síntoma más importante para que los pacientes busquen atención médica. Muchos de estos síntomas suelen superponerse necesitando de diagnósticos diferenciados para evitar los diagnósticos clínicos equívocos entre enfermedades causadas por patógenos distintos como virus de dengue (DENV), virus de chikungunya (CHIKV), *Plasmodium* spp., *Leptospira* spp., etc. El uso de nuevas tecnologías de detección y confirmación de patógenos, incluidas las pruebas cromatográficas serológicas rápidas, la amplificación de ácidos nucleicos (PCR), los ensayos inmunosorbentes ligados a enzimas, Luminex y la secuenciación genómica, han revolucionado los diagnósticos confirmatorios. Estos métodos tienen alta sensibilidad/especificidad, utilizan protocolos similares para múltiples enfermedades infecciosas, y proveen la posibilidad de análisis rápido y simultáneo de múltiples patógenos (multiplex), y tienen alta capacidad de discriminación (algunos permiten identificación de cepas). Este trabajo describe la experiencia en el Ecuador e ilustra el uso de estas técnicas con capacidad de detectar múltiples virus en la región de la costa Norte del país en el Cantón Eloy Alfaro de la provincia de Esmeraldas. Detectamos CHIKV en los meses de mayo a julio del 2019 ; luego la circulación de DENV-1 fue

confirmada de mayo de 2019 a marzo 2020, finalmente DENV-2 fue detectado de diciembre de 2020 a julio 2021. El uso de la tecnología Oxford Nanopore (ONT) para secuenciar genomas completos, permitió complementar la vigilancia con PCR con la detección de variantes de DENV y del SARS-CoV-2 y reinfecciones por SARS-CoV-2 durante los mismos años. Adicionalmente, los análisis genómicos nos permitieron encontrar evidencia que el DENV ingresó a Esmeraldas desde Colombia y las posibles dinámicas de distribución entre las comunidades (urbanas y rurales) de la provincia de Esmeraldas. En conclusión, estas experiencias subrayan el enorme potencial de las nuevas tecnologías para resolver la difícil problemática de implementar una vigilancia activa de casos febriles y diagnosticarlos en regiones donde existen diversos patógenos capaces de causar sintomatología similar.

Palabras clave: Enfermedades febriles, herramientas de diagnóstico, secuenciación, vigilancia genómica, patógenos.

ABSTRACT

Over the past 20 years, the emergence and resurgence of new and known pathogens (viruses, bacteria, parasites) has been observed worldwide. The incidence and prevalence of different pathogens can vary depending on several factors such as location (altitude, latitude, urban or rural area, environmental conditions (season, temperature, precipitation, humidity), age group, previous immunity, access to education, cultural factors, social behaviors, etc. Furthermore, most of these diseases are reported commonly in tropical and subtropical countries and are characterized by their diversity, non-specific symptomatology (fever, headache, myalgia, arthralgia, chills, and rash) of which, fever is the most important symptom for patients to seek medical attention. Clinically, these symptoms tend to overlap, giving rise to equivocal diagnoses between diseases caused by different pathogens such as dengue virus (DENV), chikungunya virus (CHIKV), *Plasmodium spp.*, *Leptospira spp.*, etc. The use of new diagnostic technologies, including rapid serological chromatographic tests, nucleic acid amplification (PCR), enzyme-linked immunosorbent assays, Luminex and genomic sequencing, have revolutionized pathogen detection to confirm diagnosis. These methods present high sensitivity/specificity, use of similar protocols for multiple infectious diseases, provide the possibility of rapid and simultaneous analysis of multiple pathogens (multiplex), and present a high discrimination capacity (some allow identification of strains). This work describes the experience in Ecuador and illustrates the use of these techniques with the capacity to detect multiple viruses in the region of the North coast of the country in the Eloy Alfaro Canton of the province of Esmeraldas. We detected CHIKV in the months of May to July 2019; CHIKV was detected in the months of May to July of 2019; then DENV-1 circulation was confirmed from May 2019 to March 2020, finally DENV-2 was detected from December 2020 to July 2021. The use of Oxford Nanopore (ONT) technology for sequencing whole genomes, made

it possible to complement PCR surveillance with the detection of DENV variants and of SARS-CoV-2 and reinfections by SARS-CoV-2 during the same years. Additionally, genomic analyses allowed us to find evidence that DENV entered Esmeraldas from Colombia and the possible distribution dynamics between the communities (urban and rural) of Esmeraldas province.

In conclusion, these experiences highlight the enormous potential of new technologies to solve the difficult problem of implementing active surveillance of febrile cases and diagnosing them in regions where there are various pathogens capable of causing similar symptoms.

Keywords: Febrile illnesses, diagnostic tools, sequencing, genomic surveillance, pathogens.

TABLE OF CONTENTS

DEDICATORIA	5
AGRADECIMIENTOS	6
RESUMEN	9
ABSTRACT	11
TABLES	16
FIGURES	17
OBJECTIVES AND JUSTIFICATION	18
Objective	18
Justification	18
CHAPTER 1	22
1. CURRENT METHODS FOR DIAGNOSIS OF TROPICAL INFECTIOUS FEBRILE DISEASE	22
1.1. Undifferentiated acute febrile illnesses	22
1.2. Previously reported febrile pathogens in Ecuador	22
1.3. Hematophagous vectors	26
1.4. Pathogens responsible for acute febrile illnesses	28
1.4.1. Dengue virus (DENV)	29
1.4.2. Zika virus (ZIKV).....	31
1.4.3. Chikungunya virus (CHIKV)	33
1.4.4. Mayaro virus (MAYV).....	34
1.4.5. Oropouche virus (OROV)	36
1.4.6. SARS-CoV-2	37
1.4.7. Leptospira	42
1.4.8. Plasmodium	43
Modern diagnostic tools for tropical febrile diseases.....	45
1.5.1. Sensitivity (S).....	46
1.5.2. Specificity (E)	46
1.5.3. Positive predictive value (PPV)	47
1.5.4. Negative predictive value (NPV)	47
1.6. Classical clinical indicators of infection	47
1.6.1. Antibody detection tests	48
1.6.2. Rapid antibody tests (RDT).....	49
1.6.3. Enzyme-linked immunosorbent assay (ELISA) for antibody detection	51

1.6.3.1. Enzyme-linked immunosorbent assay, ELISA	52
1.6.3.2. Competitive ELISA.....	53
1.7. Antigen detection tests	55
1.7.1. Rapid antigen tests	55
1.7.2. Enzyme-linked immunosorbent assay (ELISA) for antigen detection	56
1.7.2.1. Sandwich ELISA.....	56
1.7.2.2. Nucleic acid amplification test: Polymerase Chain Reaction (PCR).....	57
1.7.2.2.1. Standard or conventional PCR	58
1.7.2.2.2. Real Time PCR	59
1.7.2.2.2.1. SYBR Green.....	60
1.7.2.2.2.2. Hydrolysis probe	61
1.7.2.3. Standard curve and Limit of detection (LOD)	62
1.7.2.4. Retrotranscription PCR (rtPCR)	63
1.7.2.5. Other multiplex Real time-PCR assays.....	63
1.8. Luminex assay.....	64
1.9. Genomic analysis - Oxford nanopore technology (ONT) for sequencing	69
1.10. Metagenomic detection	69
REFERENCES.....	72
CHAPTER 2.....	98
A Chikungunya Outbreak in a Dengue-endemic Region in Rural Northern Coastal Ecuador .	98
CHAPTER 3.....	125
Phylogenetic Analysis of Transmission Dynamics of Dengue in Large and Small Population Centers, Northern Ecuador	125
CHAPTER 4.....	152
Metagenome of a Bronchoalveolar Lavage Fluid Sample from a Confirmed COVID-19 Case in Quito, Ecuador, Obtained Using Oxford Nanopore MinION Technology.....	152
PUBLICATION AS CONTRIBUTING AUTHOR	157
OTHER PUBLICATIONS AS CONTRIBUTING AUTHOR.....	165
CHAPTER 5.....	167
OVERALL PROTOCOLS AND METHODS USED IN THIS THESIS.....	167
5.1. ARBOVIRUS.....	167
5.1.1 Study site and sample collection	167
5.1.2 RNA extraction	168
5.1.3 Real time PCR for the detection and differentiation of Zika virus, chikungunya virus, and dengue virus	169
5.1.4 Conventional PCR.....	174

5.1.4.1. Electrophoresis	176
5.1.4.2. Electrophoresis	179
5.1.5. Negative samples.....	179
5.1.5.1. MAYV Real-time PCR	179
5.1.5.2 OROV Real-time PCR detection	181
5.1.5.3. <i>Leptospira</i> Real-time PCR detection.....	183
5.1.5.4. Metagenomic analysis	185
5.1.5.4.1 cDNA preparation	186
5.1.5.4.2 Library preparation.....	186
5.1.5.4.3. Library sequencing.....	187
5.1.5.5. DNA extraction	188
5.1.5.6 Nested Conventional PCR for the detection and differentiation of <i>Plasmodium falciparum</i>	189
5.1.5.6.1. ELECTROPHORESIS:.....	193
5.1.6. DENGUE WHOLE GENOME SEQUENCING	193
5.1.7. Phylogenetic analysis	194
5.2 SARS-CoV-2.....	196
5.2.1. Sample collection	196
5.2.2. RNA extraction	197
5.2.3 Real time RT-PCR for the detection of SARS-CoV-2 virus.....	197
5.2.5 SARS-CoV-2 whole genome sequencing	200
5.2.5.1 Tiling PCR	200
5.2.5.2. Sequencing in Nanopore following the NCoV-2019 v3 Sequencing (Low Cost Protocol)	200
5.2.6. Bioinformatic pipeline for sequencing analysis (ARTIC PROTOCOL)	201
CHAPTER 6.....	202
6.1. DISCUSSION	202
6.2. GENERAL CONCLUSION	212

TABLES

Table 1 Symptoms of tropical infectious diseases described in Ecuador.	24
Table 2. List of diseases and its corresponding vector	27
Table 3. Primers used for ZCD Mix preparation for 1000 µl	169
Table 4. Probes used for ZCD Mix preparation for 1000 µl.....	171
Table 5. Mastermix formulation for ZCD assay	172
Table 6. ZCD qRT-PCR cycling conditions.	173
Table 7. Primers for dengue serotype conventional RT-PCR.....	174
Table 8. Mastermix formulation for DENV serotype RT-PCR.....	175
Table 9. DENV serotype RT-PCR cycling conditions.	176
Table 10. CHIKV conventional RT-PCR assay primers	177
Table 11. Mastermix formulation for CHIKV RT-PCR.....	177
Table 12. CHIKV RT-PCR cycling conditions.	178
Table 13. MAYV qRT-PCR assay primers and probes	179
Table 14. Mastermix formulation for MAYV real-time PCR	180
Table 15. MAYV real-time PCR cycling conditions.....	181
Table 16. OROV qRT-PCR assay primers and probes.....	181
Table 17. Mastermix formulation for OROV real-time PCR.	182
Table 18. <i>Leptospira spp.</i> real-time PCR assay primers and probes	184
Table 19. Mastermix formulation for <i>Leptospira</i> real-time PCR	184
Table 20 <i>Leptospira spp.</i> real-time PCR cycling conditions.	185
Table 21. <i>Plasmodium falciparum</i> conventional nested PCR assay primers (PCR 1 and PCR2)	189
Table 22. Mastermix formulation for <i>Plasmodium falciparum</i> PCR 1	190
Table 23. <i>Plasmodium</i> PCR 1 cycling conditions	191
Table 24. Mastermix formulation for <i>Plasmodium falciparum</i> PCR 2	191
Table 25. <i>Plasmodium</i> PCR 2 cycling conditions	192
Table 26. Mastermix formulation for SARS-CoV-2 real time PCR.....	197
Table 27. SARS-CoV-2 real time PCR cycling conditions	198
Table 28. Targets and fluorophores for SARS-CoV-2 detection.....	199

FIGURES

Figure 1. RDT basic structure and performance (created with BioRender.com)	50
Figure 2. Classic ELISA basic principle and performance, created with BioRender.com	53
Figure 3. Competitive ELISA basic principle and performance, created with BioRender.com...	54
Figure 4. Rapid antigen tests test performance, created with BioRender.com	56
Figure 5. Sandwich ELISA basic principle and performance, created with BioRender.com.....	57
Figure 6. Syber Green Real time PCR performance, created with BioRender.com	60
Figure 7. Taqman probe Real time PCR performance, created with BioRender.com.....	61
Figure 8. Real time PCR fluorophore wavelengths, emission spectra, (Real-Time PCR » Clinical Laboratory Science (clinicalsci.info)).....	62
Figure 9. Multiplex real time PCR, created with BioRender.com.....	64
Figure 10. LUMINEX assay principle and performance with magnetic beads, created with BioRender.com	66
Figure 11. LUMINEX assay for nucleic acid detection, created with BioRender.com.....	68
Figure 12. RNA viral metagenomics protocol, created with BioRender.com	72

OBJECTIVES AND JUSTIFICATION

Objective

Objective 1. To test the utility of modern molecular tools for screening and differential diagnosis of febrile pathogens in a region affected by multiple tropical diseases with similar clinical symptomatology. Included COVID-19 in this study due to temporal association with the pandemic.

Objective 2. To combine molecular tools with genome sequencing (using a low-cost platform) to obtain epidemiologically relevant information about tropical diseases in this area.

Justification

Tropical infectious diseases are caused by diverse pathogens that circulate in tropical and poor regions of the world, but they are virtually absent in the industrialized world. Additionally, tropical regions have rich biodiversity that includes potential animal hosts for zoonotic diseases; arthropod vectors of viruses, bacteria or protozoa; and environmental conditions such as high temperature and humidity, which are linked to high proliferation rates of potentially pathogenic protozoa, bacteria, and fungi. These regions of our planet are affected by multiple tropical diseases that surge in epidemic waves, oftentimes overlapping and making it extremely challenging for medical professionals to provide differential diagnoses and decide on the proper treatment as patients' symptoms could be caused by a protozoa, bacteria or virus and consequently require very different treatment. Furthermore, transmission of infectious diseases is commonly driven by human

migration, which is a social phenomenon often affecting poor communities. These characteristics may discourage the development of modern diagnostic tests and specific treatments; the laboratory diagnosis of tropical diseases is notorious for the lack of innovation with the continuous use of very old techniques that are often cumbersome, dangerous, expensive, and require highly specialized personnel and unusual pieces of equipment.

These limitations and challenges contribute to high mortality and massive socio-economic burden caused by infectious diseases in the tropical world (Findlater & Bogoch, 2018); (Baker et al., 2022); (Mena et al., 2021).

Esmeraldas province is located along the northwest Pacific Coast of Ecuador, in the Choco forest sharing a border with Colombia. This province is characterized for being the poorest province in Ecuador with 57% of the population living in poverty and lacking basic needs such as potable water and garbage collection services (C. Robbins, unpub. data). During the last decade, rural areas of this province experienced important environmental and sociological changes due to the construction of a highway that connects many communities with large cities in the Coast and the Andes. Traditionally it was thought that the main febrile infectious disease in this region was malaria, however in recent years many other viral and bacterial diseases have been detected and a transition from malaria was documented. (Cifuentes *Emerg Infect Dis.* 2013 Oct; 19(10): 1642–1645; (Maljkovic Berry et al., 2020); (Wise et al., 2020); (E. Miller et al., 2021). The first DENV report in the province was in 1990, and more recently, other viruses such as Zika, chikungunya, and oropouche have been detected in the region by our group. DENV has traditionally been considered as an urban disease, however active surveillance in rural and remote areas has gained importance due to observed source-sink dynamics within rural and urban sites.

A previous study carried out in rural communities of Eloy Alfaro County in Esmeraldas province from 2013-2014, reported seroprevalence of DENV in a gradient, with more evidence of DENV circulation in proximal urban centers and less in remote riverine communities, whereas in the Esmeraldas city DENV-1 and DENV-2 were circulating. The social dynamics along the international border with legal and illegal commerce and irregular migration between Colombia and Esmeraldas province, suggest that DENV cases found in these rural communities were probably introduced from Colombia implying that rural areas have an important role in the transmission dynamics and epidemiology of different arbovirus, leading to reintroductions and changes in the patterns of transmission of febrile diseases (Márquez et al., 2023); (Márquez et al., 2018).

During 2010–2019, explosive epidemics of DENV were reported in the Americas with cases peaking at 3.1 million in 2019 (World Health Organization, 2023). In 2020, prevalence of DENV started with a high peak with a rapid drop, probably due to underreporting as the COVID-19 pandemic took hold.

SARS-CoV-2 only increased the difficulty of diagnosing tropical diseases in many countries. On February 29th, 2020, the first COVID-19 case was reported in Ecuador, being the second country in Latin America after Brazil to report COVID-19, and on March 11th, 2020, Ecuador declared the disease as a sanitary emergency leading to social distancing measures and the suspension of public events, school activities, and transportation. A mandatory curfew was imposed in April 2020. The all-cause mortality rate rose to 64% in 2020 and Guayas was the most affected province in the country reporting 77% of the cases (Reina Ortiz & Sharma, 2020). Since, the number of cases grew exponentially reaching a total of 732,038 PCR confirmed cases and

34,533 deaths. However, this official count is far below the actual number due to limitations in diagnostic testing by the public health sector. For this reason, the Ecuadorian government allowed private and public entities with molecular laboratory capacities to establish PCR based detection of SARS-CoV-2, certifying them for diagnostic use. In this manner, many universities diverted planned research and teaching activities to COVID-19 testing and research by carrying out RT-PCR testing for the public and engaging in genomic surveillance of SARS-CoV-2 variants of concern in support of the national emergency. My direct involvement in this public health effort is described in this thesis. At that time, there was a limited capacity for nucleotide sequencing in Ecuador, but the pressure of the pandemic promoted a gradual implementation of sequencing and bioinformatic platforms. These analyses allowed real time tracking of the different variants and to confirm the first reinfections. The widespread implementation of sequencing capabilities and other molecular approaches in Ecuador was one of the few positive outcomes of the pandemic.

CHAPTER 1

1. CURRENT METHODS FOR DIAGNOSIS OF TROPICAL INFECTIOUS FEBRILE DISEASE

1.1. Undifferentiated acute febrile illnesses

Acute febrile illnesses are commonly reported in tropical and subtropical countries. These illnesses are characterized by having non-specific symptoms that include fever, headache, myalgia, arthralgia, chills, and rash, with fever being the most important symptom for patients to seek medical care (Anon., 2012) (Moreira et al., 2018); (Shrestha et al., 2020); (Das et al., 2022). Acute manifestations of these illnesses requiring hospitalization have contributed to 5% to 18% of mortality in different sites worldwide (Das et al., 2022).

In the last 20 years, the emergence and reemergence of known and novel pathogens (viruses, bacteria, parasites) has been observed globally. The incidence and prevalence of different pathogens may vary according to several factors such as location (urban or rural area, season), environmental conditions, age, and prior immunity (World Health Organization, 2013). In addition, the patient's access to different levels of care, social determinants and behaviors may affect the reported incidence and prevalence of different pathogens by impacting detection (Kraemer et al., 2019); (Adhikari et al., 2019); (Moreira et al., 2018); (Agweibab, 2023).

1.2. Previously reported febrile pathogens in Ecuador

From a combination of data published from specific studies conducted throughout the country by different research groups, including ours, and the passive surveillance data reported by the Ministry of Health in its monthly Gacetas Epidemiologicas (which are based on sentinel site reporting), here we document a slew of tropical pathogens from Ecuador.

In a study conducted in 2009 in the Ecuadorian Amazon Basin, 304 serum and blood samples were collected from patients who had acute undifferentiated febrile illness. These samples were tested with different assays including IgM serology, RT-PCR and blood smear by microscopy for different pathogens. Samples tested positive for DENV, Yellow fever, OROV, MAYV, *Leptospira*, *Plasmodium*, *Coxiella*, *Rickettsia typhi*, *Rickettsia rickettsii*, *Rickettsia prowazekii*, *Brucella*, Ilhéus virus, St. Louis encephalitis and Venezuelan equine encephalitis (Manock et al., 2009)(Wise et al., 2018). Moreover, Gutierrez-Vera et al, 2021, in a seroprevalence study of arboviruses, reported IgG antibodies for West Nile virus in serum samples from the coastal region and the Amazon Basin (Gutiérrez-Vera et al., 2021). Regarding Bartonellosis, Amano et al, 1997, reported 21% seropositivity in Manabí province (Amano et al., 1997) and another outbreak was reported in the Ecuadorian provinces of Zamora Chinchipe and Loja (Lydy et al., 2018). Moreover, between 2013 and 2019, 439 cases of Chagas disease were reported by the Ecuadorian Ministry of Health, distributed in 20 provinces of the country, being Guayas, El Oro and Loja with the highest incidence (Vásconez-González et al., 2023). Furthermore, the first chikungunya cases were reported in Ecuador in 2014, and since, a total of 35,686 cases were recorded until 2020 by the Ministry of Health (Stewart-Ibarra et al., 2018); (Gaceta epidemiologica, 2020). During our study, a CHIKV outbreak was reported in 2019 in Esmeraldas province in Eloy Alfaro county (Márquez et al., 2022a).

Zika was first confirmed in 2016 in Ecuador and the virus continued circulating until 2018 with a total of 5,371 documented cases by the MOH (Gaceta Epidemiologica, 2020). The most prevalent vector borne diseases reported until 2023 were dengue, Leishmaniasis, malaria, chagas disease, and bartonellosis (Gaceta epidemiologica, 2023). The prevalence of malaria has decreased in the country following initiation of effective management in the last 15 years, however it is

prevalent in the coastal region and the Amazon basin with a total of 6,888 cases reported since 2019 until 2023 (Gaceta Epidemiologica, 2023). Referring to Mayaro, the first case was identified in a patient from Guayaquil in a study carried out between 2000-2007, and in 2019, five cases were reported in patients from Guayaquil, Babahoyo, Portoviejo and Santo Domingo (Ganjan & Riviere-Cinnamond, 2020). The presence of *Leptospira* was reported since 1924, being the annual incidence of one case per 100,000 people and 547 cases reported from the coast of the country (Calvopiña et al., 2023). From 2016 to 2018, a total of 5,363 Zika virus cases were reported by the Ministry of Health, of which the majority were from Manabí province. Moreover 20 microcephaly cases were found to be distributed throughout coastal areas and the Amazon basin, and, 3 cases of Guillain Barré syndrome associated with a ZIKV infection were confirmed (Gaceta Epidemiologica, 2018). Clinically, all these diseases manifest with an acute phase with signs and symptoms that are often similar and include fever. The clinical symptoms of these diseases are shown in **Table 1**.

Table 1 Symptoms of tropical infectious diseases described in Ecuador.

Tropical infectious disease (Agent)	Symptoms	Reference
Dengue fever (Dengue Virus)	Acute phase: Fever, headache, myalgia, arthralgia, rash Severe disease: vascular leakage leading to shock, fluid accumulation, severe bleeding, and organ involvement	(Guzman et al., 2016)
Chikungunya fever (Chikungunya Virus)	Fever (> 39°C), arthralgia, myalgia, nausea, and rash severe polyarthralgia/polyarthritis	(McFee, 2018)
Zika (Zika Virus)	Fever, rash, arthralgia, myalgia, fatigue, headache, and conjunctivitis microcephaly and Guillain–Barré	(Plourde & Bloch, 2016)

Yellow fever (Yellow fever virus)	Fever, headache, myalgia, malaise, nausea and vomiting Hepatic dysfunction, renal failure, hemorrhagic manifestations	(Waggoner, Rojas, & Pinsky, 2018)
Oropouche (Oropouche virus)	Fever, headache, muscle and joint pain and skin rash meningitis, encephalitis	(Sakkas et al., 2018a)
Mayaro (Mayaro virus)	Fever, headache, myalgia, retro-orbital pain, vomiting, and diarrhea, rash, arthralgia, conjunctivitis, neurological complications, myocarditis	(Acosta-Ampudia et al., 2018)
West Nile fever (West Nile virus)	Fever, chills, malaise, headache, backache, myalgias, arthralgias, nausea, vomiting, or diarrhea, and maculopapular rash. Neuroinvasive disease: high fever, worsening headache, neck stiffness (nuchal rigidity), confusion, stupor, tremors, seizures, muscle weakness or paralysis, and focal neurological deficits	(Bai et al., 2019)
Venezuelan equine encephalitis (Venezuelan equine encephalitis virus)	Leukopenia, tachycardia, and fever. Patients may develop interstitial pneumonia. Tremors, seizures, behavioral changes, hemiparesis, hemichorea, cranial nerve palsies, ataxia, myoclonus, confusion, somnolence, and coma	(Crosby & Crespo, 2023)
Bartonellosis (Carrion's disease) (Bartonella spp.)	Fever, hemolytic anemia, pallor, myalgia, headache, anorexia, tachycardia, and hepatomegaly. Chronic: nodular hemangioma-like lesions in the skin	(Garcia-Quintanilla et al., 2019)
Brucellosis (<i>Brucella</i> sp.)	Fever (intermittent pyrexia) arthralgia, fatigue	(Hull & Schumaker, 2018)
Leptospirosis (<i>Leptospira</i> spp.)	Fever, chills, myalgia and headache, subconjunctival hemorrhages, and icterus	(Haake & Levett, 2015)
Malaria (<i>Plasmodium</i> spp.)	Fever, shaking chills, muscle aches and, in children, digestive symptoms, paroxysms, drenching sweat, and exhaustion.	(Phillips et al., 2017a)

	Severe anaemia and multi-organ damage	
Chagas disease (<i>Trypanosoma cruzi</i>)	Fever, malaise, and lymphadenopathy, chagoma, Romana's sign, myocarditis	(Malik et al., 2015)
Rickettsiosis (<i>Rickettsia</i> sp.)	Fever, cephalgia, myalgia	(Bolaños et al., 2019)
Q fever (<i>Coxiella burnetii</i>)	Fever, chills, Myalgia, headache	(H. K. Miller et al., 2021)
St. Louis encephalitis (St. Louis encephalitis virus)	Fever, headache, vomiting, tiredness	(<i>St. Louis Encephalitis</i> <i>St. Louis Encephalitis</i> CDC, 2023)
Ilhéus fever (Ilhéus virus)	Fever, headache, myalgia, malaise, and encephalitis	(da Costa et al., 2023)

1.3. Hematophagous vectors

Arboviruses (Table 1) are viruses transmitted by hematophagous vectors between humans or from other animals to humans. Different species of mosquitoes are adapted to transmit various pathogens such as viruses and parasites; and other vectors include fleas, flies, ticks and blood sucking bugs. (Table 2)

Female Mosquitoes require a blood meal after mating, in order to develop fertile eggs. The steps that are required for viral transmission are as follows: a) virus is acquired during the blood meal, b) virus infects the midgut epithelial cells, c) virus escapes and enters the mosquito's hemolymph. Then the virus infects the peripheral tissues and organs as nerves and muscle fibers. Finally the virus arrives to the salivary glands, and it is shed in the saliva to infect a new host during the next blood meal (Azar & Weaver, 2019).

Malaria is a vector-borne disease, its etiological agent is a protozoan that belongs to the genera *Plasmodium* and it is also transmitted by mosquitoes. The life cycle of the parasite in the vector is as follows: a) the mosquito ingests the gametocytes (sexual stage of *Plasmodium*) within

the blood meal, b) gametocytes get activated in the midgut and differentiate into gametes. Male gametocytes generate eight microgametes and female gametocytes form a macrogamete. c) after fertilization occurs, the ookinete which is capable to glide, crosses the peritrophic matrix and the midgut epithelium. d) The ookinete changes to oocyst and inside of this, sporozoites undergo mitosis and arrive to the hemocoel; e) finally the sporozoites infect the salivary glands and these will infect another host (Parres-Mercader et al., 2023).

Babesiosis is also transmitted by ticks to mammalian hosts. Babesia's life cycle in the vector begins when the parasite is ingested within the blood meal of the tick. The gametocyte differentiates into gametes, and these are released into the midgut. Then a diploid zygote invades the midgut, and then meiosis division occurs to form haploid kinetes. Babesia kinetes invade tick tissues and then migrate to the salivary glands in which they stay dormant as sporoblasts. These sporoblasts replicate into sporozoites, in this phase, these will be transmitted to the mammalian host (Elsworth & Duraisingh, 2021).

In **Table 2**, a list of the vector-borne febrile infectious diseases with their respective vectors is presented.

Table 2. List of diseases and its corresponding vector

Tropical infectious disease (Agent/family)	Vector	Reference
Dengue fever (Dengue Virus,)	<i>Aedes aegypti</i> <i>Aedes albopictus</i>	(Lee et al., 2021)
Chikungunya fever (Chikungunya Virus)	<i>Aedes aegypti</i> <i>Aedes albopictus</i>	(Cevallos et al., 2017)
Zika (Zika Virus)	<i>Aedes aegypti</i> <i>Aedes albopictus</i>	(Cevallos et al., 2017)
Yellow fever	<i>Aedes spp</i>	(Chen & Wilson, 2020)

(Yellow fever virus)	<i>Haemagogus spp</i> <i>Sabethes spp</i>	
Oropouche (Oropouche virus)	<i>Culicoides paraensis</i> <i>Culex quinquefasciatus</i>	(Sakkas et al., 2018b)
Mayaro (Mayaro virus)	<i>Aedes spp</i> <i>Haemagogus spp</i>	(Lorenz et al., 2019)
West Nile fever (West Nile virus)	<i>Culex pipiens</i>	(Ciota, 2017)
Venezuelan equine encephalitis (Venezuelan equine encephalitis virus)	<i>Culex (Melaconion), Aedes,</i> <i>Mansonia, Psorophora,</i> <i>Haemagogus, Sabethes,</i> <i>Deinocerites, and Anopheles</i>	(Guzmán-Terán et al., 2020)
Bartonellosis (Carrion's disease) (Bartonella spp.)	<i>Lutzomyia spp</i>	(Zorrilla et al., 2017)
Malaria (<i>Plasmodium spp.</i>)	<i>Anopheles spp.</i>	(Arregui et al., 2015)
Chagas disease (<i>Trypanosoma cruzi</i>)	<i>Triatoma dimidiata, Rhodnius</i> <i>ecuadoriensis, Triatoma</i> <i>carrioni, Pastrongylus</i> <i>rufotuberculatus</i>	(Padilla N et al., 2019)
Rickettsiosis (Rickettsia spp.)	<i>Ixodes spp</i>	(Tomassone et al., 2018)
St. Louis encephalitis (St. Louis encephalitis virus)	<i>Culex spp.</i>	(Ridenour et al., 2021)
Ilhéus fever (Ilhéus virus)	<i>Psorophora spp</i> <i>Ochlerotatus spp</i>	(da Costa et al., 2022)

1.4. Pathogens responsible for acute febrile illnesses

The following section provides an overview of the tropical febrile pathogens tested in this project by using molecular assays. The pathogens described are dengue virus (DENV), Zika virus (ZIKV), chikungunya virus (CHIKV), Mayaro virus (MAYV), Oropouche virus (OROV), SARS-CoV-2, *Leptospira*, *Plasmodium*.

1.4.1. Dengue virus (DENV)

DENV belongs to the family *Flaviviridae* genus *orthoflavivirus*, consisting of 11 kb single stranded RNA genome. The genome encodes three structural proteins, including nucleocapsid protein, envelope protein (E), membrane associated protein (prM), and seven non-structural proteins. Four serotypes have been described as DENV-1, DENV-2, DENV-3 and DENV-4, which are further grouped into different genotypes (Kok et al., 2023). Dengue fever is a vector-borne disease transmitted by *Aedes aegypti* and *Ae. albopictus* mosquitoes with the highest occurrence in tropical and subtropical regions of the world. Dengue is endemic in over 130 countries, with Southeast Asia having the highest dengue burden (70%) followed by the western pacific and the Americas (Kularatne & Dalugama, 2022). In the Americas, outbreaks are largely cyclical following seasonal patterns, with a single DENV serotype dominating epidemics. In 2023, more than 3.1 million cases have been reported, making it the year with the highest incidence. The highest number of cases to date were reported in Brazil, Peru, and Bolivia with a case fatality rate of 0.04% and an accumulative incidence of 305 cases per 100,000 population. More recently, simultaneous circulation of all four DENV serotypes has been registered in Brazil, Colombia, Costa Rica, Guatemala, Honduras, México Venezuela, and Nicaragua, while Perú, Panama, Argentina and Puerto Rico reported circulation of DENV-1, DENV-2 and DENV-3 (WHO, 2023a). Regarding Ecuador, 22,749 cases were reported in 2023, being the highest number in the last seven years, with circulation of DENV-1 and DENV-2 reported (Gaceta epidemiológica, 2023). Recently, dengue fever outbreaks have been reported in Europe with 74 autochthonous cases from Italy, France and Spain. Moreover, 390 million cases have been estimated to occur per year and 3.9 billion of people are at risk of infection, increasing its incidence by eight-fold in 2023 (PAHO, 2023). Dengue fever is typically considered as an urban disease in the Americas, however our study shows that it also circulates in rural and remote areas with lower population densities

and suggested that the viral movement may also go from more remote communities to commercial centers (Márquez et al., 2023).

WHO in 2009 classified dengue fever into two clinical categories, non-severe and severe. Non-severe includes dengue with warning signs and no warning signs. During the febrile phase the symptoms are high fever, headache, myalgia and arthralgia. Several patients develop the most severe form of the disease (Hemorrhagic dengue) and its symptoms are severe plasma leakage and bleeding, thrombocytopenia, organ involvement hypotensive shock and death (Kularatne & Dalugama, 2022). One of the factors associated with a more severe outcome such as Dengue hemorrhagic fever is a heterotypic secondary infection that leads to antibody dependent enhancement (ADE). In ADE, cross-reactive antibodies bind to the virus, but do not neutralize it. Subsequently, these complexes are recognized by the Fc γ receptors of myeloid cells, facilitating the entry and replication of the virus in cells (Katzelnick et al., 2017). Cross-reactive antibodies have poor neutralizing activity with non-homologous DENV serotypes; thus, rather than protecting the host from infection, these antibodies facilitate the uptake of virus by mononuclear phagocytic cells, resulting in widespread dissemination with cytokine storm and vascular leakage. In addition to this, the non-structural protein NS1 has been shown to contribute to dengue pathogenesis since it is capable of triggering endothelial hyperpermeability and induce vascular leakage by releasing vasoactive cytokines from peripheral mononuclear blood cells (Puerta-Guardo et al., 2019). Furthermore, a prior primary Zika infection is capable of inducing anti-DENV2 cross reactive antibodies, leading to classical ADE and the increase of DENV severity by certain serotypes. These interactions between the four dengue serotypes and ZIKV might have a direct effect on vaccine safety and efficacy (Katzelnick et al., 2020a). Currently, there is no specific treatment for dengue, however apolipoprotein A1 (ApoA1), which is a component of HDL, was reported to

neutralize NS1-enhancement infection. Furthermore, the use of an ApoA1 mimetic peptide 4F is proposed to serve as a therapeutic strategy for symptomatic dengue (Coelho et al., n.d.). Regarding vaccines, DENGIVAXIA (Sanofi Pasteur, France) is a tetravalent live attenuated dengue vaccine (CYD-TDV), based on a YFV backbone which was licensed in 2015 in more than 20 countries. However this vaccine is recommended only in dengue immune recipients since this vaccine put vaccinated naïve younger children at a high risk of severe dengue, as it does not elicit antibodies against all serotypes equally (Sarker et al., 2023). TAK-003 or QDENGIA (Takeda Pharmaceuticals, Japan) is another tetravalent live attenuated dengue vaccine based on a DENV-2 backbone with the potential of cell mediated immunological reaction, which was licensed since 2022 nevertheless it showed lower protection for DENV-1 and DENV-3 (Sarker et al., 2023). Finally, the BUTANTAN dengue vaccine candidate is also a live attenuated, tetravalent dengue vaccine, which is an analogue of TV-003, developed by the National Health Institute of USA. In a phase-2 trial in Brazil, a single dose was tolerated and showed efficacy against DENV-1 and DENV-2, thus demonstrating its efficacy against dengue with warning signs and severe dengue. The trial will continue until 2024 with the possibility of evaluating the vaccine performance against DENV-3 and DENV-4 (Thomas, 2023).

1.4.2. Zika virus (ZIKV)

ZIKV is a single stranded RNA emerging arbovirus that belongs to the genus *orthoflavivirus*, family *Flaviviridae*. This virus was isolated for the first time in 1947 in Uganda from a rhesus monkey in the Zika forest. The first human case was reported in 1953 in Nigeria. The phylogenetic analysis showed two viral lineages, the African and the Asian (Musso & Gubler, 2016). The first reports in the Americas and the Caribbean were in 2013, however in 2014 cases

were detected in several Brazilian states and by 2015 the virus spread to other countries in South and Central America. From January 2015 to March 2017 a total of 754,460 cases were reported by PAHO. From these, the highest number of cases came from Brazil, Colombia, and Venezuela (Hills et al., 2017). Since 2017, ZIKV incidence decreased worldwide, but its transmission persists in low levels in several countries in the Americas. In 2020 a total of 22,885 cases were reported (WHO, 2022). Elsewhere, in 2019, the first three autochthonous cases were reported in France in the Var-department (*Zika-Virus-Disease-Annual-Epidemiological-Report-2021.Pdf*, n.d.).

ZIKV is transmitted to humans by the vectors *Aedes aegypti* and *Aedes albopictus*. However, there are also non-vector borne transmission routes such as perinatal transmission, sexual transmission, and blood transfusion (Sharma et al., 2020). Most of the patients with acute Zika infection (80%) are asymptomatic or present mild symptoms. The most common symptoms include rash, conjunctivitis, fever, headache, myalgia, arthralgia, myalgia, and retro-orbital pain. In areas where there is co-circulation with DENV and CHIKV, it might be complicated to differentiate cases only by clinical diagnosis (Wolford & Schaefer, 2023). In contrast with DENV and CHIKV, the infection could progress to other neurological disorders as Guillain-Barré syndrome in adults and microcephaly in the fetus of an infected mother (Krauer et al., 2017). As ZIKV and DENV are closely related flaviviruses, there was concern that prior dengue might enhance ZIKV infection. This has not borne out in studies, however Katzelnick, et al, in a study carried out in a Nicaraguan pediatric cohort, suggested that prior ZIKV infection is capable of enhancing DENV-2 disease by inducing cross reactive anti-DENV-2 antibodies. This suggests that interactions between DENV and ZIKV might also affect vaccine safety (Katzelnick et al., 2020b).

Given the cross-reactivity of ZIKV with other flaviviruses, WHO recommends the use of molecular and serological assays for diagnosis. Several serological approaches have been

developed to get a clear differentiation among both viruses, such as the blockade of binding inhibition ELISA assay (BOB-ELISA) (Balmaseda et al., 2017). Moreover, five serological assays had FDA approval in 2018, whereas others are commercially available but do not have this approval (Theel & Hata, 2018). Regarding molecular assays, ZIKV can be detected through RT-PCR with different targets such as the *E* gene, the *NS1* gene, *NS3* gene, and the *NS5* gene. Currently, there is no vaccine available for this, however there are more than eighteen ZIKA vaccine constructs in different development stages (Poland et al., 2019).

1.4.3. Chikungunya virus (CHIKV)

CHIKV is the etiological agent of Chikungunya fever or la “quebradora” (“to walk bent over”), which is an alphavirus with a single stranded positive sense RNA genome of 12 kb that belongs to the *Togaviridae* family (Chinedu Eneh et al., 2023). Phylogenetic analysis describes three main genotypes, Asian/American, ECSA and West African. This virus was isolated for the first time in 1952 in the Makonde Plateau in East Africa. At first it was suggested that the virus was maintained in the sylvatic cycle in Africa and Asia, however urban transmission is now the most important cycle. (Bartholomeeusen et al., 2023). Since the outbreak in 2004 in the Indian Ocean Islands, CHIKV has been identified in 110 countries in Asia, Africa, Europe and the Americas. Between 2013 and 2023, more than 3.7 million cases were reported only in the Americas (Chinedu Eneh et al., 2023). In 2013, the first case was reported on the island of San Martin, then spread to other Caribbean islands and in 2015 it entered the Americas, affecting 45 countries. CHIKV can cause explosive outbreaks that strain medical resources. An example of this occurred in Paraguay, from October 2022 until March 2023 in which 75,911 cases were reported, of which the majority of cases came from Central Department and the capital Asunción (Torales, 2023). CHIKV is transmitted to humans by the vectors *Aedes aegypti* and *Ae. albopictus* which are involved in the

urban cycle. The mutation A226V in E1 protein was shown to enhance the infectivity of the virus in *Aedes albopictus* (Bartholomeeusen et al., 2023). Three to seven days after the mosquito bite, 97% of people develop acute Chikungunya infection characterized by high fever, myalgia and severe arthralgia in the peripheral joints as wrists, knees, ankles and hands. 40% of the infected individuals developed chronic arthritis, and it may persist for several months and years. Other atypical manifestations include neurological (encephalitis), cardiovascular (myocarditis), renal, dermatological and respiratory (Webb et al., 2022). Important factors that contribute to the expansion of CHIKV are limited mosquito control, climate change, viral adaptation, global travel and trade and the lack of curative treatments and no vaccines up to date (Morrison, 2014). This virus has been nominated as a priority pathogen for vaccine development, thus there are several candidate vaccines that could contribute to the reduction of the burden of the disease once approved. The VLA 1553 vaccine has actually been approved, however it is not yet widely available. This vaccine targets a long-lasting immunity with a single dose (1×10^4 TCID₅₀/0.5ml), it is a vaccine construct based on the CHIKV La Reunion strain of the ECSA lineage (LR2006-OPY1) with a 61 amino acid deletion in the nsP3 gene (del5nsP3). A pivotal phase three study was carried out in individuals ≥ 18 years old with a 98.9% sero-response rate at day 29 and the antibody persistence showed to be positive with a retention of 99% of sero-response. The plaque reduction neutralization test showed that VLA 1553-induced antibodies are capable of neutralizing CHIKV strains from the three different genotypes (Schneider et al., 2023).

1.4.4. Mayaro virus (MAYV)

MAYV is a single stranded RNA alphavirus with a genome size of 11.5kb that belongs to the *Togaviridae* family transmitted by mosquito (known as alphaviruses) which was isolated for the first time in Trinidad and Tobago in 1954 from forest workers. It is classified in the Semliki

complex. Three genotypes have been described as D, L and N, with genotype D being the most widely dispersed. This virus is transmitted to humans by the primary vector belonging to the genus *Haemagogus*, however there are also secondary vectors from which the virus has been isolated as *Aedes* sp. *Culex* sp, *Psorophora* sp. and *Sabethes* sp. MAYV has been considered as endemic in the tropical forests of the Amazon basin, however in recent years it has been shown that it has the capability to spread to urban areas. In remote areas, the cycle is enzootic sylvatic involving wild vertebrates as birds and reptiles, primates and mosquitoes as *Haemagogus* (Valencia-Marín et al., 2020), however *Aedes* is considered a bridge between sylvatic and urban cycles. Mayaro fever cases in humans have occurred due to the accidental spillover from the sylvatic cycle in people who lived near forests or work in these areas. According to Ganjian et al, 2020, MAYV has been reported in 10 Latin America countries (Argentina, Brazil Bolivia, French Guiana, Haiti, Mexico, Panamá, Perú, Ecuador and Venezuela) and 1 Caribbean country (Trinidad y Tobago) with an approximate number of 901 confirmed cases, with the highest numbers in Brazil and Peru (Ganjian & Riviere-Cinnamond, 2020). The clinical symptoms for Mayaro disease are fever, headache, myalgia, retro-orbital pain, vomiting, diarrhea, rash, arthralgia, conjunctivitis, neurological complications and myocarditis (Acosta-Ampudia et al., 2018). Arthralgia may persist during severe infection and may last over several months, incapacitating the affected person (Pereira et al., 2021).

Most of the serological tests for Mayaro present cross-reactivity with other alphavirus antibodies such as CHIKV. A limitation is that ELISA assays have a reduction in their specificity in secondary infections as patients may have multiple exposures to different alphaviruses with cross reactive antibodies (Pezzi et al., 2019). There are no MAYV ELISA commercial kits, and a positive result must only be presumptive in acute infections. To confirm these positives,

seroconversion should be demonstrated between the acute and the convalescent sample and no seroconversion for other alphaviruses (PAHO, 2019). Molecular assays as RT-PCR are used in serum samples in the first five days of the viremic phase which are useful to confirm Mayaro infection. As the viral load of this virus may be low, the standard test for Mayaro diagnosis is viral isolation in C6/36 cell lines, however due its complexity, it is not commonly used as first-line diagnostic tool (Waggoner, Rojas, Mohamed-Hadley, et al., 2018).

1.4.5. Oropouche virus (OROV)

OROV is the etiological agent of Oropouche fever, which belongs to the *Orthobunyavirus* genus of the family *Peribunyaviridae*, classified in the Simbu serogroup of viruses and has a tri-segmented genome of negative sense RNA of different sizes: A large segment (L) encodes the viral RNA-dependent polymerase, a medium segment (M) which encodes a polyprotein and a small segment (S) which encodes the nucleocapsid protein. Four genotypes have been described as I, II, III and IV (Files et al., 2022). As this virus is segmented, reassortment events have been observed, which have influenced in the evolution of the virus. (Gutierrez et al., 2020). OROV has two transmission cycles, sylvatic and urban. Within the sylvatic cycle, sloths and non-human primates serve as hosts, and then the virus is transmitted by vector species as *Aedes serratus* and *Coquillettidia venezuelensis*. On the other hand, the urban cycle involves humans as unique hosts and the transmission occurred through the vector *Culicoides paraensis* and also *Culex quinquefasciatus* (Pereira et al., 2021). Since its first description in Trinidad y Tobago in 1961, more than 500,000 people have been affected, causing 30 epidemics in Latin Americas such as Panama, Brazil, Peru, Ecuador, Trinidad and Tobago, French Guiana and Peru (Durango-Chavez et al., 2022).

The most common clinical symptoms of Oropouche disease are fever, headache, arthralgia, myalgia, dizziness, photophobia, chills, retro-ocular pain, rash, nausea, and vomiting. The infection could develop into meningitis or encephalitis and also hemorrhagic symptoms as petechiae and gingival bleeding. There are several diagnostic tests for OROV, during the acute febrile illness, molecular tests as RT-PCR, real time PCR and viral isolation (Files et al., 2022).

Other tropical viruses causing febrile diseases in South America are: machupo (arenavirus), hantavirus (bunyavirus), savia virus, guanarito virus, junin virus.

1.4.6. SARS-CoV-2

SARS-CoV-2 is a betacoronavirus that belongs to the family *Coronaviridae* consisting of a positive sense single-stranded RNA genome of 30,000 nucleotides and it replicates by an RNA-dependent RNA polymerase and an exoribonuclease (ExoN) nsp14 which mediates a high-fidelity replication and enhance its proliferation. The genome encodes four structural proteins including spike protein (S), envelope protein (E), membrane protein (M) and the nucleocapsid protein (N) and also non-structural ORFs (Singh & Yi, 2021). The spike protein is a fusion protein that is subdivided into two subunits S1 and S2, and this protein is considered as the most important virulence factor. S1 subunit contains the RBD domain and is linked to viral binding to ACE2 receptor which is in charge of viral membrane fusion. The host cell has the TMPRSS2 protease that facilitates the entry of the virus (Kumar et al., 2023).

This virus belongs to the SARS associated betacoronavirus (sarbecovirus) The first report of the circulation of a novel coronavirus in the world, was in December 2019 in Wuhan, China. Subsequently, once the etiologic agent sequence was available, the virus was named as SARS-CoV-2 and the disease as COVID-19 and in March 11, 2020 it was declared as a pandemic

(Ukwishaka et al., 2023). A report of all cases from Wuhan hospitals showed that 55 cases were associated with the Huanan market. This market and other 3 were selling live mammals (wild and farmed wild animals) during 2019 in the early stages of the pandemic, suggesting that these animals were the source of these pneumonias as possible other zoonotic viruses, leading to the closure of the market and further environmental sampling. According to Worobey et al, 2022, the early lineages A and B of SARS-CoV-2 were associated with the geographic location of the market, since 11 lineage B cases from 2019 lived close to and had been to the Huanan market. Regarding lineage A, none of these cases have previous contact with the Huanan market, however these individuals were staying closer to the market, suggesting their exposure to the virus. As stated, Huanan market sold live wild animals including hog badgers, red foxes, and raccoon dogs. Five environmental samples taken from a stall that sold live mammals in 2019 as well as the sewer and the water drain proximal to the stall, were found to be positive to SARS-CoV-2 suggesting that live animal trade and live animal markets are linked to virus spillover (Worobey et al., 2022). In further support of the zoonotic origin, SARS-CoV-2 shows similarities with other zoonotic sarbecoviruses such as the SARS-CoV virus responsible for the SARS outbreak in 2002 in which the natural reservoir is a horseshoe nose bat and with the Middle East Respiratory Syndrome Virus (MERS) that was found in the bat (*Taphozous perforates*) of Arabian Peninsula and in camels. Additionally, 4 human coronaviruses as HCoV-OC43, HCoV-HKU1, HCoV-229E and HCoV-NL63 have been reported to have zoonotic origins (Holmes et al., 2021). Bats and pangolins were reported to shedding viruses that are closely related to SARS-CoV-2 in different sites of China, Thailand and Japan (Holmes et al., 2021). However, up to date there is still an evolutionary gap between SARS-CoV-2 and its closely related viruses. An example of this is RatGT13 which was sampled from *Rhinolophus affinis* bat in Yunnan, showed a higher genetic similarity with SARS-

CoV-2. Up to date no intermediate host has been identified yet, probably because the progenitor virus has a low prevalence or the animal population has not been sampled (Holmes et al., 2021). Regarding host tropism, SARS-CoV-2 is a generalist virus since it is capable of infecting several mammal species (farmed minks, white-tailed deer, non-human primates, felines, etc). (Bashor et al., 2021).

According to the WHO coronavirus Dashboard, up to November 2023, a total of 771,679,618 confirmed cases of COVID-19 and 6,977,023 deaths have been reported worldwide (<https://covid19.who.int/>). SARS-CoV2 is the etiological agent of COVID-19 disease transmitted by different routes as airborne droplets, close contact and fecal-oral contact. The virus presents an incubation period of 4 to 5 days and recovery rate of 98%, however, the severity of the infection depends on risk factors as diabetes, cardiovascular and respiratory diseases, and now vaccine and immune status. The symptoms in naïve people are fever, fatigue, cough, cardiac injury, breathlessness, sore throat, multi-organ failure, and others (Ukwishaka et al., 2023). More recently, symptoms in most infected people are fever and upper respiratory congestion, however high risk and other patients still have severe outcomes.

Genomic surveillance by February 2020 led to the identification of a non-synonymous mutation D614G in the spike protein which seemed to increase the viral fitness, enhance viral infectivity and its binding to receptor to the human ACE2 receptor (Singh & Yi, 2021). Later, since October 2020, during the evolution of SARS-CoV-2, a high number of mutations in the receptor binding domain of the spike protein as E484K, N501Y, and P681H were described to increase the binding affinity to human receptors, to enhance cell entry, to promote viral protein stability and confer higher transmissibility (Holmes et al., 2021). These mutations are also responsible for producing antigenic changes, which resulted in the decrease of antibody neutralization and the

subsequent reduction of the immunity against secondary infections. Thus, several of these mutations lead to the emergence of novel variants and subsequent waves during the pandemic, having a direct impact at an epidemiological level of the disease (Carabelli et al., 2023). These novel variants were declared by WHO as variants of interest and variants of concern, and received Greek alphabet and code names to avoid the geographic discrimination of early strain identifications (ie Whuhan, Indian, South African). Variants of interest (VOIs) are those known to affect antibody neutralization, diagnostic tests and increased transmissibility and severity, examples of these variants were Lambda (C.37) and Mu (B.1.621). Moreover, variants of concern (VOCs) include all the characteristics of VOIs, increased virulence and showed a decrease in the efficacy of public health measures, becoming dominant either regionally or globally capable of outcompeting other variants. The VOCs include Alpha (B.1.1.7), Beta (B.1.351), Gamma (P1), Delta (B.1.617.2 and AY sublineages), and Omicron (B.1.1.529 and BA sublineages, such as BA.1, BA.2, BA.4/5, BQ.1, and XBB). Given that these variants might change their phenotype due to acquisition of novel mutations, and to develop better designed vaccines, it is important to continue with their surveillance and monitoring.

According to PAHO, 2020, a case is considered as a reinfection when a symptomatic individual tests positive after 45 days since the primary infection or 90 days if the individual was asymptomatic and the confirmation was based on the sequencing of both variants and in the middle of this period, the individual presented a negative test (PAHO, 2020). The first report of reinfection was in August 2020 in Hong Kong and since, other reinfection cases were reported in other countries such as Belgium, the Netherlands, USA and Ecuador (Prado-Vivar et al., 2021). The overall proportion of COVID-19 reinfection was determined as 4.2%. Reinfection demonstrated that natural immunity wanes within weeks in some people. Omicron variant is

associated with the increase of 10% of reinfection rate due to its capacity to escape immunity and increase infectiousness. Reinfection rates seemed to be different between continents, for example the highest prevalence of reinfection is reported in Africa since social distance and consistent hand-washing were not implemented due to population density and the lack of water services (Ukwishaka et al., 2023).

According to WHO dashboard, through October 22, 2023, a total of 13,533,465,652 vaccine doses have been administered worldwide (WHO, 2023b). In general, vaccine development before the COVID pandemic took more than 5 years until a vaccine finally gets approved and distributed. In contrast for COVID-19, vaccine development and its manufacturing took 350 days (Vandeputte et al., 2021). From 138 vaccine candidates, 21 of these were approved for emergency use worldwide which consisted in different platforms as inactivated, live attenuated, protein subunit, virus like protein, viral vector and DNA and RNA (Rahman et al., 2022). On December 31, 2020, the Pfizer vaccine (BNT162b2) was the first authorized by WHO for its use. Subsequently on February 15 2021, Astra-Zeneca/Oxford was authorized followed by Johnson & Johnson vaccine on March 2021 and Moderna on April of the same year (Soheili et al., 2023). Pfizer and Moderna vaccines consist in a nucleoside-encapsulated modified mRNA that encodes viral spike protein (S2-P antigen) and is delivered in lipid nanoparticles. These vaccines elicited B and T cell immune response against the spike protein. The common side effects presented after vaccination were moderate pain in the site of the injection and others as headache, fatigue and fever. Similar adverse effects were reported for Moderna vaccine headache, fatigue, myalgia, arthralgia, pain and erythema. In contrast Oxford/Aztrazeneca vaccine is composed by a chimpanzee adenoviral vector ChAdOx1 which delivers the spike protein gene and Johnson & Johnson vaccine is a recombinant human adenovirus vector expresses the Spike protein antigen. The mRNA vaccines behaved better

in preventing infections whereas inactivated vaccines were more effective in preventing severity (Patel et al., 2022).

1.4.7. *Leptospira*

Leptospira is the etiological agent of leptospirosis, a common zoonotic and neglected disease in tropical regions. Leptospirosis was first described in 1886 by Adolf Weil and the agent was described by Stimson who named the bacteria as *Spirochaeta interrogans* and then Noguchi coined the term “*Leptospira*” due to its morphology (Rajapakse, 2022). *Leptospira* is a small, aerobic spirochaete. Phylogenetic analysis shows 3 clusters described as pathogenic, intermediate, and saprophytic clusters. The pathogenic species includes *L. interrogans*, *L.kirschneri*, *L.noguchii*, *L. borgpetersenii*, *L. weilii*, *L. santarosai*, *L. alexanderi*, *L.Kmetyi* and *L.alstonii*. The intermediate includes *L.fainei*, *L.licerasiae*, *L.inadai*, *L.broomii*, and *L.wolffii*. The saprophytic is composed by *L. biflexa*, *L. terpstrae*, *L. meyeri*, *L. yanagawae*, *L. vanthielii*, *L. parva*, and *L.wolbachii* (Calvopiña et al., 2023). The main reservoir is the brown rat (*Rattus norvegicus*) and contaminated environment as water has an important role in infections of animals and humans. Leptospirosis has been described worldwide, except in Antarctica (Browne et al., 2023). The incidence of this infection is estimated to be 1.9 cases per 100,000 population and 10,702 cases were reported to PAHO, from which 7.2% belong to Ecuador (Calvopiña et al., 2023). The clinical symptoms are similar to other febrile illnesses as dengue and malaria. Most of the cases showed fever, myalgia and headache, however the 10% of these cases developed severe disease with conjunctival suffusion, jaundice and kidney injury. In the transmission cycle, humans are incidental hosts, and the infection occurs during recreational, domestic and occupational activities (Browne et al., 2023). Moreover, proximity to animal reservoirs as cattle, pigs and dogs is also an important factor for the increase of disease prevalence. The microscopic agglutination test (MAT) is the technique

used for leptospirosis diagnosis, however it has an 80% of sensitivity, its standardization is difficult and needs trained personnel for *Leptospira* culture (Calvopiña et al., 2023). Regarding ELISA, the most common antigens used for detection (coated in ELISA wells) are whole cells or Omp and rOmp (OMSA, 2022). In a systematic review, the global sensitivity of IgM test was reported to be 86% with a specificity of 84% for initial screening of acute disease (Rosa et al., 2017). Similar values of sensitivity and specificity were reported by Niloofa et al. (Niloofa et al., 2015). The same authors reported the development of two in-house ELISAs, one for genus IgM detection and the other for serovar IgM antibodies. The genus IgM ELISA showed 83.3% of sensitivity and 91% of specificity, whereas the serovar IgM ELISA showed a sensitivity of 80.2% and a specificity of 89% (Niloofa et al., 2021). The commercial tests Panbio *Leptospira* IgM-ELISA and the Virion-Serion classic *Leptospira* IgG-ELISA are widely used; however, ELISAs are not adequate for epidemiological surveillance of *Leptospira* strains (Maneewatchararangsri et al., 2021).

For this reason, several PCR assays have been developed for detection of pathogenic *Leptospira* in clinical samples such as blood and urine. Among these targets, the gene *lipl32* has been widely used due to its specificity to pathogenic *Leptospira*. (Stoddard et al., 2009); (Ahmed et al., 2020). Other targets including *lipl21*, *lipl41*, *OmpL1* genes have been reported to present variable sensitivities and specificities. For example, for *OmpL1* gene sensitivity and specificity were reported as 97.2% and 100% respectively, while 16sRNA, these were reported as 100% and 100%, respectively (Gökmen et al., 2016); (Chandan et al., 2011).

1.4.8. Plasmodium

Plasmodium spp is a protozoan pathogen that belongs to the phylum *Apicomplexa*, commonly found in tropical areas and is responsible for producing malaria, a life-threatening disease. Five

species of *Plasmodium* have been described, *Plasmodium falciparum* and *Plasmodium vivax* are the most important ones since humans are the unique hosts. Malaria is transmitted by 40 species of mosquito from genus *Anopheles*, which are distributed worldwide (Phillips et al., 2017b). WHO reported by 2021 an estimated 247 million cases in 84 countries and 619,000 deaths (WHO, 2021). *Plasmodium* infects primarily the red blood cells and replicates to more than 10^{12} parasites during the symptomatic phase of the disease. The 88% of the disease burden is in Sub-Saharan Africa, followed by Southeast Asia (10%), the mediterranean region (2%) and Caribbean and Latin America less than 1%. In the Americas, *Plasmodium vivax* is predominant with 64% of malaria cases (Núñez et al., 2023). Clinical symptoms of malaria are fever, shaking chills, muscle aches and, in children, digestive symptoms, paroxysms, drenching sweat and exhaustion, severe anemia and multi-organ damage (Phillips et al., 2017b). Microscopy in blood smears has been the gold standard for malaria diagnosis, however it requires experts or well trained personnel (Oyegoke et al., 2022). For this reason, more than 200 rapid diagnostic tests (RDTs) are commercially available and have contributed to improving diagnosis in resource-limited areas. The RDT card is a lateral flow device that uses immunochromatography to detect antigens associated with malaria. For example, in Africa the percentage of usage of these tests increased from 36% to 87% in suspected cases, leading to the decrease in overuse of antimalarials. These RDTs are based on the detection of two antigens in blood, Histidine-rich protein (*hrp2* gene) and *Plasmodium* lactate dehydrogenase (*pLDH* gene). The use of rapid tests in Brazil increased from 1,486 tests in 2011 to 14,655 in 2015. However, deletions in genes *pfhrp2* and *pfhrp3* were reported in Peru, resulting in false negatives for rapid tests based in *Hrp2* (Recht et al., 2017). However, substandard malaria RDTs are widespread in resource-limited settings, and lot-to-lot variations may affect their

performance. Quality control panels in each country are recommended to assure the performance of RDT's.

Regarding malaria vaccines, in 2021 WHO recommended the use of RTS,S/AS01 for children due to clinical trials carried out in Ghana, Kenya and Malawi and the second vaccine recommended recently by WHO for malaria prevention is R21/Matrix-M (WHO, 2023).

Modern diagnostic tools for tropical febrile diseases

The aim of diagnostic tests is to provide etiologic confirmation to guide effective management of the illness and to provide information to conduct epidemiologic assessments such as estimating the prevalence of a disease. Classic diagnostic tools developed for detection of etiologic agents of fevers include viral isolation, microscopy, cell culture, plaque assays, biochemical reactions, immunofluorescence, and serology by microagglutination (MAT) and Huddleson agglutination, require specific skills and expertise from laboratory technicians, complex biosafety procedures, specific laboratory facilities and equipment and are time consuming. Regardless, some of these protocols still have low sensitivity and may fail to identify microbial etiology. On the contrary, new diagnostic technologies including rapid serologic chromatographic tests, nucleic acid amplification/detection, enzyme-linked immunosorbent assays, Luminex and more recently genomic sequencing have revolutionized pathogen detection because they use similar protocols for multiple infectious diseases, have high accuracy, high sensitivity, less risk to personnel, provide opportunities for multiplex detection of different targets, are faster, and many lead to precise pathogen identification (even at the strain level).

The process of selecting one or several tests for use in a diagnostic algorithm can be difficult for clinics, countries and researchers. In order to select the optimal diagnostic test, it is crucial to

consider its performance in optimal conditions (laboratory settings with controls) as well in routine conditions (with patient samples). Besides evaluation of regulatory approvals, pricing and market use, the performance properties needed for decision-making include properties such as sensitivity (S), specificity (E), positive predictive value (PPV) and negative predictive value (NPV), and are described in detail below:

1.5.1. Sensitivity (S)

Refers to the ability of a test to correctly identify the presence of a disease in a person that has the disease, meaning the proportion of true positives. The formula for sensitivity calculation is as follows:

$$\text{Sensitivity} = (\text{True Positives (A)}) / (\text{True Positives (A)} + \text{False Negatives (C)})$$

If a test has a sensitivity of 80%, this means that it identifies 80% of the positives (true positives) and the 20% remain as false negatives (Lalkhen & McCluskey, 2008).

1.5.2. Specificity (E)

Refers to the ability of a test to correctly identify the absence of a disease in a subject that does not have the disease, meaning the proportion of true negatives. The formula for specificity calculation is as follows:

$$\text{Specificity} = (\text{True Negatives (D)}) / (\text{True Negatives (D)} + \text{False Positives (B)})$$

If a test has a specificity of 80%, this means that the test detects 80% of true negatives and 20% remain as false positives. There is often an inverse relation between sensitivity and specificity and these need to be considered together for the test selection (Lalkhen & McCluskey, 2008).

1.5.3. Positive predictive value (PPV)

Determines the true positives out of the positive results, and it is dependent of incidence or prevalence of the infectious agent (Shreffler & Huecker, 2023). The formula is as follows:

$$\text{Positive Predictive Value} = (\text{True Positives (A)}) / (\text{True Positives (A)} + \text{False Positives (B)})$$

1.5.4. Negative predictive value (NPV)

Determines the true negatives out of the negative results and it is also dependent of incidence or prevalence of the infectious agent (Shreffler & Huecker, 2023), and is represented by the following formula:

$$\text{Negative Predictive Value} = (\text{True Negatives (D)}) / (\text{True Negatives (D)} + \text{False Negatives (C)})$$

Several diagnostic tests have been implemented in low-resource countries because they require less investment in laboratory facilities and equipment (compared with classical diagnostics) (Anon., 2012). These diagnostic tests are available for different pathogens as viruses, bacteria and parasites, however for the aim of this work, several diagnostic tests as antibody detection tests, antigen diagnostic tests, PCR, Luminex and metagenomics are described in the following section.

1.6. Classical clinical indicators of infection

Complete blood counts provide classical parameters to measure overall health and provide evidence that an individual may have an infection during a clinical evaluation. Typical results obtained with infections include lymphopenia and thrombocytopenia, however these effects are non-specific and thus, it is not possible to differentiate between acute viral infections from other

pathogens such as bacteria and parasites. Platelet counts may serve as a marker during symptomatic disease and might be a clue for the diagnosis and monitoring of viral infections. Platelets are anucleate cells that circulate in the blood and internalize viruses during infection affecting the inflammatory response (Raadsen et al., 2021).

Regarding chikungunya infection, mild thrombocytopenia might be observed with platelets counts $>100,000/\mu\text{l}$, Lymphopenia count $<1,000 \text{ cells}/\text{mm}^3$ and in only one third of the patients lymphopenia may be severe $<500 \text{ cells}/\text{mm}^3$ (Bartholomeeusen et al., 2023)

Dengue fever is characterized by leucopenia ($<5000 \text{ cells}/\text{mm}^3$) and possibly a rise in hematocrit in a range of 5 to 10%. Laboratory analysis suggest that during dengue hemorrhagic fever hematocrit rises to $>20\%$ and thrombocytopenia is severe $<100,000 \text{ cells}/\text{mm}^3$ (Ralapanawa et al., 2018). According to Yan et al, 2018 in a study carried out in Singapore, patients positive for DENV tend to have thrombocytopenia and monocytosis, moreover these patients present liver injury with a two-fold increase of alanine aminotransferase and aspartate aminotransferase. In contrast, ZIKV positive patients tend to present normal platelet counts, low monocyte counts and do not present any abnormality regarding alanine aminotransferase and aspartate aminotransferase levels. Even though, this seems to be a difference between Zika and Dengue infections, blood count parameters need to be validated in a prospective cohort to evaluate if these parameters might enhance diagnostic of these arboviruses (Yan et al., 2018).

1.6.1. Antibody detection tests

Elevated IgM titers are evidence of recent acute infection whereas IgG titers are used to detect past or chronic infections. Furthermore, the seroconversion criterium allows the detection of the

4x antibody titer increase between acute and convalescent samples in secondary dengue, to confirm a current acute infection.

Detectable IgM titers can persist for around 6 months, whereas IgG persist for years or indefinitely. For this reason, the result interpretation and the aim of performing the diagnostic test varies depending on the disease and the immunoglobulin type detected.

The most common serological tests are enzyme linked immunosorbent assays (ELISAS), however, more sophisticated multiplex assays such as Luminex are also now widely used for research and diagnosis.

1.6.2. Rapid antibody tests (RDT)

A rapid diagnostic test is defined as a test that provides a result in minutes, does not need any complex laboratory infrastructure or special technician skills, and does not require electricity. In general, these are membrane-based immunochromatographic tests that are performed in cassettes or on dipsticks with a single-step lateral flow (Chappuis et al., 2013). These are qualitative tests that indicate presence or absence of the analyzed target in certain sample types, including urine, serum or blood (Mohd Hanafiah et al., 2017). The lateral flow assays are composed of a chromatographic system and the immunochemical reaction (antibody, antigen or antibody and antigen). The basic structure of this assay (for antibody detection IgM or IgG) and its performance is shown in **Figure 1**. The antigen is fixed in the membrane. At specific locations (lines), the test (target desired to be detected) and control lines are located. The test line is for interaction with the sample, and the control line helps to ensure that the test is working appropriately. When the sample is added, it moves with the capillary force throughout the nitrocellulose membrane, allowing the antigen or the antibody of the sample to interact with antibodies or antigens in the conjugated pad.

The conjugated pad contains colored nanoparticles which have an antibody on the surface. When there is an interaction with the antigen of the sample, as result of this interaction, a signal is generated, and a visible line is formed. This platform meets WHO ASSURED criteria (affordable, sensitive, rapid, robust, its use is not complicated, and it is equipment-free) (Mohd Hanafiah et al., 2017).

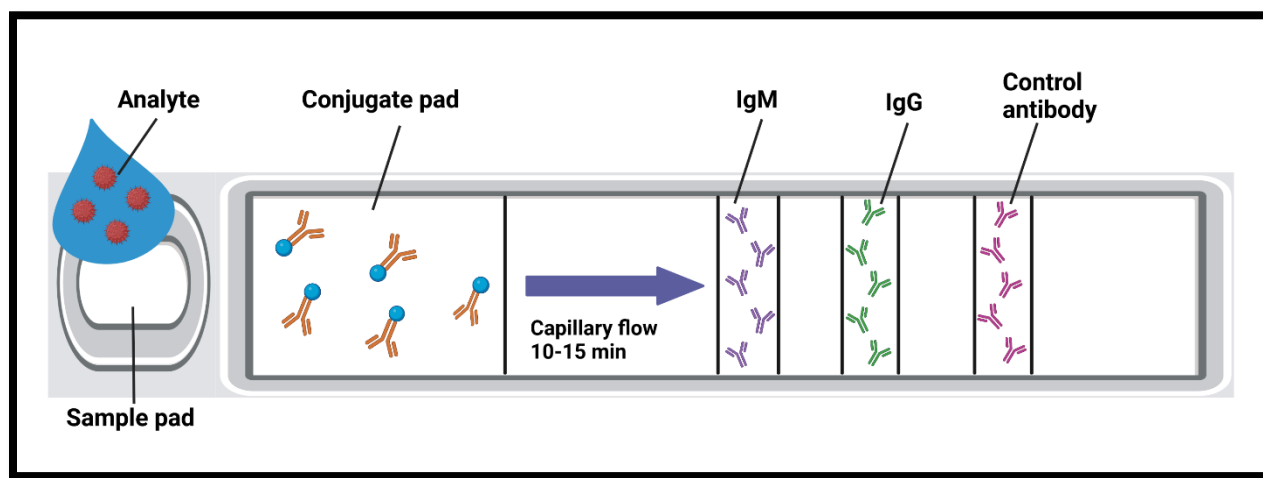


Figure 1. RDT basic structure and performance (created with BioRender.com)

The advantages of RDTs are simplicity, rapid results, portability, long storage stability, cost-effectiveness, and no equipment required. These tests are widely accepted in both developed and developing countries for rapid decision making at the bedside or in primary consultation. However, as these tests are mostly qualitative, possible cross-reactivity may occur, and their sensitivity is generally low, thus results may require an additional confirmation (Di Nardo et al., 2021). Nevertheless, RDTs have contributed to screening, diagnosis, monitoring, and surveillance efforts, especially in the field. Rapid tests have been developed for detection of IgM, IgG or antigens of several infectious diseases. It is important to carry out a prior evaluation of the accuracy of RDTs in the population in which it is going to be applied, given that genetic background,

epidemiology and cultural conditions may influence in the performance of the test (Prado et al., 2018).

1.6.3. Enzyme-linked immunosorbent assay (ELISA) for antibody detection

The ELISA is the gold standard of immunoassays and it is used for detection and quantification of different targets such as antigens and antibodies. The most common format consists of a 96-well or 384-well polystyrene plate which is coated with the target of interest. The four main steps of an ELISA are coating, detection, blocking and reading the results. The main components of the assay include coating antibody or antigen, antigen, a primary or/and secondary antibody, substrate and stop solution. The primary antibody binds to the specific target (Alhaji & Farhana, 2023) and the secondary antibody is enzyme-conjugated, most commonly to horseradish peroxidase (HRP). The enzyme reacts with a chromogenic substrate (such as 3,3',5,5'-tetramethylbenzidine), and as a result, a colored reaction will be revealed. This reaction is then stopped with a solution that alters the ideal reaction conditions, and the optic density produced by the color developed is read at a specific wavelength in a microtiter plate reader (Sakamoto et al., 2018).

The advantages of ELISA are its sensitivity and relative simplicity, and these complement the acute-phase molecular diagnostics in several diseases. The disadvantages are that cross-reactions can occur, protocols are labor-intensive (taking up to 7 hours to get a result), plasma components may affect the performance of the test, and commercial kits are expensive. Furthermore, more complex equipment and reagents are required than those required by the RDT, thus ELISAS are usually performed under controlled laboratory conditions (Hidayat & Wulandari, 2021); (Sakamoto et al., 2018). In-house assays are cheaper and could be developed *in situ*, but the cost

of antibody production is high, and in-house protocols need to be validated since temperature, tips, buffers, antigen batches and conductivity of distilled water may affect the final result.

The ELISA assay has different formats that are applied depending on the targets or specific pathogen seroconversions. The different formats are described below:

1.6.3.1. Enzyme-linked immunosorbent assay, ELISA

A classic ELISA is used for the detection and quantification of a specific analyte (e.g. antigens, antibodies, proteins, hormones, peptides, etc.) an enzyme-marked molecule detects is used to detect the analyte (Aydin, 2015).

In the typical ELISA assay shown in **Figure 2**, the plate is coated with the antigen, and then the serum sample (which has the antibodies if positive) is added. During the incubation period, the antibodies bind to their specific antigen. Then a secondary antibody conjugated with an enzyme is added, which attaches to the primary antibody. Finally, a substrate is added so the colorimetric reaction can be observed, and the optical density from the colorimetric reaction can be obtained. Positive reactions are colored while the negatives are normally colorless (Alhaji & Farhana, 2023).

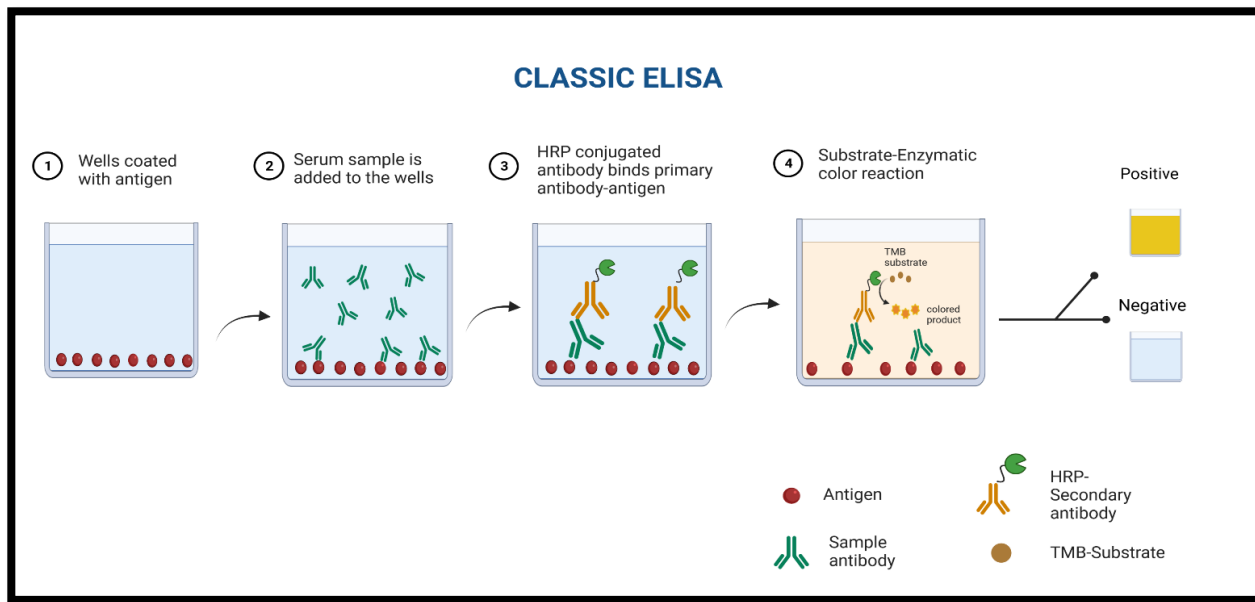


Figure 2. Classic ELISA basic principle and performance, created with BioRender.com

1.6.3.2. Competitive ELISA

The competitive ELISA (**Figure 3**) is very different from the other types of classic ELISA. In this assay, the plate is coated with antibody-specific antigen. Then a plasma or serum sample is added. After incubation, without washing the plate, a biotinylated monoclonal antibody (bMAb) that is specific to the same antigen of detection is added. This ELISA was designed to eliminate cross-reactions caused by low-affinity antibodies against closely related microorganisms. The antibodies in the serum or plasma and the bMAb will compete for the binding site of the antigen.

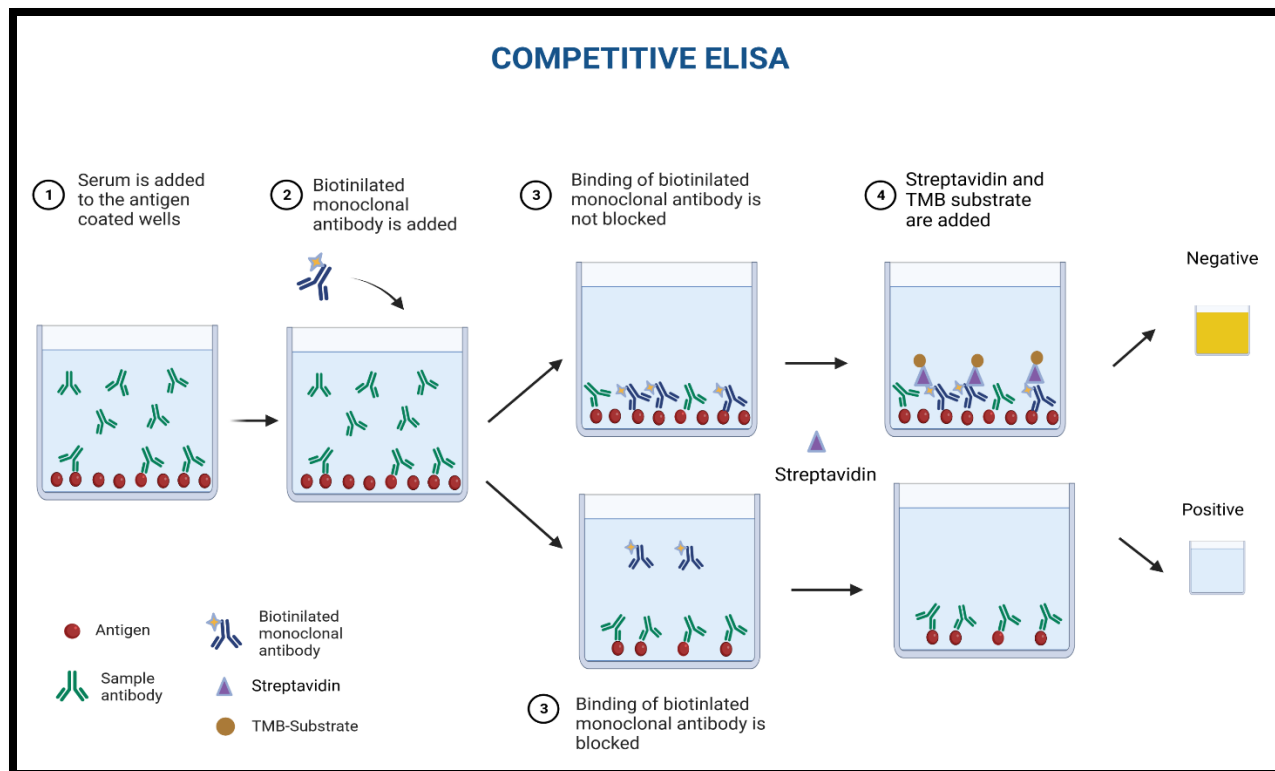


Figure 3. Competitive ELISA basic principle and performance, created with BioRender.com

The bMAB is highly specific to the antigen, so the incubation time needs to be run immediately after adding them in the first well. Streptavidin conjugated with an enzyme binds to the biotin of the monoclonal antibody and finally, a substrate reveals a colorimetric reaction. Results need to be interpreted differently from other ELISAs since positive samples are colorless reactions and optical density values are low, meaning that the number of antibodies in the sample is higher than the number of monoclonal antibodies, outcompeting them. Negative samples are presented with a yellow color and higher optical densities, meaning that the number of monoclonal antibodies is higher than sample antibodies (Sakamoto et al., 2018).

1.7. Antigen detection tests

Some infectious agents secrete proteins or peptides (antigens) that can be detected in body fluids during a period of time in the acute phase of infection. During this phase rapid tests, molecular and serological tests can be applied for diagnosis of a specific antigen in several types of samples including nasopharyngeal swabs, serum, blood, saliva and tissues depending on the pathogen.

1.7.1. Rapid antigen tests

Even though rapid antigen detection tests are used as screening and have been helpful to rapidly identify infected people, their sensitivity is usually low and molecular tests are needed for result confirmation, especially of negative samples. Laboratory technicians, consumer self-testing and practitioners must understand the performance of the tests for adequate interpretation.

The difference between antibody rapid tests and antigen rapid tests is that antigen tests detect the presence of a specific protein produced by the etiologic agent, while antibody tests detect the immune response to it (**Figure 4**). It is crucial then, that antigen tests are used during the phases of infection where the pathogen can be detected in the specific body fluid type tested (ie viremic blood, nasal swab during acute phase etc).

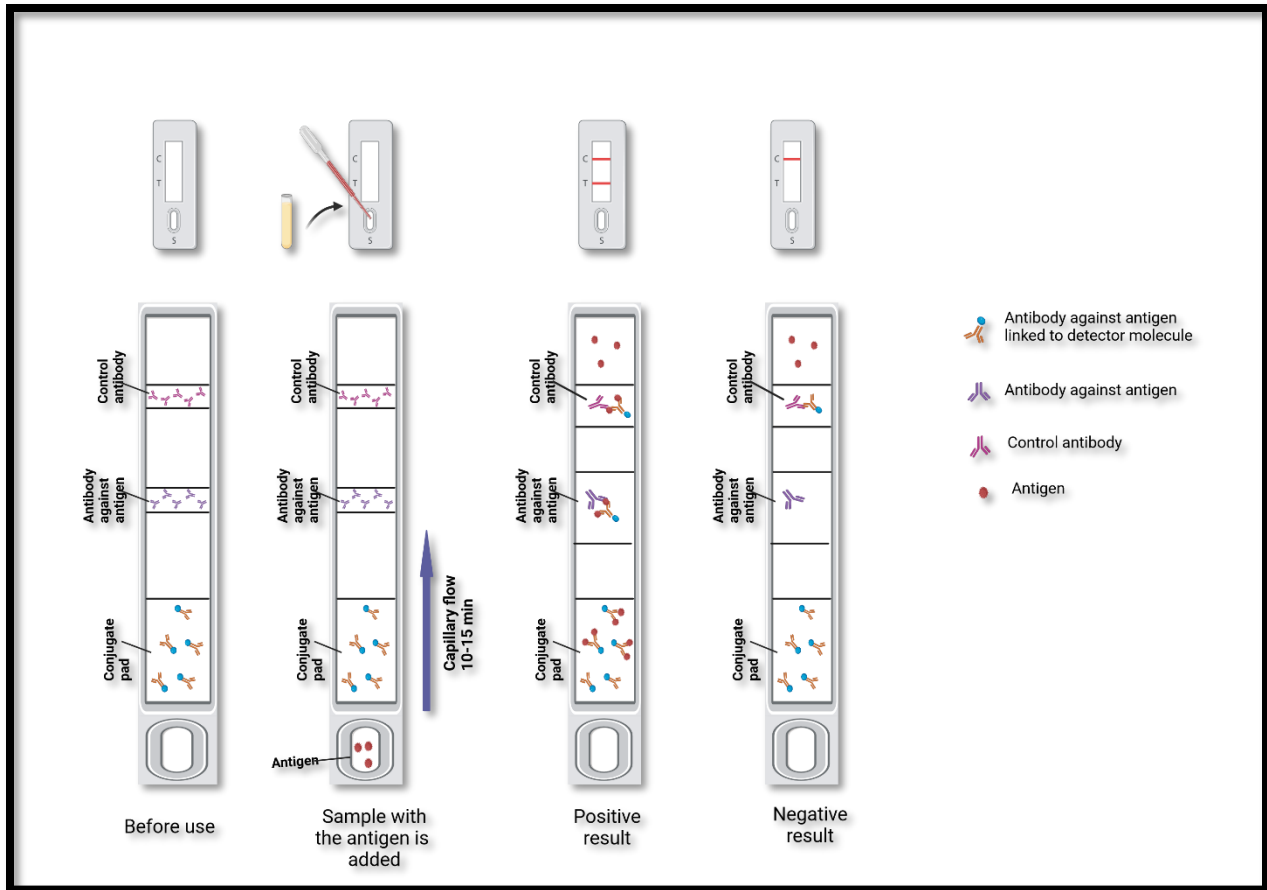


Figure 4. Rapid antigen tests test performance, created with BioRender.com

1.7.2. Enzyme-linked immunosorbent assay (ELISA) for antigen detection

1.7.2.1. Sandwich ELISA

In the sandwich ELISA (**Figure 6**) format, wells are coated with a capture antibody, the sample with the antigen is added next. After washing and incubation, a conjugated secondary antibody with an enzyme is added which will bind to the antibody-antigen complexes. Then, a substrate is added, which will react with the enzyme and reveal a colorimetric reaction. Finally,

the optical density is measured. The results are presented similarly to those for the indirect ELISA (Aydin, 2015).

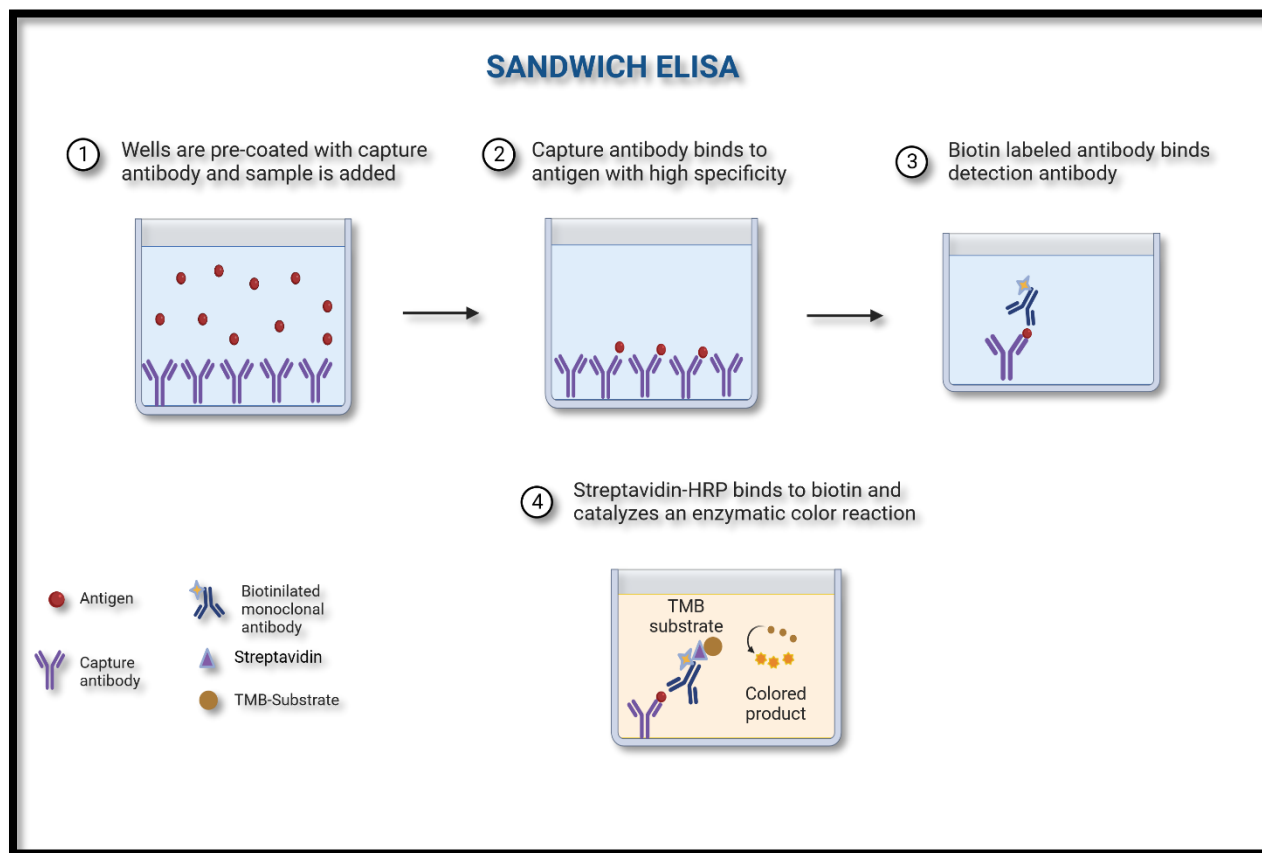


Figure 5. Sandwich ELISA basic principle and performance, created with BioRender.com

1.7.2.2. Nucleic acid amplification test: Polymerase Chain Reaction (PCR)

Polymerase chain reaction is the exponential amplification of target sequences from a DNA or RNA template using specific primers. This technique was developed for the first time in 1990 by Kary Mullis with the discovery of a polymerase from *Thermus aquaticus* and the development of the thermocyclers, which have made possible the routine usage of PCR possible in several

applications, including diagnosis of infectious diseases. PCR can be performed on a variety of samples such as blood, saliva, feces, tissue, and microorganisms, and is a very sensitive assay. The components of the PCR are the DNA template, primers, Taq polymerase and nucleotide bases (dNTPs). The template is the DNA region of interest to be amplified, from which genetic material has been extracted from a sample. The PCR could be performed in 0.2ml individual tubes, 8-tube strips or in 96-well plates and the tube caps are not transparent. For RNA viruses, it is necessary to transcribe the RNA into cDNA using reverse transcriptase. The primers or oligonucleotides are short sequences (around 20 bp) complementary to the target region including forward and reverse primers. These serve as a guide for the Taq polymerase to build the new complementary strand. Free nucleotide bases (dNTPs) include the four nitrogen bases (Adenine, Cytosine, Guanine, Thymine) and are the building blocks of the complementary strand. The Taq polymerase is an enzyme that performs the amplification of the fragment and is characterized by its resistance to heating and cooling cycles. These components are mixed in a master mix, and the template is added to the reaction. After that, these reactions are run in a thermocycler.

1.7.2.2.1. Standard or conventional PCR

The principle of standard or conventional PCR involves three main steps: denaturation, annealing and extension or elongation, which are performed by commercially available PCR thermocyclers. During denaturation, the two complementary DNA strands are separated by heating at 95°C, leading to the disruption of the hydrogen bonds. Annealing occurs in a range of 50°C to 65°C, during which the primers bind to the complementary bases of the template. Finally, the Taq polymerase begins the extension of the complementary strand by adding dNTPs in a range of temperature from 75°C to 80°C. The new DNA serves as a template for amplification in each of 30 to 40 iterative cycles, leading the DNA molecules to exponentially increase the number of

copies resulting in millions of amplified DNA fragments. The PCR products are separated by size by agarose gel electrophoresis and visualized with an intercalator agent such as ethidium bromide or Sybr Safe which is added to the buffer and/or gel.(Garibyan & Avashia, 2013); (Ghannam & Varacallo, 2022); (Kralik & Ricchi, 2017a).

1.7.2.2.2. Real Time PCR

Given that conventional PCR cannot quantify the end-product DNA, the PCR technique was refined to enable real-time detection, quantification and monitoring with several advantages, including a higher sensitivity and precision, faster analysis and no need of post-PCR processes (electrophoresis). Real-time PCR uses fluorescent reporters for detection, which are classified in two main types based on the fluorescent agent and the range of specificity: SYBR Green and Taqman probe (Artika et al., 2022); (Valones et al., 2009); (Kralik & Ricchi, 2017b). The thermocycler used for this assay is capable of detecting fluorescence of the amplification of target sequences, being more expensive than conventional thermocyclers. Another important aspect is the type of tubes used since their caps are transparent and flat. Therefore, it could be performed in a 96-well plate sealed with an optically transparent film, leading to fluorescence detection. The threshold in real-time PCR corresponds to the proportion of the signal that presented a substantial quantitative change in reference to the initial baseline signal. The threshold is set automatically by the thermocycler normally at 10 times the standard deviation of the baseline fluorescent value. Moreover, the **C_q value** refers to the cycle number at which the fluorescence signal crosses the threshold. This fluorescence signal increases proportionally to the exponential growth of the amplified DNA products, thus reflects the initial number of genomes in the sample (the smaller the C_q, the higher the amount of starting material in the reaction).

1.7.2.2.1. SYBR Green

The earliness of the fluorescent signal is proportional to the quantity of template in real time PCR. SYBR Green intercalates with double-stranded DNA molecules and can bind to specific and non-specific products. Thus, a melting curve is needed to control the binding to primer dimers. Its fluorescence depends on the amount of double stranded DNA present in the reaction and can be used with several primers. The advantages are the low cost and the sensitivity; however, one disadvantage is that specificity decreases due to the binding to non-specific products or primer dimers and the limited ability to perform multiplexed detection of more than one target in a reaction (Figure 6). (Artika et al., 2022); (Valones et al., 2009).

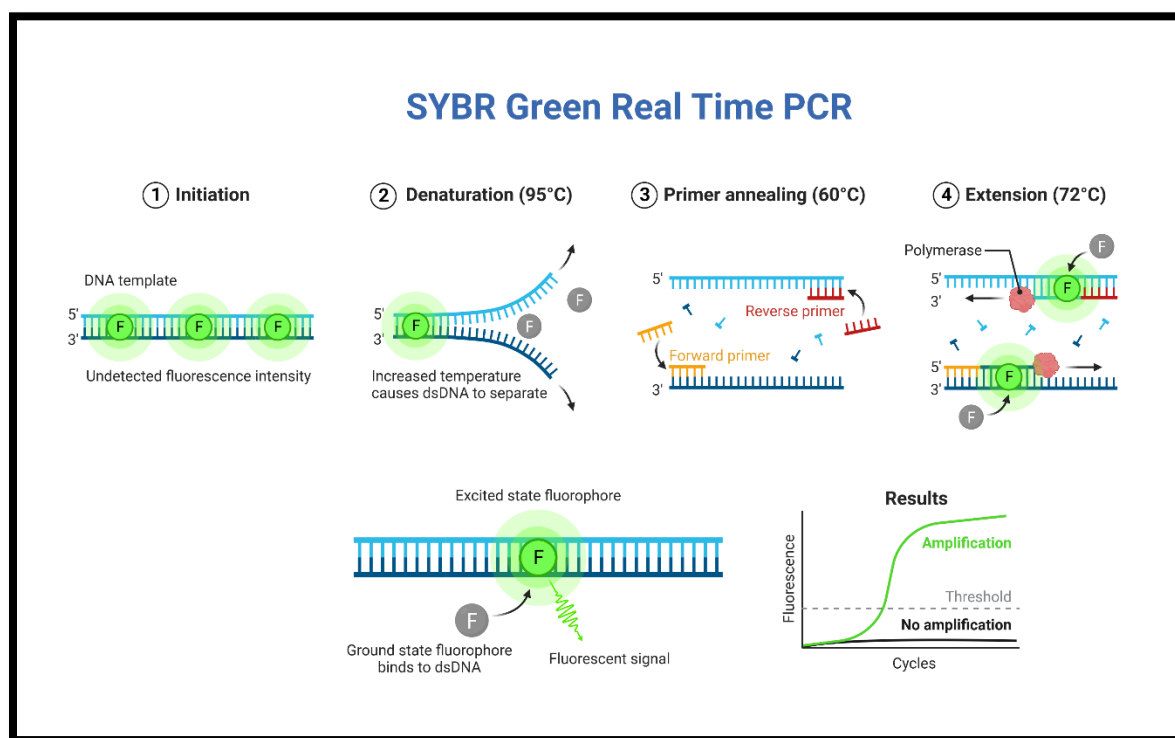


Figure 6. Syber Green Real time PCR performance, created with BioRender.com

1.7.2.2.2. Hydrolysis probe

The Taqman probe is designed to bind a specific sequence within the PCR target in the template. It has a reporter fluorophore at the 5' end and a quencher at the 3' end. When the probe binds to its site within the target, the 5'→3' nuclease activity of the Taq polymerase cleaves the probe in its 5' terminal end, releasing one of the components of the fluorescent reaction from the quencher and leading to the release of the energy as fluorescence. The Taqman probe is useful in designing multiplex PCR assays for detection of different targets in one reaction, which is useful for pathogen diagnosis given its high sensitivity and specificity. These assays can be qualitative and quantitative (**Figure 7**). (Artika et al., 2022); (Valones et al., 2009). The wavelengths for different fluorophores are shown in **Figure 8**.

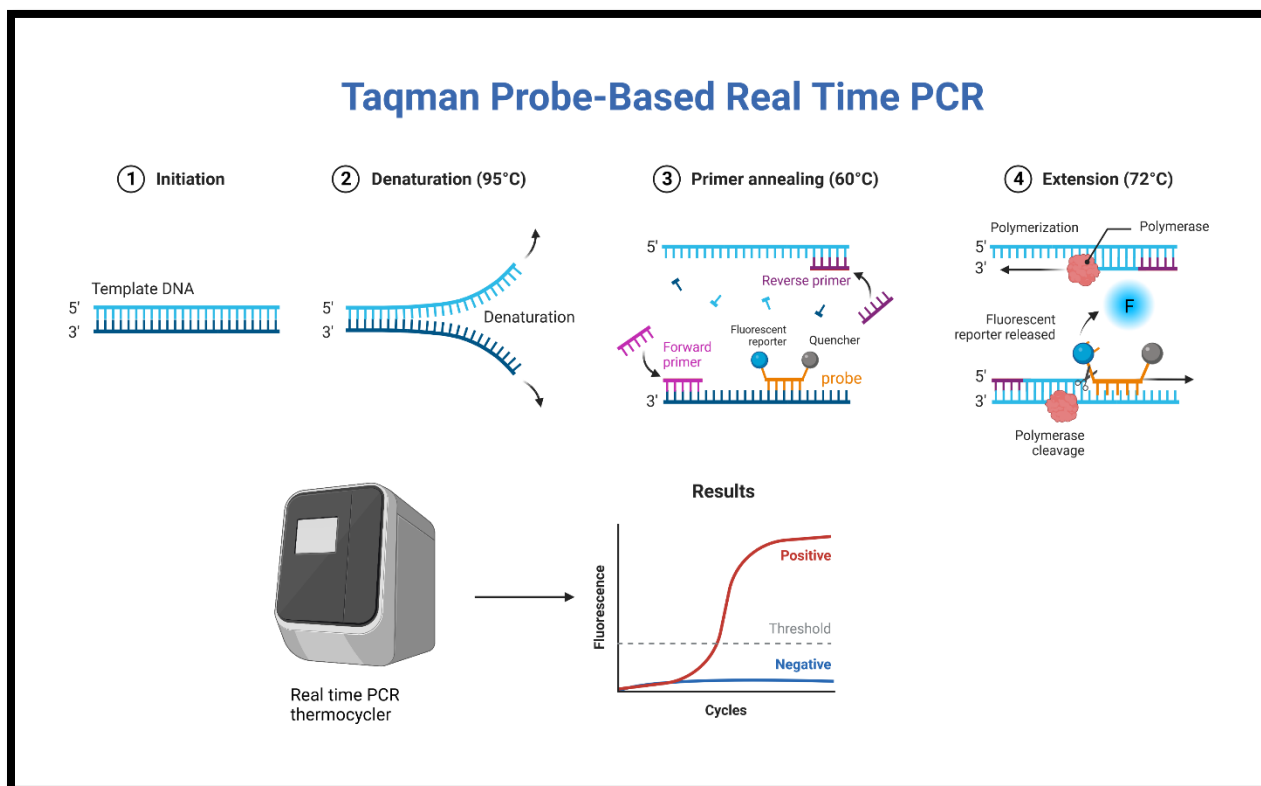


Figure 7. Taqman probe Real time PCR performance, created with BioRender.com

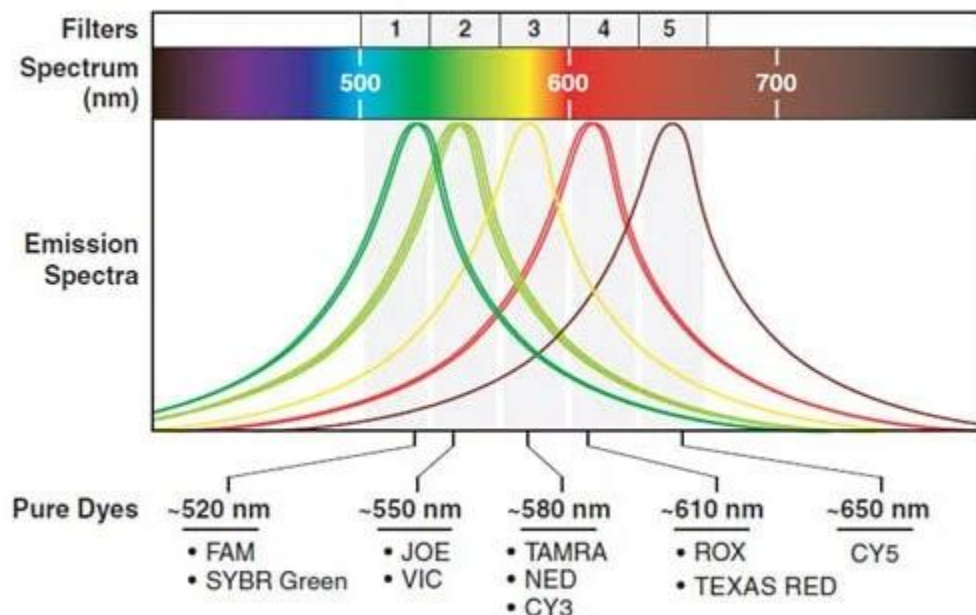


Figure 8. Real time PCR fluorophore wavelengths, emission spectra, ([Real-Time PCR » Clinical Laboratory Science \(clinicalsci.info\)](#))

1.7.2.3. Standard curve and Limit of detection (LOD)

A relative standard curve is used to quantify an unknown sample. To produce this curve, 10-fold serial dilutions of a standard DNA or RNA are prepared to get at least five data points. An example of a standard is gblock constructed with several targets that will be tested in the PCR. An interpolation from the standard curve is performed to estimate the target quantity. This standard curve is prepared and run in each plate. The reliability of the standard curve for quantification is determined by the spacing between the dilutions. The log of concentration (X axis) vs cq values (Y axis) are plotted and a linear regression value (R^2) is calculated. This value should be mostly close to 1 to be considered as ideal and get the model regression equation. The concentration of the target in the unknown samples could be calculated with the cq value of the sample by replacing

it in the equation (Kralik & Ricchi, 2017c). Moreover, the LOD value is also important to consider, since it is the minimum concentration of nucleic acid that will give a positive result in almost 95% of the positive tested samples. (Kralik & Ricchi, 2017c).

1.7.2.4. Retrotranscription PCR (rtPCR)

For pathogens whose genome is RNA, an additional stage is performed prior to amplification in which RNA is the template to generate cDNA by a reverse transcriptase enzyme at a temperature range 50°C to 55°C. The cDNA then serves as a template for PCR amplification. This reaction could be performed in one or two steps. The one-step PCR includes reverse transcription and PCR amplification in the same tube, whereas the two-step reaction means that the cDNA is first synthesized and then it is transferred to another tube for PCR amplification (Jalali et al., 2017).

Real time and conventional PCR/RT-PCR are widely used for the diagnosis and confirmation of the etiology of disease of several tropical infections leading to the identification of the pathogen.

1.7.2.5. Other multiplex Real time-PCR assays

Multiplex detection assays have been designed for testing simultaneous pathogens in a single reaction (**Figure 9**). For example, several multiplex real time RT-PCR assays for arbovirus identification have been designed, as these often co-circulate in endemic regions are available commercially or as in-house kits. An example is the CDC Triplex qRT-PCR for Dengue, Zika and Chikungunya viruses. The performance of this kit was evaluated during a dengue outbreak in Brazil using 713 serum samples, of which 99.86% had DENV and 0.14% had ZIKV. The test had a 95% sensitivity and 100% specificity (Colombo et al., 2019). In 2016, Waggoner et al. developed a similar multiplex assay, and its performance was compared with a pan-dengue-Chikungunya RT-PCR using 216 serum samples from Nicaragua in which 25 samples tested positive for DENV,

110 tested positive for CHIKV, 38 for coinfection and 43 samples tested negative for DENV, CHIKV and ZIKV (Waggoner et al., 2016). This assay is the one I have mostly used in this project.

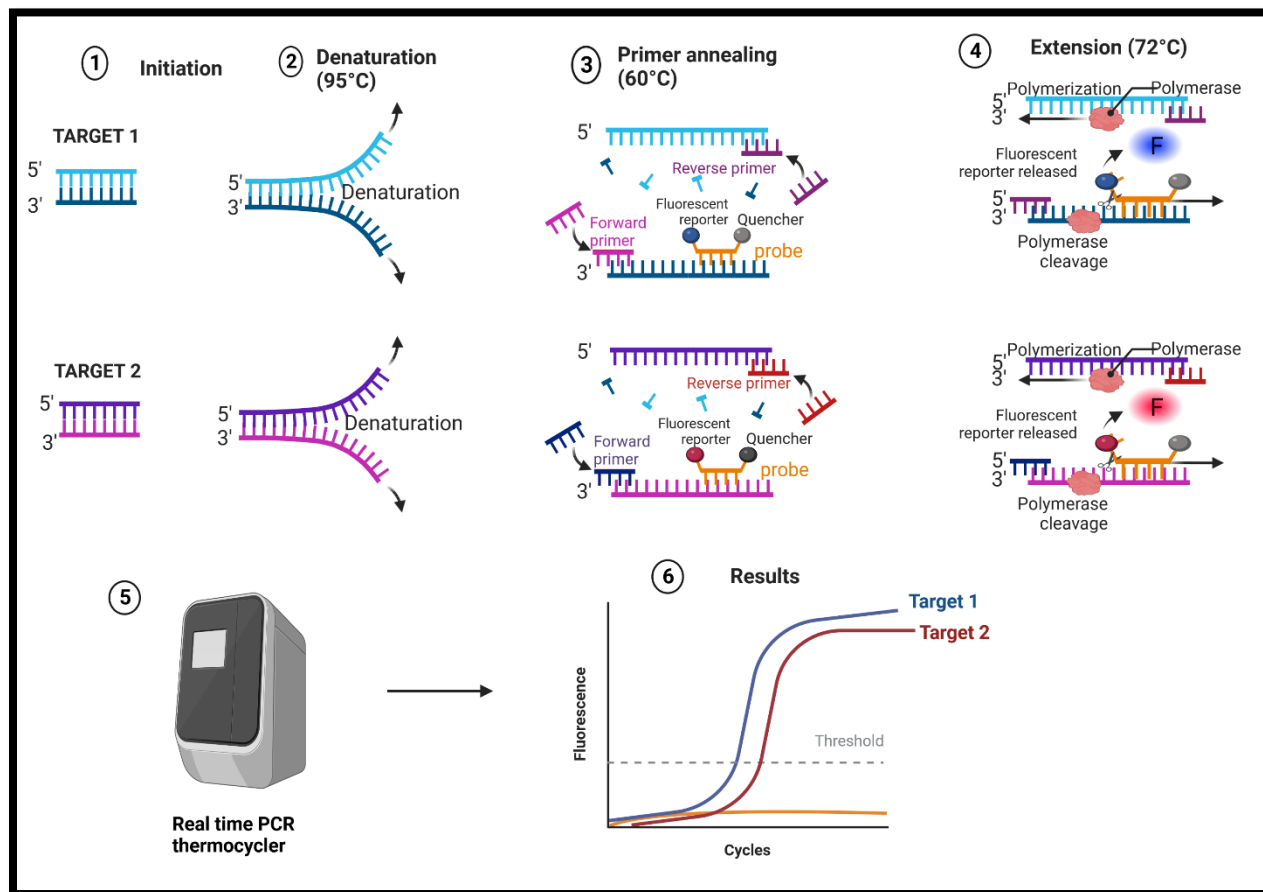


Figure 9. Multiplex real time PCR, created with BioRender.com

1.8. Luminex assay

The Luminex assay is a magnetic microparticle-based immunoassay which is centered on similar principles as ELISAs. This assay allows detection of up to one hundred biomarkers at once including antibodies, antigens, cytokines and other molecules in a multiplexed format, using less sample volume than ELISA. Microspheres or beads are dyed with different proportions of red and

infrared fluorophores which correspond to a distinct spectral signature. Detection and quantification of multiple cytokines and other biomarkers in the sample is important for obtaining information about biological processes and diseases (Weiss et al., 2020).

Beads are precoated with antibodies that are specific to an analyte, coupled to a unique region of the bead. The antibodies will be bound to the analyte of interest. These are incubated with the sample, followed by a wash of unbound materials. Then samples are incubated with biotinylated detection antibodies, which form an antibody-antigen sandwich. Subsequently, an incubation with streptavidin-phycoerythrin reporter is performed. The Luminex instrument such as Luminex 100, Luminex 200 and other instruments, has two types of lasers, the first one is going to classify the beads and determine the analyte that has been detected and the second one is going to determine the magnitude of the phycoerythrin reporter signal which is directly proportional to the analyte that has bound (Weiss et al., 2020).

Multiple reads are performed at each bead region leading to robust detection. This is in case polystyrene beads are used. In contrast, for magnetic beads, the Luminex MAGPIX analyzer is used. The main difference is that the instrument has a magnet which captures and holds the magnetic beads in a monolayer, while two distinct light LEDs are used to illuminate the beads. One LED is used for bead identification with a wavelength of 621nm and the second LED with a wavelength of 511nm is going to determine the magnitude of the phycoerythrin reporter signal. The CDC is one of the pioneers in using this assay for the simultaneous detection of IgM for West Nile and St. Louis viruses (**Figure 10**). The antigens to be detected are incorporated in these microspheres at a specific concentration. For IgM detection, IgG should be removed to avoid interference, while this is unnecessary for IgG detection. This presents an advantage over ELISA

since multiple antigens can be detected simultaneously in the same assay conditions (Basile et al., 2013).

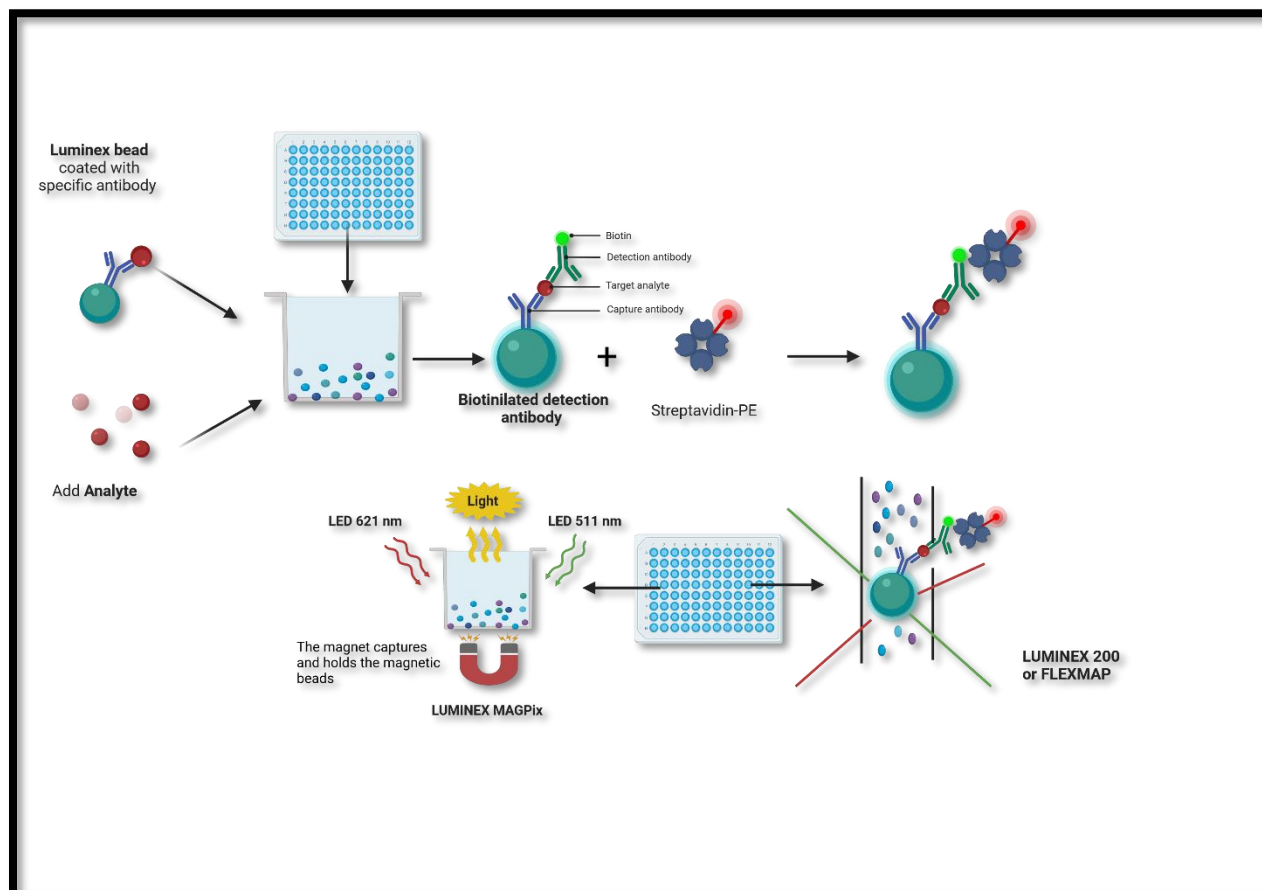


Figure 10. LUMINEX assay principle and performance with magnetic beads, created with BioRender.com

Luminex XMAP technology (Figure xx) was developed for the analysis of multiple analytes in the same sample, showing high sensitivity and specificity (**Figure 11**). The technology uses different sets of microspheres which at some point, during the analysis, are attracted by a magnet. These sets are internally conjugated to two different fluorophores with distinct spectra. This spectral address is unique for each one of the sets and is determined by different

concentrations of the dye. The surface of the sets allows to integrate several reagents which are specific to nucleic acid approaches. A fluorescent reporter as Alexa 532 or Cy3 is integrated to the target analyte leading to its detection. MagPlex-TAG microspheres are integrated with 24 bp anti-TAG oligonucleotides that will lead to the binding of the target sequences that contain a complementary sequence to TAG. This complementary sequence is added into the primer sequence resulting in the binding to the anti-TAG sequence in the microsphere (Reslova et al., 2017).

This technology has different applications including SNP genotyping, genetic disease screening, gene expression profiling, HLA DNA typing (for transplantation) and microbial detection. For bacterial pathogen detection in foodborne illnesses, in which universal PCR primers were designed to target 23S rDNA leading to differentiation among *E.coli*, *Salmonella*, *Listeria monocytogenes* and *Campylobacter jejuni*. Another example is for genotyping of *Mycobacterium tuberculosis* isolates in which the assay is based on the polymorphisms that correspond to the Direct Repeat locus. Biotinylated PCR primers were used to amplify and label the spacers. These amplicons were then detected by hybridization in a mixture of 43 bead sets which have specific probes to capture the spacer sequences (Dunbar, 2006). Discrimination of different sequence targets is carried out with the use of detection probes. This step is necessary before the amplification step. One of the major challenges is to design probes that work at similar melting temperatures, usually between 51 and 56°C. (Reslova et al., 2017).

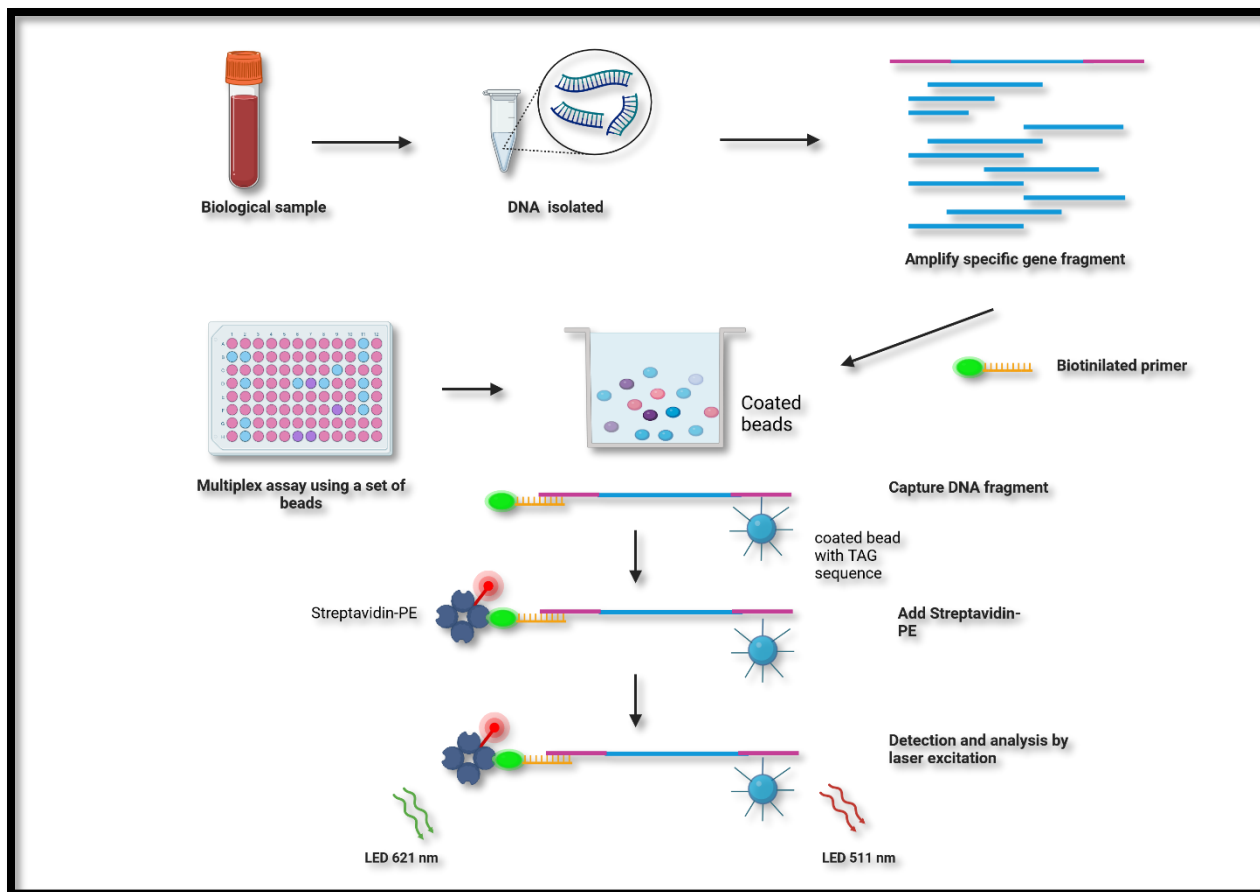


Figure 11. LUMINEX assay for nucleic acid detection, created with BioRender.com

Luminex assay has several advantages over ELISA and microarray. The first advantage is that it enables detecting up to 100 analytes in a single well, since each bead is a single test. Moreover, the 3D structure of the beads allows a faster kinetic reaction and shorter times for the assay. In Luminex, there is flexibility to attach specific probes to unique colored beads leading for its use in screening. Another advantage is that it requires small amount of sample (50 μ l) per well and produces highly accurate results. However, it also presents disadvantages as variability due to the assay manufacturer, lot number and the laboratory where it is performed. In the case of cytokine assays, human autoantibodies may alter the measurement of cytokines since these could generate nonspecific binding (Khalifian et al., 2015)

1.9. Genomic analysis - Oxford nanopore technology (ONT) for sequencing

Nanopore sequencing is a third-generation sequencing technology that directly detects the nucleotides of the DNA by passing through a protein nanopore. The first device released was MINION which is a portable sequencer and can be connected to a laptop or a computer with a USB port. This technology uses a flow cell that contains a total of 2048 nanopores with 512 channels, which are controlled by a specific integrated circuit (ASIC). Before sequencing, adapters are ligated to both ends of DNA or cDNAs fragments and subsequently the DNA strand is captured and loaded into the nanopore by using a motor enzyme which unzips DNA long strands. After that, the sensor detects the ionic current signals which are used to determine the specific base and these signals are translated into a DNA sequence (Lin et al., 2021). The main characteristic of this technology is that it is capable of generating long reads with a maximum length up to a hundred thousand base pairs and data is produced in real time. The number of reads produced varies from channel to channel depending on the number of activated pores. The software used for sequencing is MINKOW which performs functions as data acquisition and sample identification. Nanopore sequencing has been affordable for genome sequencing in middle- and low-income countries due to its low cost compared to other sequencing technologies, moreover it is not complicated to use, and the results could be obtained in hours. Another advantage is that it is useful for epidemiological surveillance for monitoring outbreaks (Wasswa et al., 2022). However a disadvantage of this technology is the higher error rate (14%) for DNA and cDNA sequencing compared to Illumina sequencing (Sahlin & Medvedev, 2021).

1.10. Metagenomic detection

Current diagnostic tests including RDTs, ELISAs, cell culture, and PCRs, are classified as traditional techniques designed to detect a specific target, requiring a prior knowledge of the

suspected pathogen (Bibby, 2013). These tests could fail in the detection due to mutations in the pathogen genome (presence of genetic variants of the pathogen), low specificity of the tests, etc. Many times, and especially in tropical regions with high diversity, scientists are confronted with unexpected pathogen, an unknown etiology and even a novel pathogen for which there are no diagnostic strategies. Metagenomic analysis provides a promising tool, as it is the process of sequencing nucleic acids as DNA or cDNA from a broad range of microorganisms present in different samples (blood, saliva, tissue, feces, respiratory swabs, bronchoalveolar lavage fluid) without prior knowledge of their identity, with the capacity to detect a broad spectrum of pathogens including bacteria, virus, protozoa. Several considerations should be taken into account for a metagenomic analysis: Sample quality and the timing of sample collection (Liu et al., 2022). The timing is critical since the pathogen could be present only in the first five days of the acute phase of the disease; the reads obtained from the sequencers are compared to pathogen databases (Kaju, Kraken, Bug Seq). The availability of rapid and affordable untargeted detection of emerging or unexpected pathogens low-cost metagenomic analysis may be of a great value.

In our hands, a Metagenomic approach has been performed in samples from febrile patients (negative to many targeted diagnostic tests) and allowed us to detect 1% reads (5,016 of 464,444) specific to OROV (Wise et al., 2018). In another study, using Nanopore sequencing, samples (negative to DENV, ZIKV, CHIKV, MAYV, OROV and *Leptospira*), showed the presence of *Plasmodium*, which was confirmed using nested PCR (Márquez et al., 2022b). Conteville et al. (2018) performed a metagenomic analysis on five serum samples that tested negative for dengue and yellow fever, using Illumina HiSeq 2500 platform system, detecting Hepatitis A virus (Conteville et al., 2018).

A modified metagenomic protocol for serum samples from febrile individuals has been described, this protocol uses a SMART-9N approach for Nanopore sequencing and demonstrated increases in sensitivity, depth and coverage (Claro et al., 2021). The SMART-9N approach was first described by Zu et al. (2001), and was modified to be used with random primers for cDNA synthesis (Zhu et al., 2001), in contrast with Wise et al, 2018 protocol, the advantages of SMART are the following: it uses a shorter list of reagents, it reduces hands-on laboratory work, the random primers sequences are largely different and reduce the cost per reaction (Claro et al., 2021). DNA metagenomic analysis is similar to the protocol for RNA, the difference is that cDNA preparation is not performed (**Figure 12**).

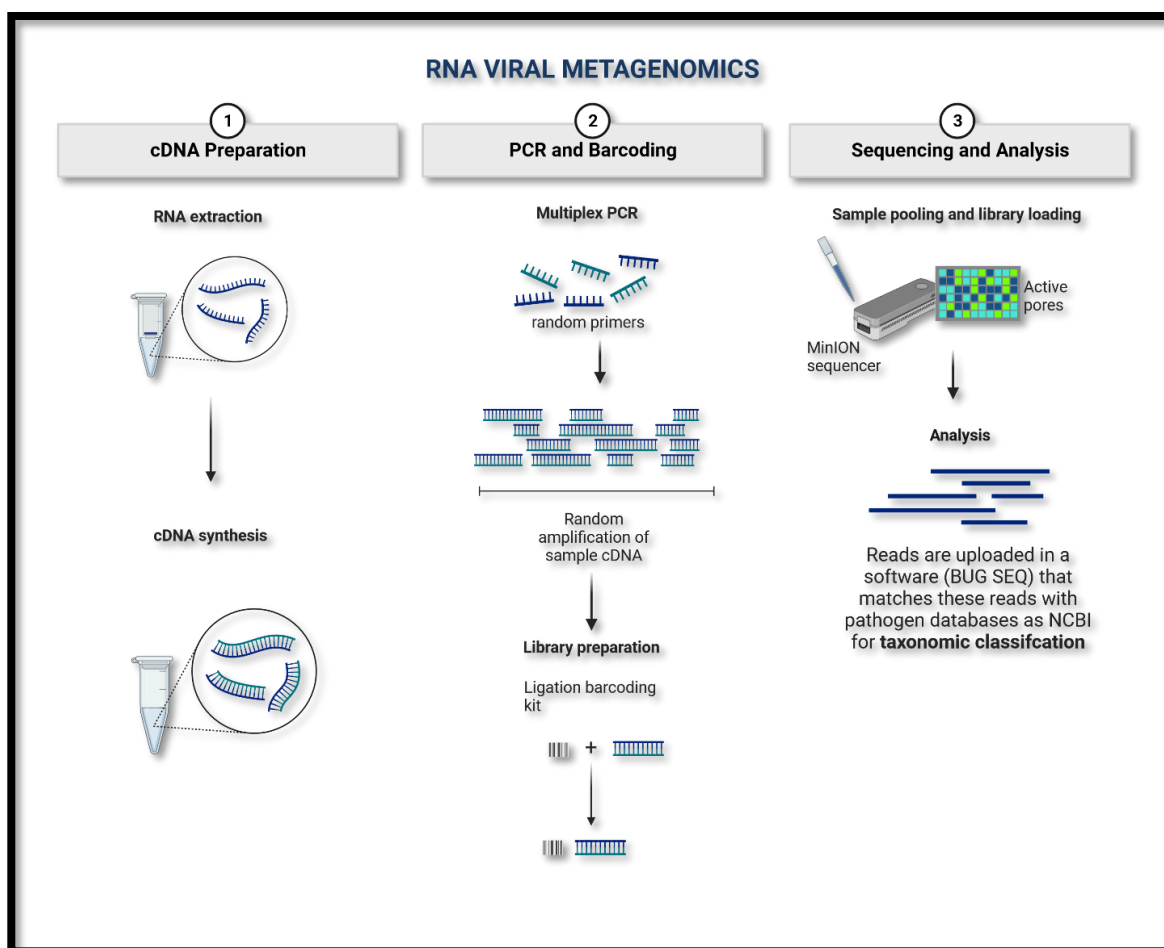


Figure 12. RNA viral metagenomics protocol, created with BioRender.com

REFERENCES

- Acosta-Ampudia, Y., Monsalve, D. M., Rodríguez, Y., Pacheco, Y., Anaya, J.-M., & Ramírez-Santana, C. (2018). Mayaro: An emerging viral threat? *Emerging Microbes & Infections*, 7(1), 1–11. <https://doi.org/10.1038/s41426-018-0163-5>
- Adhikari, B., Phommason, K., Pongvongsa, T., Koummarasy, P., Soundala, X., Henriques, G., Sirithiranont, P., Parker, D. M., Von Seidlein, L., White, N. J., Day, N. P. J., Dondorp, A. M., Newton, P. N., Cheah, P. Y., Pell, C., & Mayxay, M. (2019). Treatment-seeking behaviour for febrile illnesses and its implications for malaria control and elimination in Savannakhet Province, Lao PDR (Laos): A mixed method study. *BMC Health Services Research*, 19(1), 252. <https://doi.org/10.1186/s12913-019-4070-9>
- Agweibab, F. (2023). Why infectious diseases persist: A Rapid review of the social determinants of Malaria, Cholera, Tuberculosis and Yellow Fever in Sub-Saharan Africa. *Journal of the Cameroon Academy of Sciences*, 19(1), Article 1. <https://doi.org/10.4314/jcas.v19i1.2>
- Ahmed, A. A., Goris, M. G. A., & Meijer, M. C. (2020). Development of lipL32 real-time PCR combined with an internal and extraction control for pathogenic *Leptospira* detection. *PloS One*, 15(11), e0241584. <https://doi.org/10.1371/journal.pone.0241584>
- Alhadj, M., & Farhana, A. (2023). Enzyme Linked Immunosorbent Assay. In *StatPearls [Internet]*. StatPearls Publishing. <https://www.ncbi.nlm.nih.gov/books/NBK555922/>
- Amano, Y., Rumbea, J., Knobloch, J., Olson, J., & Kron, M. (1997). Bartonellosis in Ecuador: Serosurvey and Current Status of Cutaneous Verrucous Disease. *The American Journal of*

- Tropical Medicine and Hygiene*, 57(2), 174–179.
<https://doi.org/10.4269/ajtmh.1997.57.174>
- Anon. (2012). *FIND acute febrile syndrome strategy* (p. 40pp).
- Arregui, G., Enriquez, S., Benítez-Ortiz, W., & Navarro, J.-C. (2015). Taxonomía molecular de Anopheles del Ecuador mediante ADN mitocondrial (Citocromo c Oxidasa I) y optimización por Parsimonia Máxima. *Boletín de Malariología y Salud Ambiental*, 55(2), 132–154.
- Arroyave-Ospina, J. C., Caicedo, M. F., Navas, M. C., & Cortés-Mancera, F. M. (2018). [Human Pegivirus: Pathogenic potential and non-Hodgkin lymphoma development risk]. *Revista chilena de infectología : organo oficial de la Sociedad Chilena de Infectología*, 35(2), 164–175. <https://doi.org/10.4067/s0716-10182018000200164>
- Artika, I. M., Dewi, Y. P., Nainggolan, I. M., Siregar, J. E., & Antonjaya, U. (2022). Real-Time Polymerase Chain Reaction: Current Techniques, Applications, and Role in COVID-19 Diagnosis. *Genes*, 13(12), Article 12. <https://doi.org/10.3390/genes13122387>
- Aydin, S. (2015). A short history, principles, and types of ELISA, and our laboratory experience with peptide/protein analyses using ELISA. *Peptides*, 72, 4–15.
<https://doi.org/10.1016/j.peptides.2015.04.012>
- Azar, S. R., & Weaver, S. C. (2019). Vector Competence: What Has Zika Virus Taught Us? *Viruses*, 11(9), Article 9. <https://doi.org/10.3390/v11090867>
- Bai, F., Thompson, E. A., Vig, P. J. S., & Leis, A. A. (2019). Current Understanding of West Nile Virus Clinical Manifestations, Immune Responses, Neuroinvasion, and Immunotherapeutic Implications. *Pathogens*, 8(4), 193.
<https://doi.org/10.3390/pathogens8040193>

- Baker, R. E., Mahmud, A. S., Miller, I. F., Rajeev, M., Rasambainarivo, F., Rice, B. L., Takahashi, S., Tatem, A. J., Wagner, C. E., Wang, L.-F., Wesolowski, A., & Metcalf, C. J. E. (2022). Infectious disease in an era of global change. *Nature Reviews Microbiology*, *20*(4), Article 4. <https://doi.org/10.1038/s41579-021-00639-z>
- Balmaseda, A., Stettler, K., Medialdea-Carrera, R., Collado, D., Jin, X., Zambrana, J. V., Jaconi, S., Cameroni, E., Saborio, S., Rovida, F., Percivalle, E., Ijaz, S., Dicks, S., Ushiro-Lumb, I., Barzon, L., Siqueira, P., Brown, D. W. G., Baldanti, F., Tedder, R., ... Corti, D. (2017). Antibody-based assay discriminates Zika virus infection from other flaviviruses. *Proceedings of the National Academy of Sciences of the United States of America*, *114*(31), 8384–8389. <https://doi.org/10.1073/pnas.1704984114>
- Bartholomeeusen, K., Daniel, M., LaBeaud, D. A., Gasque, P., Peeling, R. W., Stephenson, K. E., Ng, L. F. P., & Ariën, K. K. (2023). Chikungunya fever. *Nature Reviews Disease Primers*, *9*(1), Article 1. <https://doi.org/10.1038/s41572-023-00429-2>
- Bashor, L., Gagne, R. B., Bosco-Lauth, A. M., Bowen, R. A., Stenglein, M., & VandeWoude, S. (2021). SARS-CoV-2 evolution in animals suggests mechanisms for rapid variant selection. *Proceedings of the National Academy of Sciences*, *118*(44), e2105253118. <https://doi.org/10.1073/pnas.2105253118>
- Basile, A. J., Horiuchi, K., Panella, A. J., Laven, J., Kosoy, O., Lanciotti, R. S., Venkateswaran, N., & Biggerstaff, B. J. (2013). Multiplex Microsphere Immunoassays for the Detection of IgM and IgG to Arboviral Diseases. *PLOS ONE*, *8*(9), e75670. <https://doi.org/10.1371/journal.pone.0075670>
- Bibby, K. (2013). Metagenomic identification of viral pathogens. *Trends in Biotechnology*, *31*(5), 275–279. <https://doi.org/10.1016/j.tibtech.2013.01.016>

- Bolaños, P., Chacón, M., Bolaños, P., & Chacón, M. (2019). Respecto a un caso de rickettsia rickettsii en Costa Rica. *Medicina Legal de Costa Rica*, 36(1), 14–20.
- Browne, E. S., Pereira, M., Barreto, A., Zeppelini, C. G., Oliveira, D. D., & Costa, F. (2023). Prevalence of human leptospirosis in the Americas: A systematic review and meta-analysis. *Revista Panamericana de Salud Pública*, 47, 1. <https://doi.org/10.26633/RPSP.2023.126>
- Calvopiña, M., Romero-Alvarez, D., Vasconez, E., Valverde-Muñoz, G., Trueba, G., Garcia-Bereguian, M. A., & Orlando, S. A. (2023). Leptospirosis in Ecuador: Current Status and Future Prospects. *Tropical Medicine and Infectious Disease*, 8(4), 202. <https://doi.org/10.3390/tropicalmed8040202>
- Cevallos, V., Ponce, P., Waggoner, J., Pinsky, B., Coloma, J., Quiroga, C., Morales, D., & Cardenas, M. (2017). Zika and Chikungunya Virus Detection in Naturally Infected Aedes aegypti in Ecuador. *Acta Tropica*, 177. <https://doi.org/10.1016/j.actatropica.2017.09.029>
- Chandan, S., Umesha, S., Bhure, S. K., Haraprasad, N., & Chandrashekar, S. (2011). Development of PCR assay for targeting partial *lipL21* and *lipL41* gene of *leptospira*. *Nepal Journal of Biotechnology*, 1(1), Article 1. <https://doi.org/10.3126/njb.v1i1.4170>
- Chappuis, F., Alirol, E., d'Acremont, V., Bottieau, E., & Yansouni, C. P. (2013). Rapid diagnostic tests for non-malarial febrile illness in the tropics. *Clinical Microbiology and Infection*, 19(5), 422–431. <https://doi.org/10.1111/1469-0691.12154>
- Chen, L. H., & Wilson, M. E. (2020). Yellow fever control: Current epidemiology and vaccination strategies. *Tropical Diseases, Travel Medicine and Vaccines*, 6(1), 1. <https://doi.org/10.1186/s40794-020-0101-0>

- Chinedu Eneh, S., Uwishema, O., Nazir, A., El Jurdi, E., Faith Olanrewaju, O., Abbass, Z., Mustapha Jolayemi, M., Mina, N., Kseiry, I., & Onyeaka, H. (2023). Chikungunya outbreak in Africa: A review of the literature. *Annals of Medicine and Surgery*, 85(7), 3545–3552. <https://doi.org/10.1097/MS9.0000000000000979>
- Chow, E. J., Uyeki, T. M., & Chu, H. Y. (2023). The effects of the COVID-19 pandemic on community respiratory virus activity. *Nature Reviews Microbiology*, 21(3), Article 3. <https://doi.org/10.1038/s41579-022-00807-9>
- Ciota, A. T. (2017). West Nile virus and its vectors. *Current Opinion in Insect Science*, 22, 28–36. <https://doi.org/10.1016/j.cois.2017.05.002>
- Claro, I., Ramundo, M., Coletti, T., Silva, C., Valenca, I., Candido, D., Sales, F., Manuli, E., Jesus, J., Paula, A., Felix, A., Andrade, P., Pinho, M., Souza, W., Amorim, M., Modena, J. L., Kallas, E., Levi, J., Faria, N., & Quick, J. (2021). Rapid viral metagenomics using SMART-9N amplification and nanopore sequencing. *Wellcome Open Research*, 6, 241. <https://doi.org/10.12688/wellcomeopenres.17170.1>
- Coelho, D. R., Carneiro, P. H., Mendes-Monteiro, L., Conde, J. N., Andrade, I., Cao, T., Allonso, D., White-Dibiasio, M., Kuhn, R. J., & Mohana-Borges, R. (n.d.). ApoA1 Neutralizes Proinflammatory Effects of Dengue Virus NS1 Protein and Modulates Viral Immune Evasion. *Journal of Virology*, 95(13), e01974-20. <https://doi.org/10.1128/JVI.01974-20>
- Colombo, T. E., Versiani, A. F., Dutra, K. R., Rubiato, J. G. D., Galvão, T. M., Negri Reis, A. F., & Nogueira, M. L. (2019). Performance of CDC Trioplex qPCR during a dengue outbreak in Brazil. *Journal of Clinical Virology*, 121, 104208. <https://doi.org/10.1016/j.jcv.2019.104208>

- Conteville, L. C., Filippis, A. M. B. de, Nogueira, R. M. R., Mendonça, M. C. L. de, & Vicente, A. C. P. (2018). Metagenomic analysis reveals Hepatitis A virus in suspected yellow fever cases in Brazil. *Memorias Do Instituto Oswaldo Cruz*, *113*(1), 66–67. <https://doi.org/10.1590/0074-02760170260>
- Crosby, B., & Crespo, M. E. (2023). Venezuelan Equine Encephalitis. In *StatPearls [Internet]*. StatPearls Publishing. <https://www.ncbi.nlm.nih.gov/books/NBK559332/>
- da Costa, V. G., Saivish, M. V., Lino, N. A. B., Bittar, C., de Freitas Calmon, M., Nogueira, M. L., & Rahal, P. (2022). Clinical Landscape and Rate of Exposure to Ilheus Virus: Insights from Systematic Review and Meta-Analysis. *Viruses*, *15*(1), 92. <https://doi.org/10.3390/v15010092>
- da Costa, V. G., Saivish, M. V., Lino, N. A. B., Bittar, C., de Freitas Calmon, M., Nogueira, M. L., & Rahal, P. (2023). Clinical Landscape and Rate of Exposure to Ilheus Virus: Insights from Systematic Review and Meta-Analysis. *Viruses*, *15*(1), Article 1. <https://doi.org/10.3390/v15010092>
- Das, P., Rahman, M. Z., Banu, S., Rahman, M., Chisti, M. J., Chowdhury, F., Akhtar, Z., Palit, A., Martin, D. W., Anwar, M. U., Namwase, A. S., Angra, P., Kato, C. Y., Ramos, C. J., Singleton, J., Stewart-Juba, J., Patel, N., Condit, M., Chung, I. H., ... Cohen, A. L. (2022). Acute febrile illness among outpatients seeking health care in Bangladeshi hospitals prior to the COVID-19 pandemic. *PLoS ONE*, *17*(9), e0273902. <https://doi.org/10.1371/journal.pone.0273902>
- Di Nardo, F., Chiarello, M., Cavalera, S., Baggiani, C., & Anfossi, L. (2021). Ten Years of Lateral Flow Immunoassay Technique Applications: Trends, Challenges and Future Perspectives. *Sensors*, *21*(15), Article 15. <https://doi.org/10.3390/s21155185>

- Dunbar, S. A. (2006). Applications of Luminex® xMAP™ technology for rapid, high-throughput multiplexed nucleic acid detection. *Clinica Chimica Acta; International Journal of Clinical Chemistry*, 363(1), 71–82. <https://doi.org/10.1016/j.cccn.2005.06.023>
- Durango-Chavez, H. V., Toro-Huamanchumo, C. J., Silva-Caso, W., Martins-Luna, J., Aguilar-Luis, M. A., Valle-Mendoza, J. del, & Puyen, Z. M. (2022). Oropouche virus infection in patients with acute febrile syndrome: Is a predictive model based solely on signs and symptoms useful? *PLOS ONE*, 17(7), e0270294. <https://doi.org/10.1371/journal.pone.0270294>
- Elsworth, B., & Duraisingh, M. T. (2021). A framework for signaling throughout the life cycle of *Babesia* species. *Molecular Microbiology*, 115(5), 882–890. <https://doi.org/10.1111/mmi.14650>
- Files, M. A., Hansen, C. A., Herrera, V. C., Schindewolf, C., Barrett, A. D. T., Beasley, D. W. C., Bourne, N., & Milligan, G. N. (2022). Baseline mapping of Oropouche virology, epidemiology, therapeutics, and vaccine research and development. *Npj Vaccines*, 7(1), Article 1. <https://doi.org/10.1038/s41541-022-00456-2>
- Findlater, A., & Bogoch, I. I. (2018). Human Mobility and the Global Spread of Infectious Diseases: A Focus on Air Travel. *Trends in Parasitology*, 34(9), 772–783. <https://doi.org/10.1016/j.pt.2018.07.004>
- Gaceta epidemiologica. (2018). *Enfermedades transmitidas por vectores Zika*. <https://www.salud.gob.ec/wp-content/uploads/2015/12/GACETA-ZIKA-SE14-2018.pdf>
- Ganjan, N., & Riviere-Cinamond, A. (2020). Mayaro virus in Latin America and the Caribbean. *Revista Panamericana de Salud Pública*, 44, 1. <https://doi.org/10.26633/RPSP.2020.14>

- Garcia-Quintanilla, M., Dichter, A. A., Guerra, H., & Kempf, V. A. J. (2019). Carrion's disease: More than a neglected disease. *Parasites & Vectors*, *12*(1), 141. <https://doi.org/10.1186/s13071-019-3390-2>
- Garibyan, L., & Avashia, N. (2013). Research Techniques Made Simple: Polymerase Chain Reaction (PCR). *The Journal of Investigative Dermatology*, *133*(3), e6. <https://doi.org/10.1038/jid.2013.1>
- Ghannam, M. G., & Varacallo, M. (2022). Biochemistry, Polymerase Chain Reaction. In *StatPearls [Internet]*. StatPearls Publishing. <https://www.ncbi.nlm.nih.gov/books/NBK535453/>
- Gökmen, T. G., Soyak, A., Kalayci, Y., Önlü, C., & Köksal, F. (2016). COMPARISON OF 16S rRNA-PCR-RFLP, LipL32-PCR AND OmpL1-PCR METHODS IN THE DIAGNOSIS OF LEPTOSPIROSIS. *Revista Do Instituto de Medicina Tropical de São Paulo*, *58*, 64. <https://doi.org/10.1590/S1678-9946201658064>
- Gutiérrez, B., Wise, E. L., Pullan, S. T., Logue, C. H., Bowden, T. A., Escalera-Zamudio, M., Trueba, G., Nunes, M. R. T., Faria, N. R., & Pybus, O. G. (2020). Evolutionary Dynamics of Oropouche Virus in South America. *Journal of Virology*, *94*(5), 10.1128/jvi.01127-19. <https://doi.org/10.1128/jvi.01127-19>
- Gutiérrez-Vera, E., Patiño, L., Castillo-Segovia, M., Valencia, V. M., Montesdeoca-Agurto, J., Regato-Arrata, M., Gutiérrez-Vera, E., Patiño, L., Castillo-Segovia, M., Valencia, V. M., Montesdeoca-Agurto, J., & Regato-Arrata, M. (2021). Seroprevalence of arboviruses in Ecuador: Implications for improved surveillance. *Biomédica*, *41*(2), 247–259. <https://doi.org/10.7705/biomedica.5623>

- Guzman, M. G., Gubler, D. J., Izquierdo, A., Martinez, E., & Halstead, S. B. (2016). Dengue infection. *Nature Reviews Disease Primers*, 2(1), Article 1. <https://doi.org/10.1038/nrdp.2016.55>
- Guzmán-Terán, C., Calderón-Rangel, A., Rodríguez-Morales, A., & Mattar, S. (2020). Venezuelan equine encephalitis virus: The problem is not over for tropical America. *Annals of Clinical Microbiology and Antimicrobials*, 19(1), 19. <https://doi.org/10.1186/s12941-020-00360-4>
- Haake, D. A., & Levett, P. N. (2015). Leptospirosis in Humans. *Current Topics in Microbiology and Immunology*, 387, 65–97. https://doi.org/10.1007/978-3-662-45059-8_5
- Hidayat, R., & Wulandari, P. (2021). Enzyme Linked Immunosorbent Assay (ELISA) Technique Guideline. *Bioscientia Medicina : Journal of Biomedicine and Translational Research*, 5(5), Article 5. <https://doi.org/10.32539/bsm.v5i5.228>
- Holmes, E. C., Goldstein, S. A., Rasmussen, A. L., Robertson, D. L., Crits-Christoph, A., Wertheim, J. O., Anthony, S. J., Barclay, W. S., Boni, M. F., Doherty, P. C., Farrar, J., Geoghegan, J. L., Jiang, X., Leibowitz, J. L., Neil, S. J. D., Skern, T., Weiss, S. R., Worobey, M., Andersen, K. G., ... Rambaut, A. (2021). The origins of SARS-CoV-2: A critical review. *Cell*, 184(19), 4848–4856. <https://doi.org/10.1016/j.cell.2021.08.017>
- Hull, N. C., & Schumaker, B. A. (2018). Comparisons of brucellosis between human and veterinary medicine. *Infection Ecology & Epidemiology*, 8(1), 1500846. <https://doi.org/10.1080/20008686.2018.1500846>
- Jalali, M., Zaborowska, J., & Jalali, M. (2017). Chapter 1 - The Polymerase Chain Reaction: PCR, qPCR, and RT-PCR. In M. Jalali, F. Y. L. Saldanha, & M. Jalali (Eds.), *Basic Science*

- Methods for Clinical Researchers* (pp. 1–18). Academic Press.
<https://doi.org/10.1016/B978-0-12-803077-6.00001-1>
- Katzelnick, L. C., Gresh, L., Halloran, M. E., Mercado, J. C., Kuan, G., Gordon, A., Balmaseda, A., & Harris, E. (2017). Antibody-dependent enhancement of severe dengue disease in humans. *Science*, *358*(6365), 929–932. <https://doi.org/10.1126/science.aan6836>
- Katzelnick, L. C., Narvaez, C., Arguello, S., Mercado, B. L., Collado, D., Ampie, O., Elizondo, D., Miranda, T., Carrillo, F. B., Mercado, J. C., Latta, K., Schiller, A., Segovia-Chumbez, B., Ojeda, S., Sanchez, N., Plazaola, M., Coloma, J., Halloran, M. E., Premkumar, L., ... Harris, E. (2020a). Zika virus infection enhances future risk of severe dengue disease. *Science (New York, N.Y.)*, *369*(6507), 1123–1128. <https://doi.org/10.1126/science.abb6143>
- Katzelnick, L. C., Narvaez, C., Arguello, S., Mercado, B. L., Collado, D., Ampie, O., Elizondo, D., Miranda, T., Carrillo, F. B., Mercado, J. C., Latta, K., Schiller, A., Segovia-Chumbez, B., Ojeda, S., Sanchez, N., Plazaola, M., Coloma, J., Halloran, M. E., Premkumar, L., ... Harris, E. (2020b). Zika virus infection enhances future risk of severe dengue disease. *Science (New York, N.Y.)*, *369*(6507), 1123–1128. <https://doi.org/10.1126/science.abb6143>
- Khalifian, S., Raimondi, G., & Brandacher, G. (2015). The Use of Luminex Assays to Measure Cytokines. *Journal of Investigative Dermatology*, *135*(4), 1–5.
<https://doi.org/10.1038/jid.2015.36>
- Kok, B. H., Lim, H. T., Lim, C. P., Lai, N. S., Leow, C. Y., & Leow, C. H. (2023). Dengue virus infection – a review of pathogenesis, vaccines, diagnosis and therapy. *Virus Research*, *324*, 199018. <https://doi.org/10.1016/j.virusres.2022.199018>
- Kraemer, M. U. G., Golding, N., Bisanzio, D., Bhatt, S., Pigott, D. M., Ray, S. E., Brady, O. J., Brownstein, J. S., Faria, N. R., Cummings, D. A. T., Pybus, O. G., Smith, D. L., Tatem, A.

- J., Hay, S. I., & Reiner, R. C. (2019). Utilizing general human movement models to predict the spread of emerging infectious diseases in resource poor settings. *Scientific Reports*, 9(1), 5151. <https://doi.org/10.1038/s41598-019-41192-3>
- Kralik, P., & Ricchi, M. (2017a). A Basic Guide to Real Time PCR in Microbial Diagnostics: Definitions, Parameters, and Everything. *Frontiers in Microbiology*, 8. <https://www.frontiersin.org/articles/10.3389/fmicb.2017.00108>
- Kralik, P., & Ricchi, M. (2017b). A Basic Guide to Real Time PCR in Microbial Diagnostics: Definitions, Parameters, and Everything. *Frontiers in Microbiology*, 8. <https://www.frontiersin.org/articles/10.3389/fmicb.2017.00108>
- Kralik, P., & Ricchi, M. (2017c). A Basic Guide to Real Time PCR in Microbial Diagnostics: Definitions, Parameters, and Everything. *Frontiers in Microbiology*, 8. <https://www.frontiersin.org/articles/10.3389/fmicb.2017.00108>
- Krauer, F., Riesen, M., Reveiz, L., Oladapo, O. T., Martínez-Vega, R., Porgo, T. V., Haefliger, A., Broutet, N. J., Low, N., & Group, W. Z. C. W. (2017). Zika Virus Infection as a Cause of Congenital Brain Abnormalities and Guillain–Barré Syndrome: Systematic Review. *PLOS Medicine*, 14(1), e1002203. <https://doi.org/10.1371/journal.pmed.1002203>
- Kularatne, S. A., & Dalugama, C. (2022). Dengue infection: Global importance, immunopathology and management. *Clinical Medicine*, 22(1), 9–13. <https://doi.org/10.7861/clinmed.2021-0791>
- Kumar, R., Srivastava, Y., Muthuramalingam, P., Singh, S. K., Verma, G., Tiwari, S., Tandel, N., Beura, S. K., Panigrahi, A. R., Maji, S., Sharma, P., Rai, P. K., Prajapati, D. K., Shin, H., & Tyagi, R. K. (2023). Understanding Mutations in Human SARS-CoV-2 Spike

- Glycoprotein: A Systematic Review & Meta-Analysis. *Viruses*, 15(4), Article 4.
<https://doi.org/10.3390/v15040856>
- Lalkhen, A. G., & McCluskey, A. (2008). Clinical tests: Sensitivity and specificity. *Continuing Education in Anaesthesia Critical Care & Pain*, 8(6), 221–223.
<https://doi.org/10.1093/bjaceaccp/mkn041>
- Lee, G., Vasco, L., Márquez, S., Zuniga-Moya, J., Engen, A., Uruchima, J., Ponce, P., Cevallos, W., Trueba, G., Trostle, J., Berrocal, V., Morrison, A., Cevallos, V., Mena, C., Coloma, J., & Eisenberg, J. (2021). A dengue outbreak in a rural community in Northern Coastal Ecuador: An analysis using unmanned aerial vehicle mapping. *PLOS Neglected Tropical Diseases*, 15, e0009679. <https://doi.org/10.1371/journal.pntd.0009679>
- Liu, J., Zhang, Q., Dong, Y.-Q., Yin, J., & Qiu, Y.-Q. (2022). Diagnostic accuracy of metagenomic next-generation sequencing in diagnosing infectious diseases: A meta-analysis. *Scientific Reports*, 12(1), 21032. <https://doi.org/10.1038/s41598-022-25314-y>
- Lo, S. W., & Jamroz, D. (2020). Genomics and epidemiological surveillance. *Nature Reviews Microbiology*, 18(9), Article 9. <https://doi.org/10.1038/s41579-020-0421-0>
- Lorenz, C., Freitas Ribeiro, A., & Chiaravalloti-Neto, F. (2019). Mayaro virus distribution in South America. *Acta Tropica*, 198, 105093. <https://doi.org/10.1016/j.actatropica.2019.105093>
- Lydy, S. L., Lascano, M. S., Garcia-Perez, J. E., Williams-Newkirk, A. J., & Grijalva, M. J. (2018). Seroprevalence and risk factors for infection with *Bartonella bacilliformis* in Loja province, Ecuador. *Emerging Microbes & Infections*, 7, 115.
<https://doi.org/10.1038/s41426-018-0110-5>

- Malik, L. H., Singh, G. D., & Amsterdam, E. A. (2015). The Epidemiology, Clinical Manifestations, and Management of Chagas Heart Disease. *Clinical Cardiology*, 38(9), 565–569. <https://doi.org/10.1002/clc.22421>
- Maljkovic Berry, I., Rutvisuttinunt, W., Sippy, R., Beltran-Ayala, E., Figueroa, K., Ryan, S., Srikanth, A., Stewart-Ibarra, A. M., Endy, T., & Jarman, R. G. (2020). The origins of dengue and chikungunya viruses in Ecuador following increased migration from Venezuela and Colombia. *BMC Evolutionary Biology*, 20(1), 31. <https://doi.org/10.1186/s12862-020-1596-8>
- Maneewatchararangsri, S., Doungchawee, G., Kalambaheti, T., Luvira, V., Soonthornworasiri, N., Vattanatham, P., Chaisri, U., & Adisakwattana, P. (2021). Evaluation of a genus-specific rGroEL1-524 IgM-ELISA and commercial ELISA kits during the course of leptospirosis in Thailand. *Scientific Reports*, 11(1), Article 1. <https://doi.org/10.1038/s41598-021-99377-8>
- Manock, S. R., Jacobsen, K. H., de Bravo, N. B., Russell, K. L., Negrete, M., Olson, J. G., Sanchez, J. L., Blair, P. J., Smalligan, R. D., Quist, B. K., Espín, J. F., Espinoza, W. R., MacCormick, F., Fleming, L. C., & Kochel, T. (2009). Etiology of acute undifferentiated febrile illness in the Amazon basin of Ecuador. *The American Journal of Tropical Medicine and Hygiene*, 81(1), 146–151.
- Márquez, S., Carrera, J., Espín, E., Cifuentes, S., Trueba, G., Coloma, J., & Eisenberg, J. N. (2018). Dengue Serotype Differences in Urban and Semi-rural Communities in Ecuador. *ACI Avances En Ciencias e Ingenierías*, 10(1), Article 1. <https://doi.org/10.18272/aci.v10i1.959>

- Márquez, S., Lee, G., Gutiérrez, B., Bennett, S., Coloma, J., Eisenberg, J. N. S., & Trueba, G. (2023). Phylogenetic Analysis of Transmission Dynamics of Dengue in Large and Small Population Centers, Northern Ecuador. *Emerging Infectious Diseases*, 29(5), 888–897. <https://doi.org/10.3201/eid2905.221226>
- Márquez, S., Lee, G. O., Andrade, P., Zuniga, J., Trueba, G., Eisenberg, J. N. S., & Coloma, J. (2022a). A Chikungunya Outbreak in a Dengue-endemic Region in Rural Northern Coastal Ecuador. *The American Journal of Tropical Medicine and Hygiene*, 107(6), 1226–1233. <https://doi.org/10.4269/ajtmh.22-0296>
- Márquez, S., Lee, G. O., Andrade, P., Zuniga, J., Trueba, G., Eisenberg, J. N. S., & Coloma, J. (2022b). A Chikungunya Outbreak in a Dengue-endemic Region in Rural Northern Coastal Ecuador. *The American Journal of Tropical Medicine and Hygiene*, 107(6), 1226–1233. <https://doi.org/10.4269/ajtmh.22-0296>
- McFee, R. B. (2018). Selected mosquito-borne illnesses—Chikungunya. *Disease-a-Month*, 64(5), 222. <https://doi.org/10.1016/j.disamonth.2018.01.009>
- Mena, G. E., Martinez, P. P., Mahmud, A. S., Marquet, P. A., Buckee, C. O., & Santillana, M. (2021). Socioeconomic status determines COVID-19 incidence and related mortality in Santiago, Chile. *Science*, 372(6545), eabg5298. <https://doi.org/10.1126/science.abg5298>
- Miller, E., Barragan, V., Chiriboga, J., Weddell, C., Luna, L., Jiménez, D. J., Aleman, J., Mihaljevic, J. R., Olivas, S., Marks, J., Izurieta, R., Nieto, N., Keim, P., Trueba, G., Caporaso, J. G., & Pearson, T. (2021). *Leptospira* in river and soil in a highly endemic area of Ecuador. *BMC Microbiology*, 21, 17. <https://doi.org/10.1186/s12866-020-02069-y>

- Miller, H. K., Priestley, R. A., & Kersh, G. J. (2021). Q Fever: A Troubling Disease and a Challenging Diagnosis. *Clinical Microbiology Newsletter*, 43(13), 109–118. <https://doi.org/10.1016/j.clinmicnews.2021.06.003>
- Mohd Hanafiah, K., Arifin, N., Bustami, Y., Noordin, R., Garcia, M., & Anderson, D. (2017). Development of Multiplexed Infectious Disease Lateral Flow Assays: Challenges and Opportunities. *Diagnostics*, 7(3), Article 3. <https://doi.org/10.3390/diagnostics7030051>
- Moreira, J., Bressan, C. S., Brasil, P., & Siqueira, A. M. (2018). Epidemiology of acute febrile illness in Latin America. *Clinical Microbiology and Infection*, 24(8), 827–835. <https://doi.org/10.1016/j.cmi.2018.05.001>
- Morrison, T. E. (2014). Reemergence of Chikungunya Virus. *Journal of Virology*, 88(20), 11644–11647. <https://doi.org/10.1128/jvi.01432-14>
- Musso, D., & Gubler, D. J. (2016). Zika Virus. *Clinical Microbiology Reviews*, 29(3), 487–524. <https://doi.org/10.1128/cmr.00072-15>
- Niloofo, R., Fernando, N., Silva, N. L. de, Karunanayake, L., Wickramasinghe, H., Dikmadugoda, N., Premawansa, G., Wickramasinghe, R., Silva, H. J. de, Premawansa, S., Rajapakse, S., & Handunnetti, S. (2015). Diagnosis of Leptospirosis: Comparison between Microscopic Agglutination Test, IgM-ELISA and IgM Rapid Immunochromatography Test. *PLOS ONE*, 10(6), e0129236. <https://doi.org/10.1371/journal.pone.0129236>
- Niloofo, R., Karunanayake, L., de Silva, H. J., Premawansa, S., Rajapakse, S., & Handunnetti, S. (2021). Development of in-house ELISAs as an alternative method for the serodiagnosis of leptospirosis. *International Journal of Infectious Diseases*, 105, 135–140. <https://doi.org/10.1016/j.ijid.2021.01.074>

- Núñez, A., Ntumngia, F. B., Guerra, Y., Adams, J. H., & Sáenz, F. E. (2023). Genetic diversity and natural selection of *Plasmodium vivax* reticulocyte invasion genes in Ecuador. *Malaria Journal*, 22(1), 225. <https://doi.org/10.1186/s12936-023-04640-0>
- OMSA. (2022). LEPTOSPIROSIS. In *Manual terrestre de la OIE 2022*.
- Oyegoke, O. O., Maharaj, L., Akoniyon, O. P., Kwoji, I., Roux, A. T., Adewumi, T. S., Maharaj, R., Oyebola, B. T., Adeleke, M. A., & Okpeku, M. (2022). Malaria diagnostic methods with the elimination goal in view. *Parasitology Research*, 121(7), 1867–1885. <https://doi.org/10.1007/s00436-022-07512-9>
- Padilla N, A., Moncayo, A. L., Keil, C. B., Grijalva, M. J., & Villacís, A. G. (2019). Life Cycle, Feeding, and Defecation Patterns of *Triatoma carrioni* (Hemiptera: Reduviidae), Under Laboratory Conditions. *Journal of Medical Entomology*, 56(3), 617–624. <https://doi.org/10.1093/jme/tjz004>
- PAHO. (2019). *Laboratory Diagnosis of Mayaro Virus infection*. <https://www.paho.org/es/documentos/mayaro-virus-laboratory-diagnosis-chikungunya-differential-diagnosis-2019-solo-ingles>
- PAHO. (2020). *Interim guidelines for detecting cases of reinfection by SARS-CoV-2*. <https://www.paho.org/en/documents/interim-guidelines-detecting-cases-reinfection-sars-cov-2>
- PAHO. (2023). *As dengue cases increase globally, vector control, community engagement key to prevent spread of the disease*. <https://www.paho.org/en/news/3-8-2023-dengue-cases-increase-globally-vector-control-community-engagement-key-prevent-spread>

- Parres-Mercader, M., Pance, A., & Gómez-Díaz, E. (2023). Novel systems to study vector-pathogen interactions in malaria. *Frontiers in Cellular and Infection Microbiology*, *13*. <https://www.frontiersin.org/articles/10.3389/fcimb.2023.1146030>
- Patel, R., Kaki, M., Potluri, V. S., Kahar, P., & Khanna, D. (2022). A comprehensive review of SARS-CoV-2 vaccines: Pfizer, Moderna & Johnson & Johnson. *Human Vaccines & Immunotherapeutics*, *18*(1), 2002083. <https://doi.org/10.1080/21645515.2021.2002083>
- Pereira, T. N., Virginio, F., Souza, J. I., & Moreira, L. A. (2021). Emergent Arboviruses: A Review About Mayaro virus and Oropouche orthobunyavirus. *Frontiers in Tropical Diseases*, *2*. <https://www.frontiersin.org/articles/10.3389/fitd.2021.737436>
- Pezzi, L., Rodriguez-Morales, A. J., Reusken, C. B., Ribeiro, G. S., LaBeaud, A. D., Lourenço-de-Oliveira, R., Brasil, P., Lecuit, M., Failloux, A. B., Gallian, P., Jaenisch, T., Simon, F., Siqueira, A. M., Rosa-Freitas, M. G., Vega Rua, A., Weaver, S. C., Drexler, J. F., Vasilakis, N., de Lamballerie X, ... Simmons, G. (2019). GloPID-R report on chikungunya, o'nyong-nyong and Mayaro virus, part 3: Epidemiological distribution of Mayaro virus. *Antiviral Research*, *172*, 104610. <https://doi.org/10.1016/j.antiviral.2019.104610>
- Phillips, M. A., Burrows, J. N., Manyando, C., van Huijsduijnen, R. H., Van Voorhis, W. C., & Wells, T. N. C. (2017a). Malaria. *Nature Reviews Disease Primers*, *3*(1), Article 1. <https://doi.org/10.1038/nrdp.2017.50>
- Phillips, M. A., Burrows, J. N., Manyando, C., van Huijsduijnen, R. H., Van Voorhis, W. C., & Wells, T. N. C. (2017b). Malaria. *Nature Reviews Disease Primers*, *3*(1), Article 1. <https://doi.org/10.1038/nrdp.2017.50>
- Plourde, A. R., & Bloch, E. M. (2016). A Literature Review of Zika Virus. *Emerging Infectious Diseases*, *22*(7), 1185–1192. <https://doi.org/10.3201/eid2207.151990>

- Poland, G. A., Ovsyannikova, I. G., & Kennedy, R. B. (2019). Zika Vaccine Development: Current Status. *Mayo Clinic Proceedings*, 94(12), 2572–2586. <https://doi.org/10.1016/j.mayocp.2019.05.016>
- Prado, P. S., Almeida Júnior, J. T. D., Abreu, L. T. de, Silva, C. G., Souza, L. da C., Gomes, M. C., Mendes, L. M. T., Santos, E. M. D., & Romero, G. A. S. (2018). Validation and reliability of the rapid diagnostic test “SD Bioeasy Dengue Duo” for dengue diagnosis in Brazil: A phase III study. *Memorias Do Instituto Oswaldo Cruz*, 113(8), e170433. <https://doi.org/10.1590/0074-02760170433>
- Prado-Vivar, B., Becerra-Wong, M., Guadalupe, J. J., Márquez, S., Gutierrez, B., Rojas-Silva, P., Grunauer, M., Trueba, G., Barragán, V., & Cárdenas, P. (2021). A case of SARS-CoV-2 reinfection in Ecuador. *The Lancet. Infectious Diseases*, 21(6), e142. [https://doi.org/10.1016/S1473-3099\(20\)30910-5](https://doi.org/10.1016/S1473-3099(20)30910-5)
- Puerta-Guardo, H., Glasner, D. R., Espinosa, D. A., Biering, S. B., Patana, M., Ratnasiri, K., Wang, C., Beatty, P. R., & Harris, E. (2019). Flavivirus NS1 Triggers Tissue-Specific Vascular Endothelial Dysfunction Reflecting Disease Tropism. *Cell Reports*, 26(6), 1598-1613.e8. <https://doi.org/10.1016/j.celrep.2019.01.036>
- Raadsen, M., Du Toit, J., Langerak, T., van Bussel, B., van Gorp, E., & Goeijenbier, M. (2021). Thrombocytopenia in Virus Infections. *Journal of Clinical Medicine*, 10(4), Article 4. <https://doi.org/10.3390/jcm10040877>
- Rahman, Md. M., Masum, Md. H. U., Wajed, S., & Talukder, A. (2022). A comprehensive review on COVID-19 vaccines: Development, effectiveness, adverse effects, distribution and challenges. *VirusDisease*, 33(1), 1–22. <https://doi.org/10.1007/s13337-022-00755-1>

- Rajapakse, S. (2022). Leptospirosis: Clinical aspects. *Clinical Medicine*, 22(1), 14–17.
<https://doi.org/10.7861/clinmed.2021-0784>
- Ralapanawa, U., Alawattagama, A. T. M., Gunrathne, M., Tennakoon, S., Kularatne, S. A. M., & Jayalath, T. (2018). Value of peripheral blood count for dengue severity prediction. *BMC Research Notes*, 11, 400. <https://doi.org/10.1186/s13104-018-3505-4>
- Recht, J., Siqueira, A. M., Monteiro, W. M., Herrera, S. M., Herrera, S., & Lacerda, M. V. G. (2017). Malaria in Brazil, Colombia, Peru and Venezuela: Current challenges in malaria control and elimination. *Malaria Journal*, 16(1), 273. <https://doi.org/10.1186/s12936-017-1925-6>
- Reina Ortiz, M., & Sharma, V. (2020). *Modeling the COVID-19 outbreak in Ecuador: Is it the right time to lift social distancing containment measures?* [Preprint]. *Epidemiology*.
<https://doi.org/10.1101/2020.05.21.20109520>
- Reslova, N., Michna, V., Kasny, M., Mikel, P., & Kralik, P. (2017). xMAP Technology: Applications in Detection of Pathogens. *Frontiers in Microbiology*, 8.
<https://www.frontiersin.org/articles/10.3389/fmicb.2017.00055>
- Ridenour, C. L., Cocking, J., Poidmore, S., Erickson, D., Brock, B., Valentine, M., Roe, C. C., Young, S. J., Henke, J. A., Hung, K. Y., Wittie, J., Stefanakos, E., Sumner, C., Ruedas, M., Raman, V., Seaton, N., Bendik, W., Hornstra O'Neill, H. M., Sheridan, K., ... Hepp, C. M. (2021). St. Louis Encephalitis Virus in the Southwestern United States: A Phylogeographic Case for a Multi-Variant Introduction Event. *Frontiers in Genetics*, 12.
<https://www.frontiersin.org/articles/10.3389/fgene.2021.667895>
- Rosa, M. I., Reis, M. F. dos, Simon, C., Dondossola, E., Alexandre, M. C., Colonetti, T., & Meller, F. O. (2017). IgM ELISA for leptospirosis diagnosis: A systematic review and meta-

- analysis. *Ciência & Saúde Coletiva*, 22, 4001–4012. <https://doi.org/10.1590/1413-812320172212.14112016>
- Sahlin, K., & Medvedev, P. (2021). Error correction enables use of Oxford Nanopore technology for reference-free transcriptome analysis. *Nature Communications*, 12(1), Article 1. <https://doi.org/10.1038/s41467-020-20340-8>
- Sakamoto, S., Putalun, W., Vimolmangkang, S., Phoolcharoen, W., Shoyama, Y., Tanaka, H., & Morimoto, S. (2018). Enzyme-linked immunosorbent assay for the quantitative/qualitative analysis of plant secondary metabolites. *Journal of Natural Medicines*, 72(1), 32–42. <https://doi.org/10.1007/s11418-017-1144-z>
- Sakkas, H., Bozidis, P., Franks, A., & Papadopoulou, C. (2018a). Oropouche Fever: A Review. *Viruses*, 10(4), 175. <https://doi.org/10.3390/v10040175>
- Sakkas, H., Bozidis, P., Franks, A., & Papadopoulou, C. (2018b). Oropouche Fever: A Review. *Viruses*, 10(4), 175. <https://doi.org/10.3390/v10040175>
- Sarker, A., Dhama, N., & Gupta, R. D. (2023). Dengue virus neutralizing antibody: A review of targets, cross-reactivity, and antibody-dependent enhancement. *Frontiers in Immunology*, 14. <https://www.frontiersin.org/articles/10.3389/fimmu.2023.1200195>
- Schneider, M., Narciso-Abraham, M., Hadl, S., McMahon, R., Toepfer, S., Fuchs, U., Hochreiter, R., Bitzer, A., Kosulin, K., Larcher-Senn, J., Mader, R., Dubischar, K., Zoihs, O., Jaramillo, J.-C., Eder-Lingelbach, S., Buerger, V., & Wressnigg, N. (2023). Safety and immunogenicity of a single-shot live-attenuated chikungunya vaccine: A double-blind, multicentre, randomised, placebo-controlled, phase 3 trial. *The Lancet*, 401(10394), 2138–2147. [https://doi.org/10.1016/S0140-6736\(23\)00641-4](https://doi.org/10.1016/S0140-6736(23)00641-4)

- Shreffler, J., & Huecker, M. R. (2023). Diagnostic Testing Accuracy: Sensitivity, Specificity, Predictive Values and Likelihood Ratios. In *StatPearls [Internet]*. StatPearls Publishing. <https://www.ncbi.nlm.nih.gov/books/NBK557491/>
- Shrestha, P., Dahal, P., Ogbonnaa-Njoku, C., Das, D., Stepniewska, K., Thomas, N. V., Hopkins, H., Crump, J. A., Bell, D., Newton, P. N., Ashley, E. A., & Guérin, P. J. (2020). Non-malarial febrile illness: A systematic review of published aetiological studies and case reports from Southern Asia and South-eastern Asia, 1980–2015. *BMC Medicine*, *18*(1), 299. <https://doi.org/10.1186/s12916-020-01745-0>
- Singh, D., & Yi, S. V. (2021). On the origin and evolution of SARS-CoV-2. *Experimental & Molecular Medicine*, *53*(4), Article 4. <https://doi.org/10.1038/s12276-021-00604-z>
- Soheili, M., Khateri, S., Moradpour, F., Mohammadzede, P., Zareie, M., Mortazavi, S. M. M., Manifar, S., Kohan, H. G., & Moradi, Y. (2023). The efficacy and effectiveness of COVID-19 vaccines around the world: A mini-review and meta-analysis. *Annals of Clinical Microbiology and Antimicrobials*, *22*(1), 42. <https://doi.org/10.1186/s12941-023-00594-y>
- St. Louis Encephalitis* | *St. Louis Encephalitis* | CDC. (2023, June 14). <https://www.cdc.gov/sle/index.html>
- Stewart-Ibarra, A. M., Ryan, S. J., Kenneson, A., King, C. A., Abbott, M., Barbachano-Guerrero, A., Beltrán-Ayala, E., Borbor-Cordova, M. J., Cárdenas, W. B., Cueva, C., Finkelstein, J. L., Lupone, C. D., Jarman, R. G., Maljkovic Berry, I., Mehta, S., Polhemus, M., Silva, M., & Endy, T. P. (2018). The Burden of Dengue Fever and Chikungunya in Southern Coastal Ecuador: Epidemiology, Clinical Presentation, and Phylogenetics from the First Two Years of a Prospective Study. *The American Journal of Tropical Medicine and Hygiene*, *98*(5), 1444–1459. <https://doi.org/10.4269/ajtmh.17-0762>

- Stoddard, R. A., Gee, J. E., Wilkins, P. P., McCaustland, K., & Hoffmaster, A. R. (2009). Detection of pathogenic *Leptospira* spp. Through TaqMan polymerase chain reaction targeting the LipL32 gene. *Diagnostic Microbiology and Infectious Disease*, 64(3), 247–255. <https://doi.org/10.1016/j.diagmicrobio.2009.03.014>
- Theel, E. S., & Hata, D. J. (2018). Diagnostic Testing for Zika Virus: A Postoutbreak Update. *Journal of Clinical Microbiology*, 56(4), e01972-17. <https://doi.org/10.1128/JCM.01972-17>
- Thomas, S. J. (2023). Is new dengue vaccine efficacy data a relief or cause for concern? *Npj Vaccines*, 8(1), Article 1. <https://doi.org/10.1038/s41541-023-00658-2>
- Tomassone, L., Portillo, A., Nováková, M., de Sousa, R., & Oteo, J. A. (2018). Neglected aspects of tick-borne rickettsioses. *Parasites & Vectors*, 11(1), 263. <https://doi.org/10.1186/s13071-018-2856-y>
- Torales, M. (2023). Notes from the Field: Chikungunya Outbreak — Paraguay, 2022–2023. *MMWR. Morbidity and Mortality Weekly Report*, 72. <https://doi.org/10.15585/mmwr.mm7223a5>
- Ukwishaka, J., Ndayishimiye, Y., Destine, E., Danwang, C., & Kirakoya-Samadoulougou, F. (2023). Global prevalence of coronavirus disease 2019 reinfection: A systematic review and meta-analysis. *BMC Public Health*, 23(1), 778. <https://doi.org/10.1186/s12889-023-15626-7>
- Valencia-Marín, B. S., Gandica, I. D., & Aguirre-Obando, O. A. (2020). The Mayaro virus and its potential epidemiological consequences in Colombia: An exploratory biomathematics analysis. *Parasites & Vectors*, 13(1), 508. <https://doi.org/10.1186/s13071-020-04354-1>

- Valones, M. A. A., Guimarães, R. L., Brandão, L. A. C., Souza, P. R. E. de, Carvalho, A. de A. T., & Crovela, S. (2009). Principles and applications of polymerase chain reaction in medical diagnostic fields: A review. *Brazilian Journal of Microbiology*, *40*, 1–11. <https://doi.org/10.1590/S1517-83822009000100001>
- Vandeputte, J., Saville, M., Cavaleri, M., Friede, M., Hacker, A., Mueller, S. O., Rizzi, R., Smith, D., Thirstrup, S., Wagner, R., Baay, M., & Neels, P. (2021). IABS/CEPI platform technology webinar: Is it possible to reduce the vaccine development time? *Biologicals*, *71*, 55–60. <https://doi.org/10.1016/j.biologicals.2021.04.005>
- Vásconez-González, J., Izquierdo-Condoy, J. S., Fernandez-Naranjo, R., Gamez-Rivera, E., Tello-De-la-Torre, A., Guerrero-Castillo, G. S., Ruiz-Sosa, C., & Ortiz-Prado, E. (2023). Severe Chagas disease in Ecuador: A countrywide geodemographic epidemiological analysis from 2011 to 2021. *Frontiers in Public Health*, *11*. <https://www.frontiersin.org/articles/10.3389/fpubh.2023.1172955>
- Waggoner, J. J., Gresh, L., Mohamed-Hadley, A., Ballesteros, G., Davila, M. J. V., Tellez, Y., Sahoo, M. K., Balmaseda, A., Harris, E., & Pinsky, B. A. (2016). Single-Reaction Multiplex Reverse Transcription PCR for Detection of Zika, Chikungunya, and Dengue Viruses. *Emerging Infectious Diseases*, *22*(7), 1295–1297. <https://doi.org/10.3201/eid2207.160326>
- Waggoner, J. J., Rojas, A., Mohamed-Hadley, A., de Guillén, Y. A., & Pinsky, B. A. (2018). Real-time RT-PCR for Mayaro virus detection in plasma and urine. *Journal of Clinical Virology*, *98*, 1–4. <https://doi.org/10.1016/j.jcv.2017.11.006>

- Waggoner, J. J., Rojas, A., & Pinsky, B. A. (2018). Yellow Fever Virus: Diagnostics for a Persistent Arboviral Threat. *Journal of Clinical Microbiology*, *56*(10), e00827-18. <https://doi.org/10.1128/JCM.00827-18>
- Wasswa, F. B., Kassaza, K., Nielsen, K., & Bazira, J. (2022). MinION Whole-Genome Sequencing in Resource-Limited Settings: Challenges and Opportunities. *Current Clinical Microbiology Reports*, *9*(4), 52–59. <https://doi.org/10.1007/s40588-022-00183-1>
- Webb, E., Michelen, M., Rigby, I., Dagens, A., Dahmash, D., Cheng, V., Joseph, R., Lipworth, S., Harriss, E., Cai, E., Nartowski, R., Januraga, P. P., Gedela, K., Sukmaningrum, E., Cevik, M., Groves, H., Hart, P., Fletcher, T., Blumberg, L., ... Sigfrid, L. (2022). An evaluation of global Chikungunya clinical management guidelines: A systematic review. *eClinicalMedicine*, *54*. <https://doi.org/10.1016/j.eclinm.2022.101672>
- Weiss, S., Klingler, J., Hioe, C., Amanat, F., Baine, I., Arinsburg, S., Kojic, E. M., Stoeber, J., Liu, S. T. H., Jurczynszak, D., Bermudez-Gonzalez, M., Simon, V., Krammer, F., & Zolla-Pazner, S. (2020). A High-Throughput Assay for Circulating Antibodies Directed Against the S Protein of Severe Acute Respiratory Syndrome Coronavirus 2. *The Journal of Infectious Diseases*, *222*(10), 1629–1634. <https://doi.org/10.1093/infdis/jiaa531>
- WHO. (2023a). *Dengue – the Region of the Americas*. <https://www.who.int/emergencies/disease-outbreak-news/item/2023-DON475>
- WHO. (2023b). *WHO Coronavirus (COVID-19) Dashboard*. <https://covid19.who.int/>
- Wise, E. L., Márquez, S., Mellors, J., Paz, V., Atkinson, B., Gutierrez, B., Zapata, S., Coloma, J., Pybus, O. G., Jackson, S. K., Trueba, G., Fejer, G., Logue, C. H., & Pullan, S. T. (2020). Oropouche virus cases identified in Ecuador using an optimised qRT-PCR informed by

- metagenomic sequencing. *PLOS Neglected Tropical Diseases*, 14(1), e0007897.
<https://doi.org/10.1371/journal.pntd.0007897>
- Wise, E. L., Pullan, S. T., Márquez, S., Paz, V., Mosquera, J. D., Zapata, S., Jackson, S. K., Fejer, G., Trueba, G., & Logue, C. H. (2018). Isolation of Oropouche Virus from Febrile Patient, Ecuador. *Emerging Infectious Diseases*, 24(5), 935–937.
<https://doi.org/10.3201/eid2405.171569>
- Wolford, R. W., & Schaefer, T. J. (2023). Zika Virus. In *StatPearls*. StatPearls Publishing.
<http://www.ncbi.nlm.nih.gov/books/NBK430981/>
- World Health Organization. (2013). *WHO informal consultation on fever management in peripheral health care settings: A global review of evidence and practice*. World Health Organization; WHO IRIS. <https://apps.who.int/iris/handle/10665/95116>
- World Health Organization. (2023, April 3). *Geographical expansion of cases of dengue and chikungunya beyond the historical areas of transmission in the Region of the Americas*.
<https://www.who.int/emergencies/disease-outbreak-news/item/2023-DON448>
- Worobey, M., Levy, J. I., Malpica Serrano, L., Crits-Christoph, A., Pekar, J. E., Goldstein, S. A., Rasmussen, A. L., Kraemer, M. U. G., Newman, C., Koopmans, M. P. G., Suchard, M. A., Wertheim, J. O., Lemey, P., Robertson, D. L., Garry, R. F., Holmes, E. C., Rambaut, A., & Andersen, K. G. (2022). The Huanan Seafood Wholesale Market in Wuhan was the early epicenter of the COVID-19 pandemic. *Science*, 377(6609), 951–959.
<https://doi.org/10.1126/science.abp8715>
- Yan, G., Pang, L., Cook, A. R., Ho, H. J., Win, M. S., Khoo, A. L., Wong, J. G. X., Lee, C. K., Yan, B., Jureen, R., Ho, S. S., Lye, D. C., Tambyah, P. A., Leo, Y. S., Fisher, D., Oon, J., Bagdasarian, N., Chow, A., Smitasin, N., & Chai, L. Y. A. (2018). Distinguishing Zika and

- Dengue Viruses through Simple Clinical Assessment, Singapore. *Emerging Infectious Diseases*, 24(8), 1565–1568. <https://doi.org/10.3201/eid2408.171883>
- Zhu, Y. Y., Machleder, E. M., Chenchik, A., Li, R., & Siebert, P. D. (2001). Reverse Transcriptase Template Switching: A SMARTTM Approach for Full-Length cDNA Library Construction. *BioTechniques*, 30(4), 892–897. <https://doi.org/10.2144/01304pf02>
- Zika-virus-disease-annual-epidemiological-report-2021.pdf*. (n.d.). Retrieved October 9, 2023, from <https://www.ecdc.europa.eu/sites/default/files/documents/zika-virus-disease-annual-epidemiological-report-2021.pdf>
- Zorrilla, V., Vásquez, G., Espada, L., & Ramírez, P. (2017). Vectores de la leishmaniasis tegumentaria y la enfermedad de carrión en el Perú: Una actualización. *Revista Peruana de Medicina Experimental y Salud Pública*, 34, 485–496. <https://doi.org/10.17843/rpmesp.2017.343.2398>

CHAPTER 2

The American Journal of Tropical Medicine and Hygiene. First published: 14 November 2022
doi:10.4269/ajtmh.22-0296

A Chikungunya Outbreak in a Dengue-endemic Region in Rural Northern Coastal Ecuador

Sully Márquez,¹ Gwennyth O. Lee,² Paulina Andrade,^{3,4} Julio Zuniga,² Gabriel Trueba,¹ Joseph N. S. Eisenberg,^{2*†}
and Josefina Coloma^{4*†}

¹Instituto de Microbiología, Universidad San Francisco de Quito, Quito, Ecuador; ²Department of Epidemiology, School of Public Health, University of Michigan, Ann Arbor, Michigan; ³Colegio de Ciencias Biológicas y Ambientales COCIBA, Universidad San Francisco de Quito, Quito, Ecuador; ⁴Division of Infectious Diseases and Vaccinology, School of Public Health, University of California, Berkeley, Berkeley, California

Abstract

Dengue virus (DENV) reemerged in the Americas in the 1980s and 1990s, whereas chikungunya virus (CHIKV) emerged in 2014. Although CHIKV produced large epidemics from 2014 to 2017, dengue fever has been the prominent arboviral disease identified through passive surveillance, bringing to question the degree to which cases are misdiagnosed. To address this concern, we conducted an active household-based surveillance of arboviral-like illnesses in six rural and remote communities in northern coastal Ecuador from May 2019 to February 2020. Although passive surveillance conducted by the Ecuadorian Ministry of Health reported only DENV cases in the region, more than 70% of the arbovirus-like illnesses detected by active surveillance in our study were positive for CHIKV. These findings underline the need for active surveillance of arboviral

infections with laboratory confirmation, especially in rural communities where arboviral illnesses are more likely to be underreported.

INTRODUCTION

Dengue virus (DENV), genus *Flavivirus*, family *Flaviviridae*, and chikungunya virus (CHIKV), genus *Alphavirus*, family *Togaviridae*, share many traits. Both viruses are transmitted to humans by *Aedes aegypti* and *Aedes albopictus* mosquitoes. Both have single-stranded positive RNA genomes. DENV has four distinct serotypes (DENV1–4), whereas CHIKV has one serotype with three genotypes known as West African, East/Central/South African (ECSA), and Asian.^{1,2}

Dengue fever (DF) and chikungunya fever (CHIKF) share similar symptoms, including fever, myalgia, arthralgia, and rash. Most DF cases are self-limited but can progress to dengue with warning signs or severe disease, characterized by vascular leakage leading to shock, fluid accumulation, severe bleeding, and organ involvement.^{3,4} Likewise, most CHIKF cases are self-limited.⁵ In rare cases, musculoskeletal symptoms can cause a chronic polyarthritis, which may lead to severe polyarthralgia/polyarthritis.^{5,6} Differential diagnosis of DF and CHIKF, therefore, has been historically difficult. Given that there is less clinical awareness of CHIKF, and passive surveillance relies on symptoms due to the limited capacity for laboratory testing, underreporting CHIKF by passive surveillance is likely higher than for DF.⁷

Both DF and CHIKF are ancient diseases that have reemerged multiple times throughout history.⁸ DF case counts and geographic spread have increased 8-fold over the past 2 decades,³ whereas CHIKV's global reach has increased since the early 2000s. An estimated 105 million dengue infections and 51 million dengue fever cases per year have been recorded in 128 countries,⁹

whereas an estimated 10 million Chikungunya cases were reported worldwide from 2005 to 2017.

10

In the Americas, DF was introduced in the early 1980s, with a total of 2,733,635 cases of dengue reported in 2019¹¹; whereas CHIKF was introduced in the Americas in 2013, with more than 2.1 million cases reported.¹² In Ecuador, dengue virus type I (DENV-1) emerged in 1988, followed by DENV-2 in 1990, DENV-4 in 1993, and DENV-3 10 years later. The four serotypes are now endemic, producing yearly outbreaks.¹³ The first CHIKF case was detected in Ecuador in 2014. By 2015, 33,619 cases were reported,¹⁴ and by 2019 CHIKF had subsided with only 2 cases reported nationwide.¹⁵ An entomological study suggested the circulation of CHIKV Asian lineage in Ecuador.¹⁶

The northwest Pacific Coast of Ecuador (Esmeraldas province) is one of the poorest regions in the country. In the 1980s, rapid deforestation, accompanied by the construction of a highway connecting previously remote communities to the coast and the Andes in the early 2000s, resulted in rapid socioecological change in the area.¹⁷ After this transition, the province underwent an etiologic transition in febrile diseases from malaria to arboviral infections in the 1990s, with periodic dengue outbreaks that were largely underreported.¹⁸ CHIKV was first reported in Esmeraldas in 2014. From 2014 to 2018, the Ecuadorian Ministry of Health (MOH) reported 10,791 CHIKF cases and 2,913 dengue cases. In 2019, the MOH reported 1,750 dengue cases and no chikungunya cases.¹⁵

Suspected arbovirus cases require mandatory notification to the Ecuadorian MOH, the national surveillance system of which includes passive surveillance of cases from state-run clinics and hospitals. Only a subset of suspected cases is confirmed for DENV infection using IgM antibody-capture enzyme-linked immunosorbent assay (MAC-ELISA) or NS1 antigen ELISAs in

health posts or and hospital diagnostic laboratories; a smaller subset of cases is sent to the national reference laboratory (the National Institute for Public Health Research) to be confirmed by reverse transcription polymerase chain reaction (RT-PCR) for etiology. In the case of malaria, the MOH performs microscopy for diagnosis.

Only a fraction of DENV cases is tested by the national system, and thus many cases are misclassified or misdiagnosed. Thus, it is necessary to integrate strategies involving surveillance and differential diagnosis supported by serological and virological laboratory testing of arboviral diseases at national, regional, and local levels. Here we use confirmation by real-time RT-PCR to describe a CHIKV outbreak in 2019. This outbreak was identified through an active household-based surveillance study of arbovirus-like illness in a semiurban town (Borbón) and five rural and remote communities in northern coastal Ecuador.

MATERIALS AND METHODS

Study site. Located in the northwestern coastal Ecuadorian province of Esmeraldas, in Eloy Alfaro County, our study communities—Borbón, Colón Eloy, Maldonado, Santa María, Santo Domingo, and Timbiré—lie along three rivers that flow toward the Pacific Ocean (Figure 1). The communities were selected to represent different levels of remoteness as defined by our previously published remoteness metric,¹⁷ which we have shown to be associated with regional-scale patterns of human movement,¹⁹ community cohesion, and different antimicrobial resistance and enteric infection risk.^{17,20} The population in our study site primarily self-identifies as Afro-Ecuadorian, Indigenous Chachi, and mestizo; the majority group is Afro-Ecuadorian.²¹

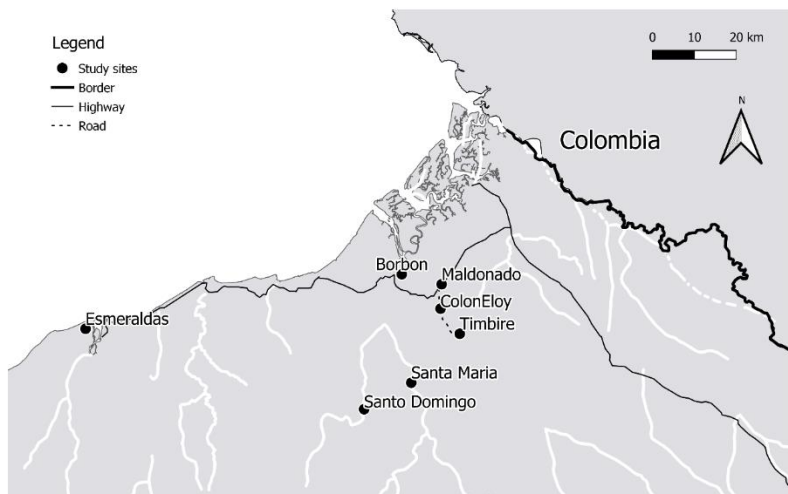


FIGURE 1. Map of the study area. The towns of Borbón, Maldonado, Colon Eloy, Timbiré, Santa María, and Santo Domingo are located approximately 100 kilometers north of the provincial capital of Esmeraldas.

Study design and population. We developed an active household-based surveillance system for arboviral-like illness within our six study communities. This surveillance includes an annual census of each study community to generate a record of the age, sex, occupation, and other key demographic and socioeconomic characteristics of individuals living in each household. Cases were identified through weekly household visits during the rainy season (June–October) when there is a higher risk for dengue virus transmission. During the low-risk dry season (November–December), household visits decreased to every 2 weeks. A trained study team of community residents, called *brigadistas*, began household-based fever surveillance in May 2019. For this analysis, we include household surveillance data collected from May 2019 until the end of February 2020, at which time household visits were shifted to phone-based surveillance due to the COVID-19 pandemic and movement restrictions.

The brigadistas visit involved a symptom survey administered to the household key informant, asking whether there were any cases of fever, red eyes, or rash in the home. When a positive case was identified, the brigadista notified a study nurse who visited the household within 24 hours to complete a follow-up survey with the symptomatic participant to determine whether the participant's symptoms were consistent with an arbovirus-like illness. Participants were excluded from further follow-up if the nurse considered their symptoms to be associated with an upper respiratory or gastrointestinal infection (on the basis of the presence of diarrhea, bloody stool, cough, or nasal congestion and confirmed by the nurse's clinical judgment). For those with an arbovirus-like illness, a serum sample was collected, and an aliquot was used for onsite testing with Dengue DUO NS1 IgG/IgM rapid test (Standard Diagnostic Inc., Suwon, Korea; data not shown). Another aliquot was frozen in liquid nitrogen and transported for further testing at the Institute of Microbiology at Universidad San Francisco de Quito (USFQ). The study was approved by the Bioethics committee of the Universidad San Francisco de Quito, the University of Michigan, and the Ecuadorian Ministry of Health, Ecuador.

RNA extraction, PCR detection, and metagenomic analysis. Viral RNA was extracted from a total of 182 febrile serum samples using the Qiagen viral RNA mini kit according to the manufacturer's instructions (Qiagen, Hilden, Germany) and was tested using a triplex real time RT-PCR Zika-Dengue-Chikungunya (ZDC) assay to confirm infection and etiology.²² Samples positive for dengue were next analyzed for their serotype using a conventional multiplex RT-PCR following the Harris et al. (1998) protocol.²³ Primers are shown in Supplemental Table 1. An additional screening for Oropouche,²⁴ Mayaro,²⁵ and *Leptospira* spp.²⁶ was conducted for samples

that were negative for dengue, Zika, and chikungunya. Primers and probes for each pathogen are shown in Supplemental Table 1.

PCR detection for CHIKV. A conventional RT-PCR protocol for Chikungunya confirmation was developed by our team for a subset of positive samples, primers are shown in Supplemental Table 1, using the kit Superscript III one step RT-PCR system. The reaction mix contained: 12.5 μ L 2X reaction mix, 1- μ L primers CHIKV F 10011, CHIKV R 10396 at a concentration of 10 μ M, 80 U SuperScript III Taq Platinum mix (Invitrogen, Waltham, MA), and 5 μ L of Rnase-free water. The amplification protocol was used as follows: 50°C for 30 minutes, 95°C for 15 minutes, 40 cycles of 94°C for 1 minute, 52°C for 1 minute, 72°C for 1 minute, and a final extension of 72°C for 10 minutes. For additional confirmation, the amplicons were sent for sequencing by Sanger.

We conducted a metagenomic analysis for two randomly selected febrile samples that were negative for DENV, CHIKV, and ZIKV using the cDNA preparation protocol from Public Health England Genomics laboratory (RNA viral metagenomics MINION one-pot)²⁷ and the Oxford Nanopore Technologies Ligation kit protocol (SQK-LSK109; Oxford Nanopore Technologies, Oxford, United Kingdom) and Native barcoding kit (NB-114) following manufacturer's instructions for library preparation. This library was sequenced using MinKNOW version 4.05 for 24 hours. Base calling was performed using Guppy v. 3.4.5. Porechop v. 0.2.4 was performed for demultiplexing and to remove adapters and barcodes. The taxonomic profile of the sequences of each sample was classified with the Kaiju web server platform.²⁸ The database "NCBI Blast nr 1 euk" was selected (includes bacteria, archaea, fungi, viruses, and eukaryotes), the running method used was the MEM algorithm (maximum exact matches), and the rest of the parameters were kept

by default. For the analysis of the taxonomic profiles, the number of assigned readings and the generated Krona charts were considered.

DNA extraction and PCR detection for *Plasmodium*. DNA was extracted from negative serum samples using the kit pure link genomic DNA following the manufacturer's instructions (Life Technologies, Carlsbad, CA). These samples were tested with a nested PCR for *Plasmodium falciparum* detection following the Snounou (1996) protocol.²⁹ Primers are shown in Supplemental Table 1.

Passive surveillance. The Ecuadorian MOH reports dengue cases using a standardized case report form. The MOH provided us with the case report on all dengue cases reported from January 2019 to the end of February 2020 including data on cases living in the six communities in our study. For each case, the MOH also reported demographic and symptoms data.

Statistical analysis. Outcome variables. Active surveillance samples were considered positive for DENV or CHIKV if they were positive by qPCR. Our laboratory also uses other diagnostic methods to define a dengue case DENV (e.g., NS1 and IgM); however, for this analysis, these results were not included. Moreover, a coinfection was defined as two pathogens detected with the triplex real time RT-PCR ZDC in the same serum sample.

Comparing DF and CHIKF clinical symptoms. To analyze differences in the prevalence of reported symptoms for CHIKF versus DF, we performed two-sided t tests, excluding samples co-infected with DENV and CHIKV. Differences at the $P < 0.05$ were considered statistically significant. We used radar plots to visualize differences in symptom prevalence between dengue with and without warning signs and between DENV and CHIKV cases. We included those symptoms that were present in at least 5% of the cases.

Risk factor analysis. To compare characteristics of individuals with a symptomatic DENV or CHIKV infection to the study population overall, we calculated the incidence of each virus (symptomatic cases per 10,000 person-years). We then developed bivariate and multivariate logistic models to test the association between common arboviral risk factors and symptomatic dengue and chikungunya. The risk factors we considered were age, sex, ethnicity, community of residence, occupation, and whether the individual had ever lived outside of their current community.

Comparison of active and passive surveillance. On the basis of reported symptoms, dengue cases from the MOH passive surveillance were divided into dengue with and without warning signs. We compared the number of episodes of dengue and chikungunya reported by passive and active surveillance. We also compared the prevalence of symptoms reported in our study active surveillance and the MOH passive surveillance. For a subset of individuals whose case episode was captured by both active and passive surveillance, we compared laboratory results between the two systems. All analyses were conducted in R version 4.0.3 (R Foundation for Statistical Computing, Vienna, Austria) or Stata version 16.1 (Stata Corp., LLC, College Station, TX)

RESULTS

DENV and CHIKV cases were detected in all six rural communities. From May 2019 to the end of February 2020, the active surveillance study collected 182 serum samples from 172 unique individuals with acute arbovirus-like illness; 10 individuals had two illness episodes (mean= 129 days apart; range= 32–229 days). A distinct episode was considered when the individual presented fever separated by at least 15 fever-free days. The blood draw was completed, on average, 3 days after symptoms reportedly began (mean =3.2, SD= 2.2).

Laboratory testing was completed for 174 of 182 episodes. More than 80% of these episodes were diagnosed with a CHIKV, DENV, or CHIKV-DENV coinfection (145 of 174). More than half of these 145 pathogen-positive episodes (61%) were diagnosed with a CHIKV infection only ($N = 88$), 30% with DENV infection only ($N = 42$), and 10% with a coinfection ($N = 15$). The conventional RT-PCR for CHIKV performed in 11 randomly selected positive samples and the amplicon sequences, confirmed the presence of CHIKV (Accession IDs: ON959484–ON959494). All DENV infections were identified as the DENV-1 serotype.

Of the 29 samples that were negative for DENV and CHIKV, 10 samples (all from 2019) were screened for additional viral pathogens by qPCR: these were found to be negative for ZIKV, Oropouche, Mayaro, and *Leptospira* spp. Two of these negative samples were randomly selected and subjected to metagenomic analysis and showed *Plasmodium* spp nucleotide sequences (Accession ID: SAMN27568483, SAMN27568586); nested PCR confirmed the presence of *Plasmodium falciparum* in these samples.

Symptom analysis. Cases positive for DENV reported more severe illness than cases positive for CHIKV; symptoms that were more frequent in DENV than CHIKV included fever, headache, myalgia, arthralgia, chills, anorexia, backache, stomachache, and vomiting. In contrast, CHIKV cases showed more frequently rash than DENV cases (28.4% versus 11.9%) (Figure 2). There were no statistically significant differences in the prevalence of reported symptoms by patient age for either illness (Supplemental Figures 1 and 2)



FIGURE 2. Prevalence of reported symptoms from DENV1 and CHIKV1 arbovirus cases. The prevalence of symptoms reported by participants in active surveillance who were confirmed to have a dengue virus (DENV) infection, a chikungunya virus (CHIKV) infection, a coinfection, or neither a DENV nor a CHIKV infection. *** Statistically significant difference in symptom prevalence between DENV and CHIKV cases.

Risk factor analysis of dengue and chikungunya cases. A total of 5,189 individuals were censused in 2018 and 2019 in our study. Unadjusted risk factors for symptomatic CHIKV infection (using logistic regression) were sex (female 1.65, 95% CI: 1.10–2.48), living in a more remote community (Santo Domingo odds ratio [OR]=3.60, 95% CI: 1.89–6.85; Santa María OR=3.88, 95% CI: 2.16–6.96 relative to living in Borbón), and occupation (Domestic OR=11.63, 95% CI: 1.59–85.37 relative to individuals reporting that they were unemployed). After adjusting for sex and occupation, living in a more remote community remained statistically significant risk for

Table 1. Community of residence and occupation are associated with symptomatic chikungunya virus infection

	Proportion of population	Incidence per 10,000	Bivariate	Multivariate
Age (years)				
OR				
0-18	46.10%	148.8 (108.4, 205.6)	Ref	-
19-36	25.20%	214.3 (149.2, 307.0)	1.43 (0.88, 2.33) (p=0.145)	-
37+	28.70%	220.2 (157.7, 306.9)	1.47 (0.93, 2.35) (p=0.102)	-
Sex				
Male	49.20%	139.6 (94.9, 184.4)	Ref	-
Female	50.80%	230.3 (173.9, 286.6)	1.65 (1.10, 2.48) (p=0.016)	1.63 (0.96, 2.77) (p=0.068)
Ethnicity				
Afro- Ecuadorian	72.80%	193.9 (155.1, 242.3)	Ref	-
Mestizo/other	21.50%	121.1 (71.8, 203.7)	0.62 (0.35, 1.10) (p=0.106)	-
Chachi	5.80%	302.9 (173.3, 587.7)	1.65 (0.86, 3.20) (p=0.134)	-
Community				
Borbón	35.20%	115.9 (76.4, 175.6)	Ref	Ref
Colon Eloy	15.60%	83.3 (39.8, 173.9)	0.72 (0.31, 1.68) (p=0.447)	0.69 (0.29, 1.62) (p=0.393)
Timbire	11.60%	128.5 (64.4, 255.2)	1.11 (0.49, 2.49) (p=0.803)	1.08 (0.48, 2.43) (p=0.957)
Maldonado	21.10%	211.1 (141.8, 313.4)	1.82 (1.02, 3.25) (p=0.042)	1.78 (0.99, 3.18) (p=0.052)
Sto Domingo	7.10%	417.4 (257.0, 672.2)	3.60 (1.89, 6.85) (p<0.001)	3.59 (1.87, 6.88) (p<0.001)
Sta Maria	9.50%	449.5 (300.2, 668.9)	3.88 (2.16, 6.96) (p<0.001)	3.73 (2.06, 6.74) (p<0.001)
Ever lived outside community				
No	43.80%	157.4 (114.2, 216.6)	Ref	-
Yes	56.20%	207.9 (162.7, 265.4)	1.32 (0.88, 1.98) (p=0.179)	-
Occupation				
None	6.30%	29.6 (4.2, 207.8)	Ref	Ref
Domestic work	16.20%	344.5 (241.7, 489.2)	11.63 (1.59, 85.37) (p=0.016)	8.75 (1.18, 65.02) (p=0.034)
Young child	34.30%	146.1 (100.3, 212.3)	4.93 (0.67, 36.33) (p=0.117)	4.66 (0.63, 34.33) (p=0.131)
Student	11.80%	188.7 (107.4, 329.9)	6.37 (0.83, 49.05) (p=0.075)	5.68 (0.74, 43.72) (p=0.094)
Teacher, works with children	2.70%	69.8 (9.8, 481.1)	2.36 (0.15, 37.69) (p=0.545)	1.78 (0.11, 28.58) (p=0.683)
Manual Labor	16.00%	209.3 (132.2, 330.2)	7.07 (0.94, 54.98) (p=0.057)	8.00 (1.05, 61.00) (p=0.045)
Small business	6.80%	164.4 (74.0, 361.8)	5.55 (0.67, 46.14) (p=0.983)	6.04 (0.72, 50.41) (p=0.097)
Government or healthcare	2.80%	-	-	-
Other	3.30%	281.7 (117.6, 661.8)	9.51 (1.11, 81.48) (p=0.040)	10.72 (1.25, 92.16) (p=0.031)

Table 2. Community of residence is associated with symptomatic dengue virus infection

	Proportion of population	Incidence per 10,000	Bivariate	Multivariate
Age, years				
			IRR	
0-18	46.10%	108.9 (74.8, 158.5)	Ref	-
19-36	25.20%	88.7 (50.4, 155.6)	0.81 (0.41, 1.61) (p=0.552)	-
37+	28.70%	103.6 (63.6, 168.6)	0.95 (0.51, 1.76) (p=0.873)	-
Sex				
				-
Male	49.20%	83.0 (54.7, 125.8)	Ref	-
Female	50.80%	120.6 (85.9, 169.3)	1.45 (0.85, 2.49) (p=0.175)	-
Race				
				-
Afro-Ecuadorian	72.80%	81.7 (57.8, 115.3)	Ref	Ref
Mestizo/other	21.50%	60.6 (28.9, 126.6)	0.74 (0.3, 1.68) (p=0.474)	0.88 (0.38, 2.00) (p=0.753)
Chachi	5.80%	513.4 (316.4, 824.2)	6.29 (3.45, 11.46) (p<0.001)	0.59 (0.31, 1.12) (p=0.106)
Community				
				-
Borbón	35.20%	15.8 (5.1, 48.9)	Ref	Ref
Colón Eloy	15.60%	-	-	-
Timbiré	11.60%	48.2 (15.5, 148.5)	3.05 (0.62, 15.10) (p=0.172)	2.93 (0.59, 14.65) (p=0.191)
Maldonado	21.10%	70.4 (35.2, 140.2)	4.45 (1.18, 16.78) (p=0.027)	4.36 (1.16, 16.48) (p=0.030)
Sto Domingo	7.10%	-	-	-
Sta María	9.50%	801.3 (594.4, 1073.4)	50.68 (15.69, 163.66) (p<0.001)	61.85 (18.60, 205.69) (p<0.001)
Ever lived outside community				
				-
No	43.80%	59.6 (35.3, 100.4)	Ref	-
Yes	56.20%	135.3 (99.8, 183.4)	0.99 (0.98, 1.02) (p=0.858)	-
Occupation				
				-
None	6.30%	29.6 (4.2, 207.8)	Ref	-
Domestic	16.20%	126.3 (70.1, 226.9)	4.26 (0.55, 33.02) (p=0.165)	-
Small child	34.30%	81.2 (49.0, 134.3)	2.74 (0.36, 20.73) (p=0.329)	-
Student	11.80%	188.7 (107.4, 329.9)	6.37 (0.83, 48.98) (p=0.075)	-
Teacher, works with children	2.70%	139.5 (34.9, 543.5)	4.71 (0.43, 51.93) (p=0.206)	-
Manual Labor	16.00%	127.9 (70.9, 229.7)	4.32 (0.56, 33.44) (p=0.161)	-
Small business	6.80%	27.4 (3.9, 192.3)	0.92 (0.06, 14.78) (p=0.959)	-
Government or healthcare	2.80%	65.2 (9.2, 450.6)	2.20 (0.14, 35.19) (p=0.577)	-
Other	3.30%	56.3 (7.9, 390.7)	1.90 (0.12, 30.40) (p=0.650)	-

symptomatic CHIKV infection (Santa Maria OR= 3.73, 95% CI: 2.06–6.74; Santo Domingo OR= 3.59, 95% CI: 1.87–6.88 relative to living in Borbón) (Table 1).

Risk of symptomatic DENV was associated with individuals who reported indigenous Chachi ethnicity (compared with Afro-Ecuadorian) and who lived in the remote community of Santa Maria (compared with Borbón) (OR=6.29, 95% CI: 3.45–11.46); (OR=50.68, 95% CI: 15.69–163.66), respectively (Table 2). These results were due to a DENV outbreak in the Chachi neighborhood of Santa Maria.

Comparison of dengue and chikungunya infections from the active versus passive surveillance. During the same period as the active surveillance (May 2019–February 2020), the MOH passive surveillance system identified 65 cases of dengue in our six study communities. No CHIKF, Zika, Oropouche, or Mayaro cases were identified by the MOH during this time (Figure 3). The highest number of dengue ($N = 19$) and chikungunya ($N = 40$) cases, identified through active surveillance, was reported during the month of June (Figure 3). Similarly, the MOH also reported the greatest number of dengue cases in June (21 cases).

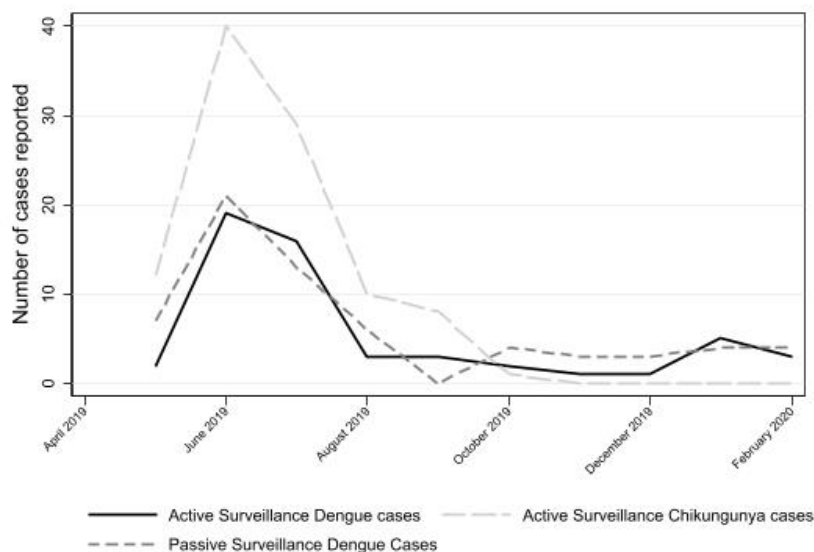


FIGURE 3. Number of dengue cases reported according the passive surveillance from the Ministry of Health; number of Dengue and Chikungunya cases reported by active Surveillance from May 2019 to February 2020

Symptoms reported by dengue cases captured by the MOH were more severe than dengue and chikungunya cases identified through active community surveillance (Table 3). Twenty cases were identified by both the MOH surveillance and the study active surveillance, and 18 of these had complete laboratory results. Of these 18 cases, 14 cases were DENV+, one was CHIKV+, two were DENV-CHIKV coinfections, and one was PCR negative for both viruses.

Table 3. Demographic/Clinical characteristics of individuals with dengue virus/ chikungunya virus stratified by passive vs. active surveillance.

Variable	Active Surveillance Dengue Cases	Active Surveillance Chikungunya Cases	Passive Surveillance Dengue Cases
	<i>N</i> = 80 (%)	<i>N</i> = 96 (%)	<i>N</i> = 152
Age, median years (IQR)	18.5 (11 – 36.5)	6.5 (13-40.2)	19 (12-28.5)
Female Sex	47 (58.8)	59 (61.5)	67 (44.1)
Clinical Characteristics			
Fever	77 (96.2)	82 (85.4)	141 (92.8)
Headache	70 (87.5)	66 (68.8)	99 (65.1)
Myalgia	43 (53.8)	26 (27.1)	88 (57.8)
Arthralgia	39 (48.8)	35 (36.5)	98 (64.5)
Abdominal Pain	21 (26.2)	13 (13.5)	24 (15.8)
Rash	10 (12.5)	23 (24.0)	5 (3.3)
Diarrhea	1 (1.3)	1 (1.0)	6 (3.9)
IQR = interquartile range			

DISCUSSION

We found that CHIKV infections went undetected in our study region in northern coastal Ecuador. In 2019 and early 2020, DENV and CHIKV co-circulated and were responsible for approximately 85% of febrile cases captured by our active surveillance (70% of these arbovirus cases were caused by CHIKV). As expected, reported symptoms were similar between the two illnesses, reinforcing the importance of arboviral screening using molecular tools such as real-time PCR as a method for detection of multiple arboviral diseases. Given that molecular screening is limited in many settings with high arbovirus burden and given that DENV infections are assumed to be the primary arbovirus, CHIKV circulation may be under-appreciated globally.

In this study, 14.5% (*N* = 10) of arbovirus-like illnesses were negative for DENV, CHIKV, and other common important viral pathogens in our study area. We found that two arbitrarily

selected negative samples were positive for *Plasmodium falciparum*. The MOH reported 146 cases of *Plasmodium falciparum* in 2019 in the region.^{15,30} In a previous study, Oropouche virus was identified in a dengue negative serum sample from our affiliated hospital in Esmeraldas.³¹ These results indicate that although DENV is common cause of febrile disease, diverse tropical pathogens with common fevers affect these communities. Our reports underline the need of a multiplex approach for febrile diseases detection because different therapeutic regimes and public health measures are necessary to control these pathogens.

Our analysis likely underestimates the true prevalence of DENV in these communities because we used only PCR-confirmed cases and excluded cases that were positive by NS1 (Standard Diagnostic Inc.) and confirmed by IgM ELISA (PanBio, Abbott, Brisbane, Australia). This choice was made to maximize our ability to differentiate between DENV and CHIKV; however, as a result, prevalence estimates are slightly lower compared with other reports by our study team.³²

Febrile diseases like DF and CHIKF show similar clinical presentation³³ We found that individuals with DENV infections reported a higher rate of symptoms, with the exception of rash, which was more often reported in CHIKV cases. Other studies have also suggested that although rash may be present in both illnesses, it is more common in early chikungunya cases.³⁴ On the other hand, the prevalence of arthralgia was higher among DENV cases than CHIKV cases. This finding is in accordance with Kuno's 2015 review reporting more arthralgia among severe dengue cases due to consecutive outbreaks of different dengue serotypes or chikungunya.³⁵ This result is, however, in contrast with many previous studies that have shown that arthralgia is often more prominent in patients with chikungunya.³⁶ Our active surveillance identified cases an average of 3

days after symptom onset; therefore, recall bias was unlikely to account for this unexpected finding.

The chikungunya risk factors we identified in our study were female, reside in a more rural community and reporting an occupation involving domestic work (i.e., being a housewife) or manual labor. These findings are similar to a previous study in a rural Malaysian cohort in which sex and rural occupancy were predictors of seropositivity for CHIKV, estimating that rural occupancy had 3.9 higher odds than urban occupancy.³⁷ Fred et al.³⁸ reported that outdoor activities such as farm work was a risk factor for CHIKV. Similarly, in a cross-sectional study performed in Quinindé, Esmeraldas, found that women were more likely to have CHIKF than men.³⁹

Our active surveillance data indicated that chikungunya cases went undetected by the passive surveillance system operated by the Ecuadorian Ministry of Public Health. A major challenge with the use of passive surveillance data is the reliance of clinical symptoms for diagnosis, which results in greater underreporting of the diseases that present with broad symptoms similar to other more known diseases.⁴⁰ Typically, active community-based surveillance captures significantly more arboviral disease including mild cases, like dengue, when compared with passive surveillance studies that focus on more severe cases.⁴¹ Despite research demonstrating that active surveillance is an important tool for estimating disease burden, the expense and logistics required for active surveillance posed a challenge to its implementation.⁴²

Therefore, active surveillance data from sentinel sites and research studies around the world like our study provide key insights into the dynamics of arboviral diseases such as dengue and chikungunya; however, for many countries, active surveillance is not feasible for multiple arboviruses given resource limitations. This study demonstrated that active surveillance of febrile illness in remote rural sites is key for the identification of possible sources and routes of

transmission for infectious diseases that may circulate endemically. Here we show that CHIKV is still prevalent in rural localities of northwestern Ecuador despite significant CHIKV circulation not been reported since 2018 in Esmeraldas province. Moreover, our data demonstrate that active surveillance using molecular characterization is able to differentiate dengue and chikungunya cases with similar symptoms that are often misdiagnosed clinically. These findings highlight the value of active surveillance data from sentinel sites and prospective research studies to provide key epidemiological insights into dynamics of arboviral diseases like dengue and chikungunya in Ecuador.

Received April 29, 2022. Accepted for publication September 10, 2022.

Published online November 14, 2022.

Note: Supplemental tables and figures appear at www.ajtmh.org.

Acknowledgments: We thank Veronica Barragan for running the polymerase chain reaction (PCR) test to detect *Leptospira*, Fabián Saenz for his PCR protocol test for *Plasmodium falciparum* detection, and Lesly Simbaña for helping in metagenomic analysis

Financial support: This study was funded by the National Institute of Allergy and Infectious Diseases, National Institute of Health (R01 AI132372-02), titled “Zika and Dengue Co-circulation Under Environmental Change and Urbanization” and by Universidad San Francisco de Quito (USFQ) Collaboration Grant Hubi 12477, titled “Detección metagenómica de nuevos virus causantes de enfermedades febriles en la población de la Costa Ecuatoriana.”

Authors' addresses: Sully Márquez and Gabriel Trueba, Instituto de Microbiología, Universidad San Francisco de Quito, Quito, Ecuador, E-mails: smarqueza@usfq.edu.ec and gtrueba@usfq.edu.ec. Gwenyth O. Lee, Julio Zuniga, and Joseph N. S. Eisenberg, Department of

Epidemiology, School of Public Health, University of Michigan, Ann Arbor, Michigan, E-mails: golee@umich.edu, julioz@umich.edu, and jnse@umich.edu. Paulina Andrade, Colegio de Ciencias Biologicas y Ambientales COCIBA, Universidad San Francisco de Quito, Quito, Ecuador, and Division of Infectious Diseases and Vaccinology, School of Public Health, University of California, Berkeley, California, E-mail: paulinaandradeproano@berkeley.edu. Josefina Coloma, Division of Infectious Diseases and Vaccinology, School of Public Health, University of California, Berkeley, California, Email:colomaj@berkeley.edu.

REFERENCES

1. Wijesinghe C, Gunatilake J, Kusumawathie PHD, Sirisena PDNN, Daulagala SWPL, Iqbal BN, Noordeen F, 2021. Circulating dengue virus serotypes and vertical transmission in Aedes larvae during outbreak and inter-outbreak seasons in a high den-gue risk area of Sri Lanka. *Parasit Vectors 14*: 614.
2. Harapan H, Michie A, Mudatsir M, Nusa R, Yohan B, Wagner AL, Sasmono RT, Imrie A, 2019. Chikungunya virus infection in Indonesia: a systematic review and evolutionary analysis. *BMC Infect Dis 19*: 243.
3. World Health Organization, 2022. Dengue and severe dengue. Available at: <https://www.who.int/news-room/fact-sheets/detail/dengue-and-severe-dengue>. Accessed November 1, 2021.
4. Guzman MG, Gubler DJ, Izquierdo A, Martinez E, Halstead SB, 2016. Dengue infection. *Nat Rev Dis Primers 2*: 16055.

5. McFee RB, 2018. Selected mosquito-borne illnesses-Chikungunya. *Dis Mon* 64: 222–234.
6. Pathak H, Mohan MC, Ravindran V, 2019. Chikungunya arthritis. *Clin Med* 19: 381–385.
7. Carabali M, Jaramillo-Ramirez GI, Rivera VA, Possu NJM, Restrepo BN, Zinszer K, 2021. Assessing the reporting of dengue, chikungunya and zika to the national surveillance system in Colombia from 2014–2017: a capture-recapture analysis accounting for misclassification of arboviral diagnostics. *PLoS Negl Trop Dis* 15: 1–16.
8. Gould E, Pettersson J, Higgs S, Charrel R, de Lamballerie X, 2017. Emerging arboviruses: why today? *One Health* 4: 1–13.
9. Cattarino L, Rodriguez-Barraquer I, Imai N, Cummings DAT, Ferguson NM, 2020. Mapping global variation in dengue transmission intensity. *Sci Transl Med* 12: eaax4144.
10. de Brito CAA, Freitas ARR, Said RF, Falc~ao MB, da Cunha RV, Siqueira AM, Teixeira MG, Ribeiro GS, de Brito MCM, Cavalcanti LP de G, 2020. Classification of chikungunya cases: a proposal. *Rev Soc Bras Med Trop* 53: 1–5.
11. Pan-American Health Organization/World Health Organization, 2019. Epidemiological update. Available at: https://www3.paho.org/hq/index.php?option=com_docman&view=download&category_slug=dengue-2217&alias=50963-11-november-2019-dengue-epidemiological-update-1&Itemid=270&lang=en. Accessed January 8, 2022.
12. de Lima STS et al., 2021. Fatal outcome of chikungunya virus infection in Brazil. *Clin Infect Dis* 73: e2436–e2443.

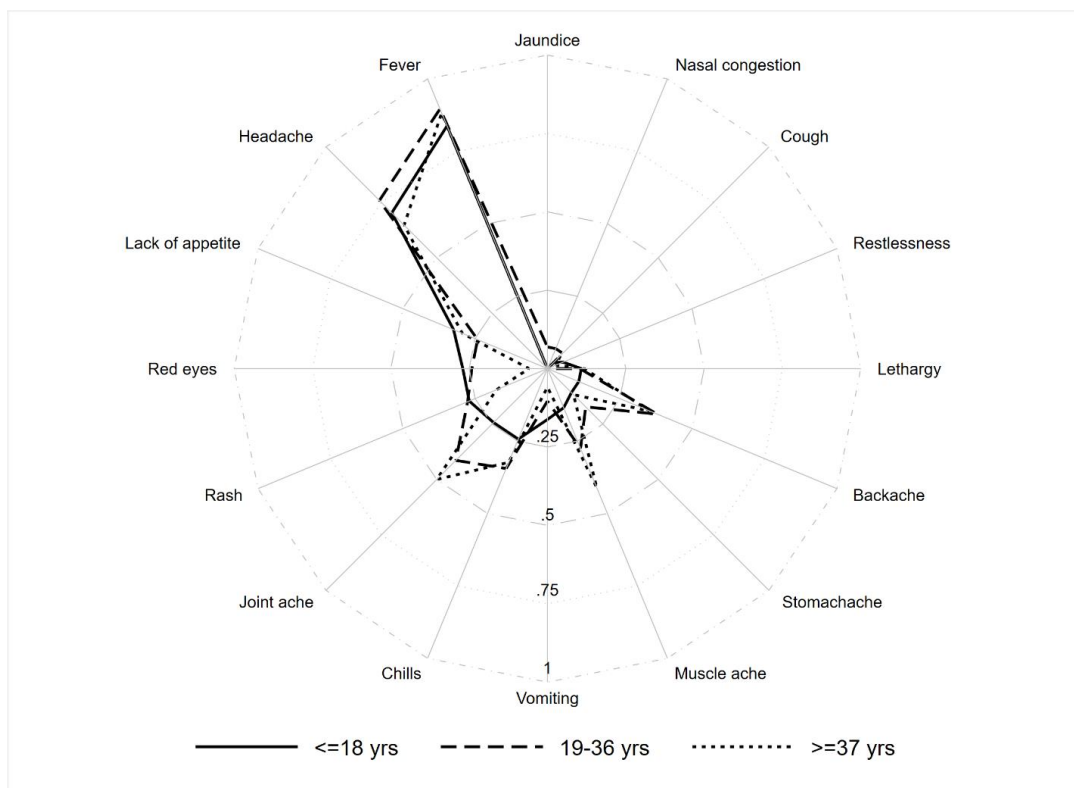
13. Real J, Regato M, Burgos V, Jurado E, 2017. Evolucion del virus dengue en el Ecuador: Periodo 2000 a 2015 [Evolution of dengue virus in Ecuador 2000–2015]. *An Fac Med (Peru)* 78: 29–35.
14. Ministerio de Salud Publica, 2021. Gaceta vectores SE 12.
15. Ministerio de Salud Publica, 2019. Gaceta vectores SE 52. Available at: <https://www.salud.gob.ec/wp-content/uploads/2020/02/GACETA-VECTORES-SE-52.pdf>. Accessed January 10, 2022.
16. Cevallos V, Ponce P, Waggoner JJ, Pinsky BA, Coloma J, Quiroga C, Morales D, Cardenas MJ, 2018. Zika and Chikungunya virus detection in naturally infected *Aedes aegypti* in Ecuador. *Acta Trop* 177: 74–80.
17. Eisenberg JNS et al., 2012. In-roads to the spread of antibiotic resistance: regional patterns of microbial transmission in northern coastal Ecuador. *J R Soc Interface* 9: 1029–1039.
18. Cifuentes SG, Trostle J, Trueba G, Milbrath M, Baldeon ME, Coloma J, Eisenberg JNS, 2013. Transition in the cause of fever from malaria to dengue, northwestern Ecuador, 1990–2011. *Emerg Infect Dis* 19: 1642–1645.
19. Zelner JL, Trostle J, Goldstick JE, Cevallos W, House JS, Eisenberg JNS, 2012. Social connectedness and disease transmission: social organization, cohesion, village context, and infection risk in rural Ecuador. *Am J Public Health* 102: 2233–2239.
20. Eisenberg JNS et al., 2006. Environmental change and infectious disease: how new roads affect the transmission of diarrheal pathogens in rural Ecuador. *Proc Natl Acad Sci USA* 103:19460–19465.

21. Sierra R, 1999. Traditional resource-use systems and tropical deforestation in a multi-ethnic region in north-west Ecuador. *Environ Conserv* 26: 136–145.
22. Waggoner JJ et al., 2016. Single-reaction multiplex reverse transcription PCR for detection of Zika, chikungunya, and dengue viruses. *Emerg Infect Dis* 22: 1295–1297.
23. Harris E, Roberts TG, Smith L, Selle J, Kramer LD, Valle S, Sandoval E, Balmaseda A, 1998. Typing of dengue viruses in clinical specimens and mosquitoes by single-tube multiplex reverse transcriptase PCR. *J Clin Microbiol* 36: 2634–2639.
24. Wise EL et al., 2020. Oropouche virus cases identified in Ecuador using an optimised qRT-PCR informed by metagenomic sequencing. *PLoS Negl Trop Dis* 14: 1–15.
25. Powers ARJ, 2010. Diagnostic Virology Protocols, 2nd edition. Totowa, NJ: Humana Press.
26. Stoddard RA, Gee JE, Wilkins PP, McCaustland K, Hoffmaster AR, 2009. Detection of pathogenic *Leptospira* spp. Through TaqMan polymerase chain reaction targeting the LipL32 gene. *Diagn Microbiol Infect Dis* 64: 247–255.
27. Kafetzopoulou LE et al., 2018. Assessment of metagenomic Nanopore and Illumina sequencing for recovering whole genome sequences of chikungunya and dengue viruses directly from clinical samples. *Euro Surveill* 23: 1800228.
28. Menzel P, Ng KL, Krogh A, 2016. Fast and sensitive taxonomic classification for metagenomics with Kaiju. *Nat Commun* 7: 11257.
29. Snounou G, 1996. Detection and identification of the four malaria parasite species infecting humans by PCR amplification. *Methods Mol Biol* 50: 263–291.

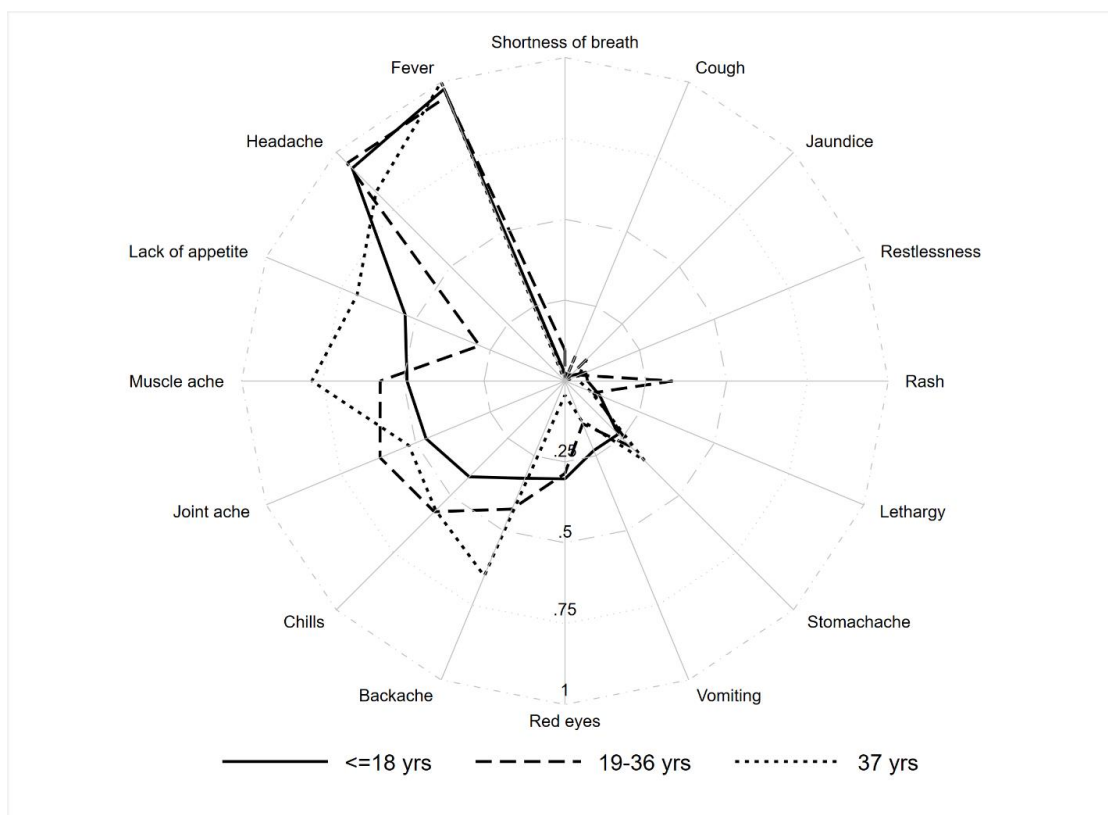
30. Vera-Arias CA, Castro LE, Gomez-Obando J, Saenz FE, 2019. Diverse origin of *Plasmodium falciparum* in northwest Ecuador. *Malar J* 18: 251.
31. Wise EL et al., 2018. Isolation of Oropouche virus from febrile patient, Ecuador. United States.
32. Lee GO et al., 2021. A dengue outbreak in a rural community in Northern Coastal Ecuador: an analysis using unmanned aerial vehicle mapping. *PLoS Negl Trop Dis* 15: e0009679.
33. Beltrán-Silva SL, Chacon-Hernandez SS, Moreno-Palacios E, Pereyra-Molina JA, 2018. Clinical and differential diagnosis: dengue, chikungunya and Zika. *Rev Med Hosp Gen (Mex)* 81:146–153.
34. Mohd Zim MA, Sam I-C, Omar SFS, Chan YF, AbuBakar S, Kamarulzaman A., 2013. Chikungunya infection in Malaysia: comparison with dengue infection in adults and predictors of persistent arthralgia. *J Clin Virol* 56: 141–145.
35. Kuno G, 2015. A re-examination of the history of etiologic confusion between dengue and Chikungunya. *PLoS Negl Trop Dis* 9: e0004101.
36. Laoprasopwattana K, Kaewjungwad L, Jarumanokul R, Geater A, 2012. Differential diagnosis of Chikungunya, dengue viral infection and other acute febrile illnesses in children. *Pediatr Infect Dis J* 31: 459–463.
37. Vong S et al., 2010. Dengue incidence in urban and rural Cambodia: results from population-based active fever surveillance, 2006–2008. *PLoS Negl Trop Dis* 4: e903.
38. Fred A et al., 2018. Individual and contextual risk factors for chikungunya virus infection: the SEROCHIK cross-sectional population-based study. *Epidemiol Infect* 146: 1056–1064.

39. Chis Ster I, Rodriguez A, Romero NC, Lopez A, Chico M, Montgomery J, Cooper P, 2020. Age-dependent seroprevalence of dengue and chikungunya: inference from a cross-sectional analysis in Esmeraldas province in coastal Ecuador. *BMJ Open* 10: e040735.
40. Chow A, Ho H, Win M-K, Leo Y-S, 2017. Assessing sensitivity and specificity of surveillance case definitions for Zika virus disease. *Emerg Infect Dis* 23: 677–679.
41. Sarti E, L’Azou M, Mercado M, Kuri P, Siqueira JBJ, Solis E, Noriega F, Ochiai RL., 2016. A comparative study on active and passive epidemiological surveillance for dengue in five countries of Latin America. *Int J Infect Dis* 44: 44–49.
42. World Health Organization, 2018. A Toolkit for National Dengue Burden Estimation. Geneva, Switzerland: WHO.

SUPPLEMENTAL FIGURES



Supplemental Figure 1. Reported symptoms among individuals with chikungunya, by age



Supplemental Figure 2. Reported symptoms among individuals with dengue, by age

SUPPLEMENTAL TABLES

Supplementary table 1. PCR/RT-PCR assays used for DENV, OROV, MAYV and *Leptospira* detection

Pathogen (s)	Assay	Forward and reverse primers sequence (5'-3')	Probe sequence (5'-3')	Reference
CHIKV	Conventional RT-PCR	CHIK F 10011: 5'-CAA ATA GCA ACA AAC CCG CHIK R 10396: 5'-GGC CGT CGA GAA AGA GAT		
DENV serotypes 1 to 4	Conventional RT-PCR	DI: 5'-TCA ATA TGC TGA AAC GCG CGA GAA ACC G TS1: 5'-CGT CTC AGT GAT CCG GGG G TS2: 5'-CGC CAC AAG GGC CAT GAA CAG TS3: 5'-TAA CAT CATCAT GAG ACA GAG C TS4: 5'-TGT TGT CTT AAA CAA GAG AGGC		Harris <i>et al</i> , 1998 (23)
OROV	qPCR	OROV F 5-CATTTGAAGCTAGATACGGACAA Ec2 R 5'-CATCTTTGGCCTTCTTTTRG	OROV P FAM-CAATGCTGGTGTGTAG	Wise <i>et al</i> , 2020 (24)
MAYV	qPCR	MAYARO 9666 F 5'-CATGGCCTACCTGTGGGATAATA MAYARO 9797 R 5'-GCACTCCCGACGCTCACTG	MAYARO 9734(-) P FAM TCGGCGCAACATGTAGTCAGGATAA BHQ1	Powers 2010 (25)
<i>Leptospira</i> spp.	qPCR	LipL32-45F 5'-AAG CAT TACCGC TTG TGG TG LipL32-286R 5'-GAACTCCA TTTCAGCGATT	LipL32-189P FAM-5'-AAAGCCAGGACAAGCGCCG-3'-BHQ1	Stoddard <i>et al</i> , 2009 (26)
<i>Plasmodium falciparum</i>	Conventional nested PCR	PLU5 5'-CCTGTTCCTTAACTTC PLU6 5'-TTAAAATTGTTGCAGTTAAAACG FAL 1 5'-TTAAACTGGTTTGGGAAAACCAATATATT FAL 2 5'-ACACAATGAACTCAATCATCATGACTACCCGTC		Snounou, 1996 (29)

CHAPTER 3

Emerging infectious diseases. First published: April 11 2023

doi: [10.3201/eid2905.221226](https://doi.org/10.3201/eid2905.221226)

Phylogenetic Analysis of Transmission Dynamics of Dengue in Large and Small Population Centers, Northern Ecuador

Sully Márquez✉, Gwenyth Lee, Bernardo Gutiérrez, Shannon Bennett, Josefina Coloma¹, Joseph N.S. Eisenberg¹, and Gabriel Trueba¹

Author affiliations: Universidad San Francisco de Quito, Quito, Ecuador (S. Márquez, B. Gutiérrez, G. Trueba); University of Michigan, Ann Arbor, Michigan, USA (G. Lee, J.N.S. Eisenberg); University of Oxford, Oxford, UK (B. Gutiérrez); Institute for Biodiversity Science and Sustainability, California Academy of Sciences, San Francisco, California, USA (S. Bennett); University of California, Berkeley, Berkeley, California, USA (J. Coloma)

Abstract

Although dengue is typically considered an urban disease, rural communities are also at high risk. To clarify dynamics of dengue virus (DENV) transmission in settings with characteristics generally considered rural (e.g., lower population density, remoteness), we conducted a phylogenetic analysis in 6 communities in northwestern Ecuador. DENV RNA was detected by PCR in 121/488 serum samples collected from febrile case-patients during 2019–2021. Phylogenetic analysis of 27 samples from Ecuador and other countries in South America confirmed that DENV-1 circulated during May 2019–March 2020 and DENV-2 circulated during December 2020–July 2021. Combining locality and isolation dates, we found strong evidence that DENV entered Ecuador through the northern province of Esmeraldas. Phylogenetic patterns suggest that, within this province, communities with larger populations and commercial centers were more often the source of DENV but that smaller, remote communities also play a role in regional transmission dynamics.

INTRODUCTION

Dengue virus (DENV) is a vectorborne tropical disease transmitted by *Aedes aegypti* and *Ae. albopictus* mosquitoes. Globally, an estimated 390 million cases occur per year, and 3.9 billion persons are at risk for infection (1). Dengue is endemic to 100 countries; southeast Asia is the most severely affected region, followed by the western Pacific and the Americas (1).

Dengue is considered an urban disease because transmission is often reported in areas with high population density. However, human mobility and active commerce have increased in classically defined rural sectors where population density is generally lower, influencing DENV transmission. DENV transmission in rural sectors is often reported to occur at similar rates as urban areas (2–4). More remote rural areas can also serve as a source for emerging febrile diseases, often through cases introduced through cross-border movement. For instance, in Laos, surveillance of fevers in rural areas provided evidence that more DENV serotypes were circulating in rural areas than in urban ones (5). Those introductions highlight the need for highly coordinated and timely arbovirus surveillance at the local and national level to enable early warning of potential DENV outbreaks among neighboring countries (6,7). In Asia, cross-border surveillance systems and networks such as UNITEDengue have been established to share data on disease outbreaks to monitor and control the disease more effectively (8).

DENV has been endemic to South America since the 1980s and to Ecuador since 1988. Generally, only 1 serotype circulates episodically within a region in South America, but all serotypes have circulated and reemerged in cycles (9,10). During 2010–2019, explosive epidemics were reported in the Americas; cases peaked at 3.1 million in 2019 (11) After a period of low prevalence in 2020,

likely because of underreporting caused by the COVID-19 pandemic (12) and limited human movement between regions, Ecuador reported an increase of DENV cases in 2021.

Esmeraldas Province is located in the northern coast of Ecuador and shares a border with the Nariño department of Colombia. Fifty-seven percent of the population lives in poverty and lacks basic needs such as potable water and garbage collection services (C. Robbins, unpub. data, [https://digitalrepository.trincoll.edu/cgi/viewcontent.cgi?article=1857&context=thesesExternal Link](https://digitalrepository.trincoll.edu/cgi/viewcontent.cgi?article=1857&context=thesesExternalLink)). In a previous study conducted in rural communities in Esmeraldas during 2013–2014, we detected circulation of all DENV serotypes, whereas in the city of Esmeraldas, the largest city in the province, we detected only 2 serotypes (DENV-1 and DENV-2) (13). Those findings suggest that rural communities can act as a source of DENV transmission. High human mobility and levels of commerce reported in towns along the Colombia border suggest that DENV cases found in rural communities in Ecuador were likely introduced from Colombia (C. Robbins, unpub. data).

On the basis of this previous evidence, the aim of this study was to extract DENV nucleotide sequences obtained from serum samples from active DENV cases collected during 2019–2021 in Esmeraldas Province. We investigated the phylogenetic relationship of those sequences to DENV nucleotide sequences from throughout Ecuador to learn more about the role of rural DENV transmission dynamics in northwestern Ecuador.

MATERIALS AND METHODS

Study Site

The study was conducted as part of an ongoing arboviral surveillance study in Cantón Eloy Alfaro, Esmeraldas Province, northwestern Ecuador. In brief, we selected 6 communities according to

their gradient of remoteness: 2 remote riverine communities with no road access (Santa María and Santo Domingo), 3 communities with road access (Colón Eloy, Timbiré, and Maldonado), and 1 commercial center (Borbón) ([Figure 1](#)).



Figure 1. Locations of the 6 rural communities in Esmeraldas Province and the city of Esmeraldas for study of transmission dynamics of dengue in large and small population centers, northern Ecuador.

Sample Collection

We collected data during May 2019–December 2021 by using active fever surveillance at the individual level. Except in the town of Borbón, community residents >2 years of age were invited to participate in prospective active surveillance. In Borbón, we invited a random sample of 500 households located in the town center to participate. In total, 1,460 households and 5,957 participants provided ≥ 1 month of active surveillance data from the study period of May 2019–December 2021. A group of community members trained to identify cases (brigadistas) conducted home visits weekly during the rainy season (June–October) and every 2 weeks during the dry

season (November–December). The surveillance protocol began with brigadistas inquiring whether any household members had experienced fever, red eyes, or rash within the previous 7 days. When a symptomatic person was identified, the brigadista alerted the study nurse, who then followed up with a questionnaire asking about ≈21 symptoms associated with DENV and travel history. Participants experiencing diarrhea or upper respiratory symptoms were excluded. When a DENV-like illness was identified (fever plus rash, myalgia, arthralgia), a blood sample was immediately collected and a rapid diagnostic test performed (data not shown). Serum derived from the blood sample was stored in liquid nitrogen for transportation to the laboratory, where the samples were kept at -80°C until processing. The study was approved by the Bioethics committee at the Universidad San Francisco de Quito, the University of Michigan, and the Ecuadorian Ministry of Health.

RNA Extraction, Reverse Transcription PCR, and Sequencing

We extracted viral RNA from 488 febrile serum samples by using the QIAamp Viral RNA Mini Kit (QIAGEN, <https://www.qiagen.com>External Link), according to manufacturer instructions. We used this RNA as a template for the triplex real time reverse transcription PCR (RT-PCR) Zika-Dengue-Chikungunya assay, which we performed to confirm infection and etiology (14). We serotyped 121 samples positive for dengue using a conventional RT-PCR with some modifications (15).

We considered 27 positive samples with a real-time PCR cycle threshold (Ct) value of <30 optimal for sequencing. We amplified a 20- μL aliquot of cDNA obtained using the Superscript IV protocol by multiplex PCR, combining 5 μL of 5X Q5 Reaction Buffer, 0.5 μL of 10 mM dNTPs, 0.25 μL of Q5 DNA polymerase, 15.25 μL nuclease-free water, and 1.5 μL primer pool A (10 μM). For DENV-1 and DENV-2, we added 1.5 μL primer pool B (10 μM) (16). We selected the samples

that showed a 900 bp band in pool A and pool B mix for sequencing. Using 2.5 µl of PCR products from each pool diluted in 45 µl of PCR water, we prepared the cDNA MinION library by using a native barcoding kit (NB-114) with a ligation sequencing kit (LSK-109) following manufacturers' instructions and loaded it into the MinION flow cell (FLO-MIN 106) (Oxford Nanopore Technologies, <https://nanoporetech.com>External Link). We performed demultiplexing and adaptor removal with Porechop version 0.2.3_seqan 2.1.1 (<https://github.com/rrwick/Porechop>External Link) and assembled the sequencing reads with a de novo assembly approach using Spades version 3.13.0 (<http://cab.spbu.ru/files/release3.13.0/manual.html>External Link). Next, we mapped the reads in Minimap2 version 2.17-R941 (<https://github.com/lh3/minimap2>External Link) against reference genomes for DENV-1 (GenBank accession no. NC_001477.1) and DENV-2 (accession no. NC_001474.2). The consensus sequence was generated with Samtools version 1.7 (<http://www.htslib.org/doc/1.7/samtools.html>External Link) and the serotype was confirmed using Genome Detective Arbovirus Typing software Tool version 1.137 (17) and BLAST (<https://blast.ncbi.nlm.nih.gov/Blast.cgi>External Link).

Phylogenetic Analysis

In total, we generated 9 DENV-1 and 13 DENV-2 genome sequences from our field site and used them for the phylogenetic analysis (22 samples). In addition, we sequenced 5 samples from the national surveillance system at the reference hospital of the city of Esmeraldas, the capital of the province (3 DENV-1 and 2 DENV-2) (accession nos. SRR1593089–SRR15793115). The hospital samples were selected for patients residing in Esmeraldas on the basis of the patient's clinical record. To augment the Ecuador data for phylogenetic analysis, we incorporated 22 sequences from GenBank, 21 representing El Oro Province (located in southern Ecuador) and 1 sample from Esmeraldas. To enable cross-country analysis, we included available GenBank sequences from

Argentina, Brazil, Perú, Nicaragua, Belize, Venezuela, and Colombia. Before generating an alignment, we identified genomes from the National Center for Biotechnology Information by randomly selecting the results of a BLAST of our whole-genome sequences for each serotype separately. We generated alignments by using MAFFT on XSEDE version 7.471 (<https://mafft.cbrc.jp/alignment/server>External Link), then visually inspected and refined them in Aliview version 1.28 (<https://github.com/Aliview/Aliview>External Link).

We constructed a maximum-likelihood phylogenetic tree for each serotype by using RaxML-HPC Blackbox version 8.2.12 (<https://cme.h-its.org/exelixis/web/software/raxml>External Link) under a general time-reversible substitution model with 1,000 bootstrap replicates and plotting the resulting tree in FigTree version 1.4.4 (<http://tree.bio.ed.ac.uk/software/figtree>External Link). We explored the temporal signal of the datasets by performing a root-to-tip genetic distance analysis using TempEst version 1.5.3 (18) and rooted the trees using the R^2 method. To explore the temporal patterns of DENV spread, we constructed Bayesian time-calibrated trees by using BEAST version 1.10.4 under a Hasegawa-Kishino-Yano substitution model and an uncorrelated lognormal relaxed molecular clock (19). We used a Bayesian skyline tree prior (20) with 10 groups and a piece-wise constant reconstruction. We ran Markov chain Monte Carlo chains for 100 million steps and logged trees every 1,000 steps; we discarded the first 10% of the trees as burn-in by using TreeAnnotator version 1.10.4 (<https://beast.community/treeannotator>). We assessed adequate mixing and convergence of model parameters, defined by effective sample sizes of >200, in Tracer version 1.7.1 (21) and summarized maximum clade credibility (MCC) trees for each run using TreeAnnotator version 1.10.4, summarizing node ages as median heights.

RESULTS

Samples Collected and DENV Serotypes Identified

During May 2019–December 2021, we collected 488 serum samples from febrile patients during the household-based active fever surveillance study: 187 samples from remote riverine communities with no road access (146 from Santa María patients and 41 from Santo Domingo); 181 samples from communities with road access (61 from Colon Eloy, 78 from Maldonado, and 42 from Timbiré), and 120 samples from the commercial center, Borbón. Of the 488 samples, 121 were PCR-positive for DENV. A percentage of the samples were positive for chikungunya virus, as reported elsewhere (22). Common symptoms among patients were fever, headache, muscle aches, joint aches, chills, backache, and stomachache. Cases confirmed in June 2019 (19 cases) and July 2019 (16 cases) were all identified as DENV-1, whereas cases detected in January and March 2021 (12 cases) were all identified as DENV-2 (Figure 2). We did not obtain any samples during April 2020–November 2020 because of COVID-19 pandemic lockdown restrictions in Ecuador.

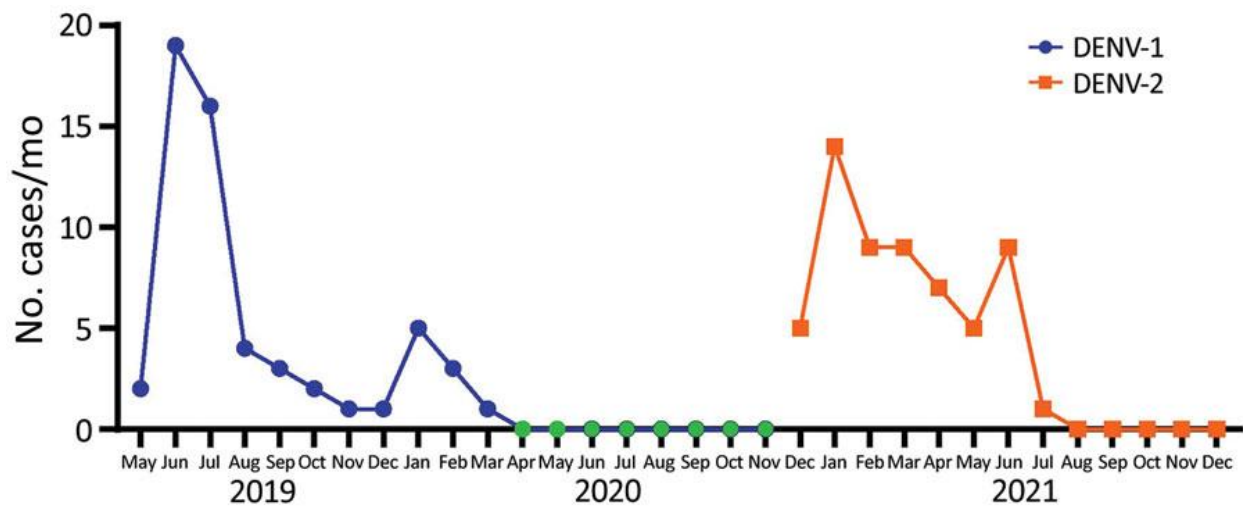


Figure 2. Number of febrile cases per month for DENV-1 (blue) and DENV-2 (orange) in study of transmission dynamics of dengue in large and small population centers, northern Ecuador, May 2019–December 2021. During April 2020–November 2020 (green), sampling was not conducted because of COVID-19 lockdown in Ecuador. DENV, dengue virus.

Phylogenetic Analysis of DENV-1 Serotype in Ecuador

The MCC tree for DENV-1 generated in BEAST software (<http://beast.community>) using whole-genome sequencing indicated at least 2 instances of viral variant exchange (viral exchanges) between countries. Those viral exchanges, inferred from the genetic similarities highlighted in the phylogeny, suggest that the strains were introduced into Ecuador. In one instance, a single Ecuador sequence collected in 2014 from Esmeraldas province ([Figure 3](#)), lower portion of clade I) shares

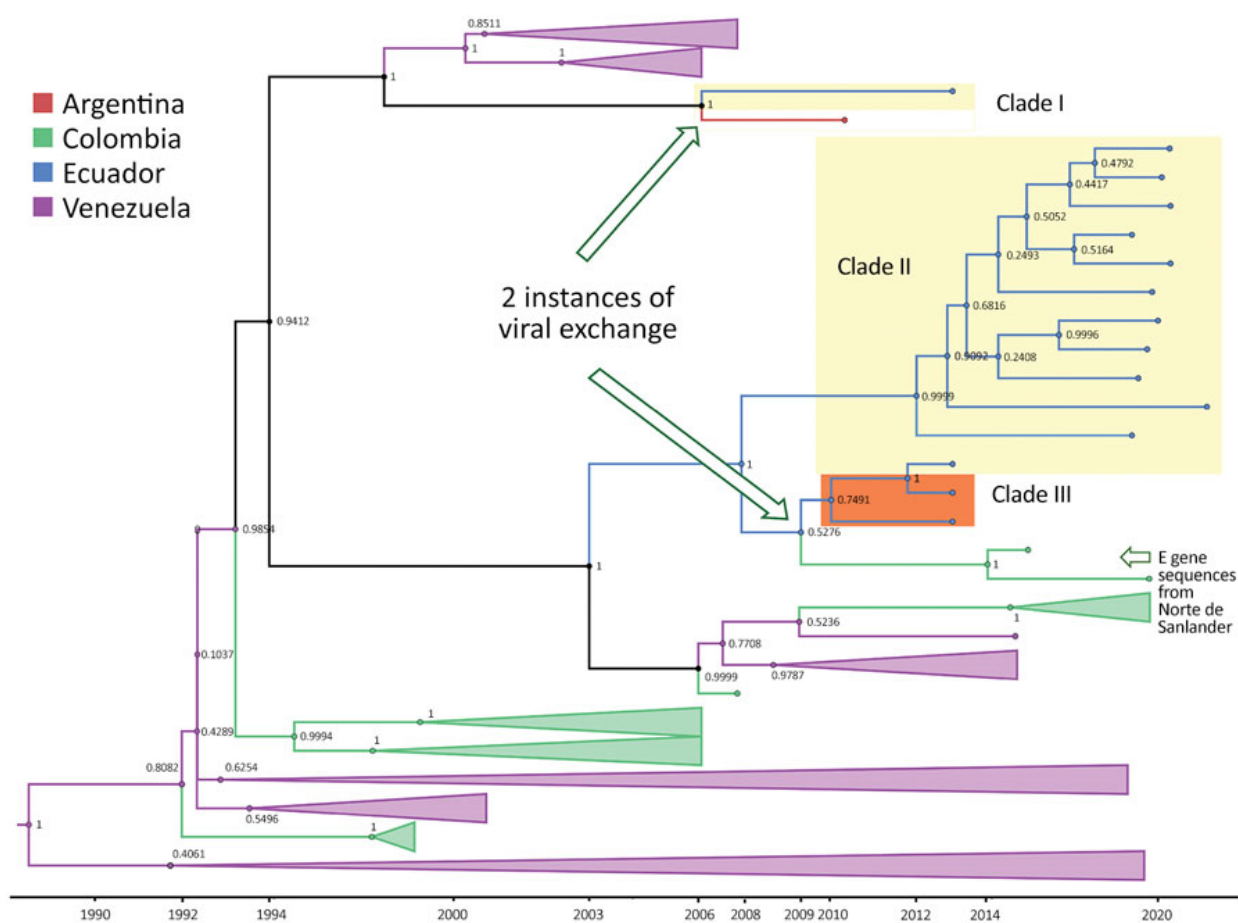


Figure 3. Maximum-clade credibility tree for dengue virus serotype 1 in study of transmission dynamics of dengue in large and small population centers, northern Ecuador. Tree was constructed using whole-genome sequences from Ecuador (blue), Colombia (green), Venezuela (purple), and Argentina (red) generated in BEAST software (<https://beast.community>). Within Ecuador, Esmeraldas Province samples are within the yellow rectangles and El Oro

Province samples are within the orange rectangle, combined with E gene sequences from Norte de Santander department, Colombia. Posterior probabilities are shown in internal nodes. E, envelope.

a common ancestor with a sequence obtained in 2010 in Argentina. The theoretical most recent common ancestor of those 2 sequences was estimated to date back to 2006 and shared a common ancestor with viral sequences from Venezuela comprising the bulk of clade I ([Figure 3](#)).

No additional sequences from this clade were detected in Ecuador, suggesting limited transmission after this potential introduction. The other DENV-1 viral exchange occurred no later than 2008 and was associated with the bulk of subsequent DENV-1 sequences from Ecuador. Those sequences formed 2 clusters, 1 from Esmeraldas Province and 1 primarily from El Oro Province that also included a sequence from Esmeraldas province ([Figure 3](#), top portion of clade II and clade III). El Oro is located 600 km south of Esmeraldas Province ([Figure 4](#)). The introduction of those viruses into the rural communities of Esmeraldas Province is estimated to have occurred no later than 2012. Persistence of clade II lineage in Ecuador over time without the presence of other sequences from other countries suggests that Ecuador has sustained transmission that is continuing to evolve independent of external viral introductions.



Figure 4. Location of El Oro Provinces in Ecuador, Nariño and Putumayo departments in Colombia, and Venezuela in relationship to Esmeraldas Province in study of transmission dynamics of dengue in large and small population centers, northern Ecuador.

Phylogenetic Analysis of DENV-2 Serotype in Ecuador

The MCC tree for DENV-2 whole-genome sequencing (along with some partial genomes) also suggests ≥ 2 exchanges of distinct viruses among Ecuador, Colombia, and Venezuela. In one instance, a cluster composed of 20 sequences collected in 2014–2015 from Machala, a city in El Oro Province, shares a most recent common ancestor dating back to 2007 with sequences from Colombia ([Figure 5](#), clade II). The closest related sequence to this Ecuador clade is a Colombia envelope gene sequence from Valle del Cauca collected in 2013. In addition, 2 envelope gene sequences from Colombia (Putumayo) sampled in 2013 clustered within the Ecuador clade II. The other instance of viral exchange is suggested by 2 clusters, a cluster of 15 Ecuador sequences collected from 2020–2021 active surveillance of rural communities in Esmeraldas Province, which share a most recent common ancestor dating back to 2013, and a cluster of sequences from

Colombia ([Figure 5](#), clade I). The sequences from Machala arrived in Ecuador earlier than those from Esmeraldas Province, possibly because the Machala study predates the Esmeraldas study ([Figure 5](#)).

Phylogenetic Analysis of DENV-1 Serotype from Esmeraldas Province

Focusing on the DENV-1 serotype from our study in Esmeraldas Province ([Figure 3](#), clade II), we labeled sequences on the basis of their gradient of remoteness: remote communities with no road access (Santa María and Santo Domingo), communities with road access (Colon Eloy, Timbiré,

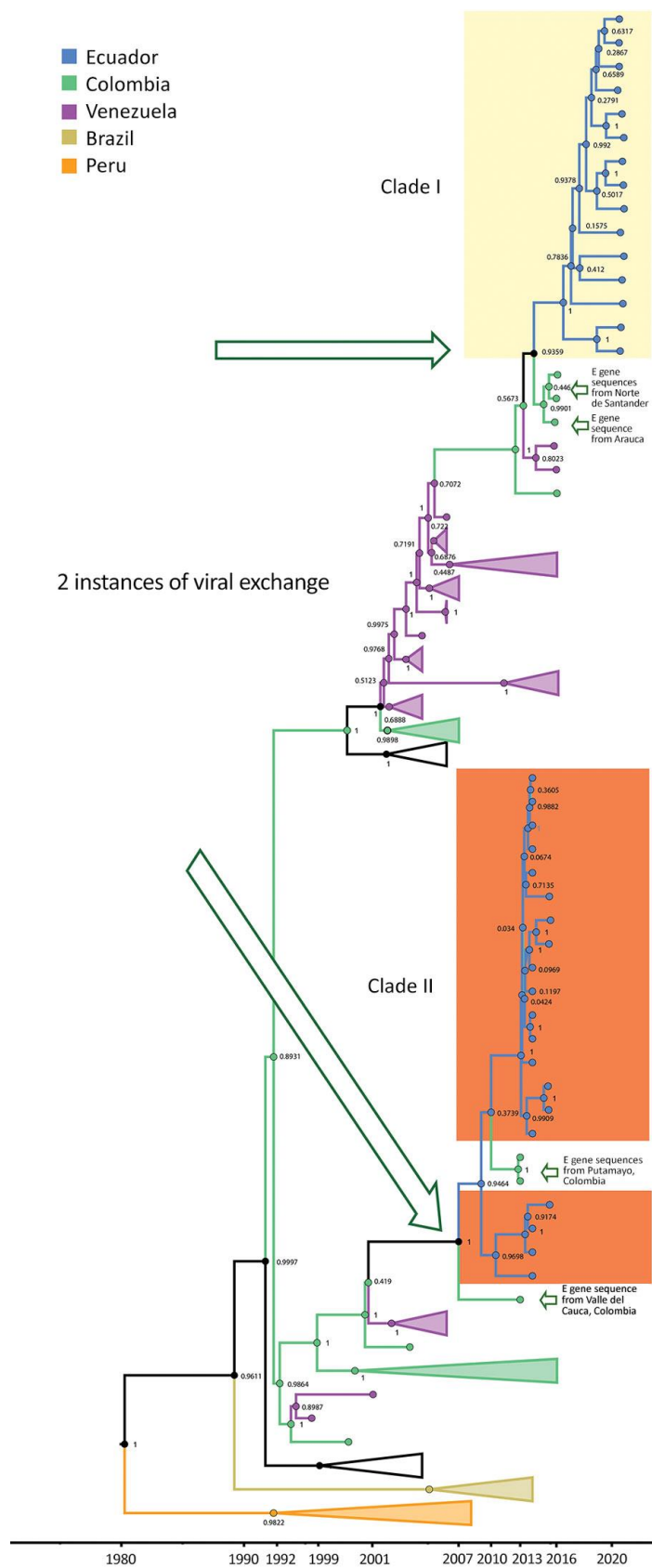


Figure 5. Maximum-clade credibility tree for dengue virus serotype 2 in study of transmission dynamics of dengue in large and small population centers, northern Ecuador. Tree was constructed using whole-genome sequences from Ecuador (blue), Colombia (green), and Venezuela (purple), combined with envelope gene sequences from Colombia departments (Nariño, Valle del Cauca, Putumayo, and Norte de Santander), and generated in BEAST software (<https://beast.community>). Within Ecuador, samples from Esmeraldas Province are within the yellow shaded area, and El Oro Province samples are within the orange shaded area. Posterior probabilities are shown in internal nodes.

and Maldonado), the commercial center (Borbón), and the large population center of Esmeraldas Province (Esmeraldas city) ([Figure 6](#)). This DENV-1 subclade tree does not show distinct clustering by gradient of remoteness, although it does support the hypothesis that the cities of Esmeraldas and Borbón are sources of the viruses circulating in the smaller communities in our study site. A sequence from the city of Esmeraldas collected in 2019 (root position posterior node probability 0.9999) and a sequence from the Borbón hospital collected in 2021 (root position posterior node probability 0.9092) shared a most recent common ancestor dating back to 2012 ([Figure 6](#)). The descendants of those 2 ancestral sequences are found in remote communities and communities with road access; however, an Esmeraldas city sequence collected in 2019 derived within this cluster is suggestive of a subsequent exchange back into the large population center.

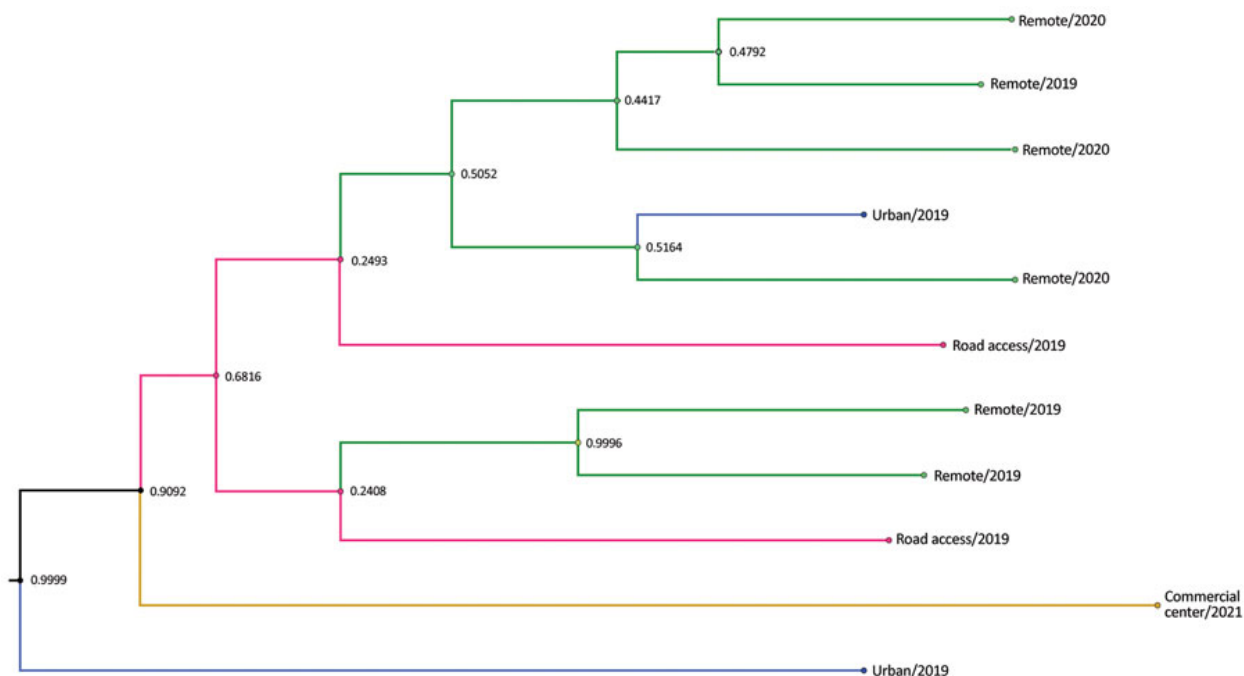


Figure 6. Subclade tree of dengue virus serotype 1 from rural communities of Esmeraldas Province in study of transmission dynamics of dengue in large and small population centers, northern Ecuador. Gradient of remoteness is classified as remote communities with no road access (green), communities with road access (pink), commercial center (yellow), and urban (blue). Subclade nodes are labeled with posterior probabilities generated in BEAST software (<https://beast.community>).

Phylogenetic Analysis of DENV-2 Serotype from Esmeraldas Province

The DENV-2 Ecuador lineage from Esmeraldas Province demonstrates clustering by community ([Figure 7](#), clade I). We also found strong support (0.9378) for the commercial center (Hospital of Borbón) and for those communities with road access (Colon Eloy and Timbire) being intermediate sources (0.992) of DENV-2 strains moving between the city of Esmeraldas and 2 remote communities (Santa Maria and Santo Domingo). The most recent common ancestor dates back to 2018 for a subset of the remote samples. Although much of the data support viral movement from cities and commercial centers to more remote communities, our phylogeny also supports

movement from a remote community (Santo Domingo) to the commercial center of the region (Borbón) ([Figure 7](#)).

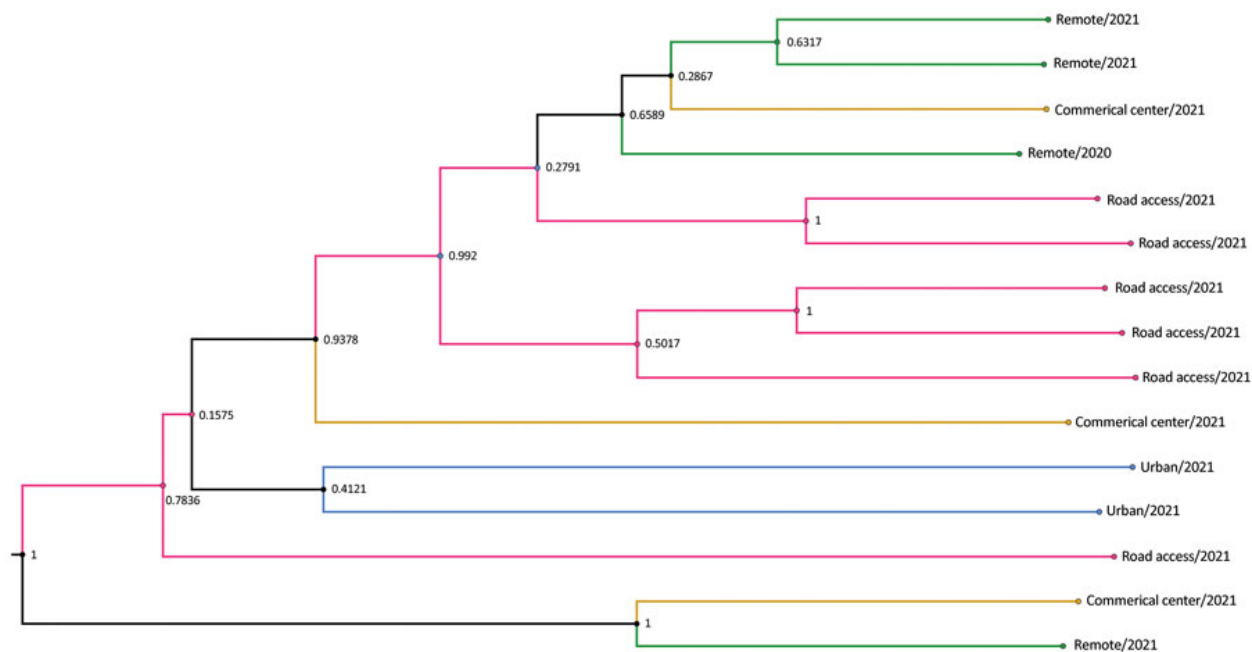


Figure 7. Subclade tree of dengue virus serotype 2 from rural communities of Esmeraldas Province in study of transmission dynamics of dengue in large and small population centers, northern Ecuador. Gradient of remoteness is classified as remote communities with no road access (green), communities with road access (pink), commercial center (yellow), and urban (blue). Subclade nodes are labeled with posterior probabilities generated in BEAST software (<https://beast.community>).

DISCUSSION

Human mobility is one of the main determinants of DENV transmission ([23](#)) because the flight range of *Aedes* mosquitoes is minimal ([24](#)). The social dynamics of the region combined with our results suggest that Esmeraldas Province is an entry point for DENV strains arriving in Ecuador from Colombia. Legal and illegal commerce (mostly by sea) between Esmeraldas Province and

Colombia is robust ([25,26](#)) and occurs primarily in small, mostly rural communities with weak customs controls that favor informal and illegal commerce and irregular human migration.

Our data suggest that DENV-1 entered Ecuador no later than 2009 and moved to at least 2 Coastal provinces in Ecuador (Esmeraldas and El Oro). Sequences found in those provinces were most closely related to nucleotide sequences from Colombia, but they also showed similarity to sequences from Venezuela ([Figure 3](#)). Another DENV-1 sequence shares a theoretical most recent common ancestor from 2006 with an Argentina sequence and also shares high similarity with sequences from Venezuela ([Figure 3](#)). The first DENV-2 introduction might have occurred earlier than 2009, and the virus circulated in Ecuador until 2015. This DENV-2 strain was most closely related to Colombia strains circulating until 2013 ([Figure 5](#)). The second introduction probably occurred no later than 2013, resulting in an Ecuador lineage that persisted at least until 2021. Those DENV-2 sequences showed high similarity to both Colombia and Venezuela sequences.

The perspective that large tropical cities are the primary source of DENV (and other *Ae. aegypti* mosquito-transmitted viruses) has resulted in establishment of surveillance centers in large urban centers, but in Ecuador, social (and commercial) dynamics suggest that DENV is also entering through small rural community centers and subsequently disseminating to the cities. Although most of our data suggest that DENV is brought to remote communities from urban centers, we also found instances of DENV movement from remote communities to larger commercial centers (e.g., Esmeraldas and Borbon). Smaller communities with road access probably provide a bridge between more remote communities and larger commercial centers, such as Esmeraldas and Borbón, thereby serving as intermediate sources. Large population centers, such as Esmeraldas, are hubs for public transportation and therefore may become the epicenter of viral spread ([27–30](#)). Further studies are needed to understand how a heterogeneous landscape (including biological,

social, and environmental factors) among communities in the region drive epidemic dynamics (31).

One reason that DENV transmission has remained endemic to regions such as Ecuador (in contrast to the diminished transmission of Zika and chikungunya viruses) is that there is continual serotype and lineage replacement to which cross immunity is only partial (31,32). For example, the Ministry of Health reported a 2.8-fold increase in the number of dengue cases from 2014 to 2015 (15,031 to 42,459 cases) (32,33). This increase was likely caused by introduction of a new lineage of DENV-2 from Colombia to Ecuador, leading to the replacement of the previously dominant lineage that had been circulating since 2012 (Figure 5). The replacement of lineages has been reported in several studies associated with outbreaks linked to the introduction of novel lineages (34,35) and has long been considered a part of DENV transmission dynamics in endemic and hyperendemic regions (25,26,36). Those replacements might be fueled by viruses displaying novel antigenic variations for which the local population lacks immunity (37) or by viral variants with higher fitness (38). Another reason for the observed increases might be that cases reported by the Ministry of Health are other *Ae. aegypti* mosquito-transmitted arboviruses, such as chikungunya virus (22).

Several surveillance gaps should be considered when interpreting our data, including minimal historical specimens, lower resolution in rural sites than in urban sites, and limited country-specific data from countries in South America (including Ecuador). Although those gaps are reflective of working in a resource-limited setting, our data also reflect a unique contribution to dengue transmission dynamics in a resource-limited setting. Additional gaps in our data are a result of the COVID-19 pandemic, which might have resulted in our missing DENV cases and potential DENV introductions. Ecuador's countrywide state of emergency (March 16–April 24, 2020) and

subsequent restrictions forced us to stop or sharply curtail our active household-based surveillance study ([Figure 2](#), period of no surveillance shown in green). This state of emergency similarly affected the government's passive surveillance program.

We believe our conclusions are robust for several reasons. First, we are using complete genome sequences. Second, we obtained posterior probabilities by using a Bayesian Skyline analysis that provides us with a level of confidence for our phylogenetic relationships. Third, our results are biologically plausible and are supported by the social dynamics we observed.

For example, evidence is ample that Colombian viruses are ancestral to and a potential source of Ecuador DENV ([Figures 3, 5](#)). Colombia has numerous, very active Caribbean ports that likely serve as entry points to South America for the virus ([39,40](#); B. Gutierrez, University of Oxford, pers. comm., 2023 Feb 14). In contrast to previous reports that suggest migration from Venezuela drives DENV lineage introduction into Ecuador ([39](#)), we believe its role is minimal. Ecuador does not share a border with Venezuela, and 75% of immigrants from Venezuela travel through Colombia (a 5-day journey). In addition, the main border crossing point in the highlands (Rumichaca, Ecuador) ([41](#)) is a region with no *Ae. aegypti* mosquito activity. A recent report, however, shows that migrants from Venezuela play a vital role in the introduction of DENV to Colombia ([42](#)), so further introductions to Ecuador through the Colombia border are likely.

Although our findings are consistent with what is known about the social dynamics of the study region, samples collected through community-based surveillance studies and previously reported strains were opportunistically gathered, usually from clinical settings. DENV cases are likely underestimated in Ecuador. Viral genomic characterization from countries such as Colombia and Venezuela are similarly limited, further adding uncertainty to our capacity to estimate the precise source and direction of exchanges.

Cases in smaller population centers are increasingly recognized as playing a vital role in broader DENV transmission dynamics (43). Our phylogenetic analyses in Ecuador shed light on those dynamics. Esmeraldas Province might be a key site from which DENV is introduced, amplified through local transmission, and then spread throughout Ecuador by human travel and movement of infected mosquitoes. Our results underline the need for coordinated efforts in DENV strain monitoring and control across national borders. Ministries of Health should intensify dengue surveillance in neglected remote regions, especially along national borders. Surveillance can also elucidate how DENV diffuses and becomes endemic, which requires an understanding of how large population centers affect viral dynamics regionally, and whether smaller, more remote communities represent a silent reservoir of ongoing dengue circulation.

Dr. Márquez is a graduate student at the Instituto de Microbiología in Universidad San Francisco de Quito. Her primary research interest is virology.

Acknowledgments

We thank Belén Prado for providing the pipeline for dengue genome assembly, obtaining the final consensus sequences, and submitted sequences to GenBank.

We also thank Yuri Villalobos for his help in creating the map for locations of the 6 rural communities in Esmeraldas Province.

This study was funded by the National Institute of Allergy and Infectious Diseases, National Institute of Health, R01 AI132372-02, entitled: “Zika and Dengue Co-circulation Under Environmental Change and Urbanization,” 1U01AI151788 entitled “American and Asian Centers

for Arboviral Research and Enhanced Surveillance- A2CARES-CREID” and Sustainable Sciences Institute.

REFERENCES

1. World Health Organization. Dengue and severe dengue [cited 2022 Apr 11]. <https://www.who.int/news-room/fact-sheets/detail/dengue-and-severe-dengue>
2. Gómez-Dantés H, Willoquet JR. Dengue in the Americas: challenges for prevention and control. *Cad Saude Publica*. 2009;25(Suppl 1):S19–31. [PubMed](#) <https://doi.org/10.1590/S0102-311X2009001300003>
3. Vong S, Khieu V, Glass O, Ly S, Duong V, Huy R, et al. Dengue incidence in urban and rural Cambodia: results from population-based active fever surveillance, 2006-2008. *PLoS Negl Trop Dis*. 2010;4:e903. [PubMed](#) <https://doi.org/10.1371/journal.pntd.0000903>
4. Chew CH, Woon YL, Amin F, Adnan TH, Abdul Wahab AH, Ahmad ZE, et al. Rural-urban comparisons of dengue seroprevalence in Malaysia. *BMC Public Health*. 2016;16:824. [PubMed](#) <https://doi.org/10.1186/s12889-016-3496-9>
5. Mayxay M, Sengvilaipaseuth O, Chanthongthip A, Dubot-Pérès A, Rolain JM, Parola P, et al. Causes of fever in rural southern Laos. *Am J Trop Med Hyg*. 2015;93:517–20. [PubMed](#) <https://doi.org/10.4269/ajtmh.14-0772>
6. Lawpoolsri S, Kaewkungwal J, Khamsiriwatchara A, Sovann L, Sreng B, Phommasack B, et al. Data quality and timeliness of outbreak reporting system among countries in Greater Mekong subregion: challenges for international data sharing. *PLoS Negl Trop Dis*. 2018;12:e0006425. [PubMed](#) <https://doi.org/10.1371/journal.pntd.0006425>

7. Ng LC, Chem YK, Koo C, Mudin RNB, Amin FM, Lee KS, et al. 2013 dengue outbreaks in Singapore and Malaysia caused by different viral strains. *Am J Trop Med Hyg.* 2015;92:1150–5. [PubMed https://doi.org/10.4269/ajtmh.14-0588](https://doi.org/10.4269/ajtmh.14-0588)
8. National Environmental Agency. Surveillance and Epidemiology Programme [cited 2022 Jun 10]. <https://www.nea.gov.sg/corporate-functions/resources/research/surveillance-and-epidemiology-programme>
9. Real J, Regato M, Burgos V, Jurado E. Evolution of dengue virus in Ecuador 2000–2015 [in Spanish]. *An Fac Med (Perú).* 2017;78:29–35.
10. Cifuentes SG, Trostle J, Trueba G, Milbrath M, Baldeón ME, Coloma J, et al. Transition in the cause of fever from malaria to dengue, Northwestern Ecuador, 1990-2011. *Emerg Infect Dis.* 2013;19:1642–5. [PubMed https://doi.org/10.3201/eid1910.130137](https://doi.org/10.3201/eid1910.130137)
11. Navarro JC, Arrivillaga-Henríquez J, Salazar-Loor J, Rodriguez-Morales AJ. COVID-19 and dengue, co-epidemics in Ecuador and other countries in Latin America: Pushing strained health care systems over the edge. *Travel Med Infect Dis.* 2020;37:101656. [PubMed https://doi.org/10.1016/j.tmaid.2020.101656](https://doi.org/10.1016/j.tmaid.2020.101656)
12. Márquez S, Carrera J, Espín E, Cifuentes S, Trueba G, Coloma J, et al. Dengue serotype differences in urban and semi-rural communities in Ecuador. *ACI Avances en Ciencias e Ingenierías.* 2018 [cited 2022 Jan 12]. <https://revistas.usfq.edu.ec/index.php/avances/article/view/959>
13. Waggoner JJ, Gresh L, Mohamed-Hadley A, Ballesteros G, Davila MJV, Tellez Y, et al. Single-reaction multiplex reverse transcription PCR for detection of Zika, chikungunya, and

dengue viruses. *Emerg Infect Dis.* 2016;22:1295–7. [PubMed](#)
<https://doi.org/10.3201/eid2207.160326>

14. Harris E, Roberts TG, Smith L, Selle J, Kramer LD, Valle S, et al. Typing of dengue viruses in clinical specimens and mosquitoes by single-tube multiplex reverse transcriptase PCR. *J Clin Microbiol.* 1998;36:2634–9. [PubMed](#) <https://doi.org/10.1128/JCM.36.9.2634-2639.1998>

15. Quick J, Grubaugh ND, Pullan ST, Claro IM, Smith AD, Gangavarapu K, et al. Multiplex PCR method for MinION and Illumina sequencing of Zika and other virus genomes directly from clinical samples. *Nat Protoc.* 2017;12:1261–76. [PubMed](#) <https://doi.org/10.1038/nprot.2017.066>

16. Cleemput S, Dumon W, Fonseca V, Abdool Karim W, Giovanetti M, Alcantara LC, et al. Genome Detective Coronavirus Typing Tool for rapid identification and characterization of novel coronavirus genomes. *Bioinformatics.* 2020;36:3552–5. [PubMed](#)
<https://doi.org/10.1093/bioinformatics/btaa145>

17. Rambaut A, Lam TT, Max Carvalho L, Pybus OG. Exploring the temporal structure of heterochronous sequences using TempEst (formerly Path-O-Gen). *Virus Evol.* 2016;2:vew007. [PubMed](#) <https://doi.org/10.1093/ve/vew007>

18. Drummond AJ, Ho SYW, Phillips MJ, Rambaut A. Relaxed phylogenetics and dating with confidence. *PLoS Biol.* 2006;4:e88. [PubMed](#) <https://doi.org/10.1371/journal.pbio.0040088>

19. Drummond AJ, Rambaut A, Shapiro B, Pybus OG. Bayesian coalescent inference of past population dynamics from molecular sequences. *Mol Biol Evol.* 2005;22:1185–92. [PubMed](#)
<https://doi.org/10.1093/molbev/msi103>

20. Rambaut A, Drummond AJ, Xie D, Baele G, Suchard MA. Posterior summarization in Bayesian phylogenetics using Tracer 1.7. *Syst Biol.* 2018;67:901–4. [PubMed https://doi.org/10.1093/sysbio/syy032](https://doi.org/10.1093/sysbio/syy032)
21. Márquez S, Lee GO, Andrade P, Zuniga J, Trueba G, Eisenberg JNS, et al. A chikungunya outbreak in a dengue-endemic region in rural northern coastal Ecuador. *Am J Trop Med Hyg.* 2022;107:1226–33. [PubMed https://doi.org/10.4269/ajtmh.22-0296](https://doi.org/10.4269/ajtmh.22-0296)
22. Allicock OM, Sahadeo N, Lemey P, Auguste AJ, Suchard MA, Rambaut A, et al. Determinants of dengue virus dispersal in the Americas. *Virus Evol.* 2020;6:veaa074. PMID 33408877
23. Vavassori L, Saddler A, Müller P. Active dispersal of *Aedes albopictus*: a mark-release-recapture study using self-marking units. *Parasit Vectors.* 2019;12:583. [PubMed https://doi.org/10.1186/s13071-019-3837-5](https://doi.org/10.1186/s13071-019-3837-5)
24. Zhang C, Mammen MP Jr, Chinnawirotpisan P, Klungthong C, Rodpradit P, Monkongdee P, et al. Clade replacements in dengue virus serotypes 1 and 3 are associated with changing serotype prevalence. *J Virol.* 2005;79:15123–30. [PubMed https://doi.org/10.1128/JVI.79.24.15123-15130.2005](https://doi.org/10.1128/JVI.79.24.15123-15130.2005)
25. Carrillo-Valenzo E, Danis-Lozano R, Velasco-Hernández JX, Sánchez-Burgos G, Alpuche C, López I, et al. Evolution of dengue virus in Mexico is characterized by frequent lineage replacement. *Arch Virol.* 2010;155:1401–12. [PubMed https://doi.org/10.1007/s00705-010-0721-1](https://doi.org/10.1007/s00705-010-0721-1)
26. Gubler DJ. Dengue, urbanization and globalization: the unholy trinity of the 21(st) century. *Trop Med Health.* 2011;39(Suppl):3–11. [PubMed https://doi.org/10.2149/tmh.2011-S05](https://doi.org/10.2149/tmh.2011-S05)

27. Lana RM, Gomes MFDC, Lima TFM, Honório NA, Codeço CT. The introduction of dengue follows transportation infrastructure changes in the state of Acre, Brazil: a network-based analysis. *PLoS Negl Trop Dis.* 2017;11:e0006070. [PubMed](#) <https://doi.org/10.1371/journal.pntd.0006070>
28. Sanna M, Hsieh YH. Ascertaining the impact of public rapid transit system on spread of dengue in urban settings. *Sci Total Environ.* 2017;598:1151–9. [PubMed](#) <https://doi.org/10.1016/j.scitotenv.2017.04.050>
29. Ren H, Wu W, Li T, Yang Z. Urban villages as transfer stations for dengue fever epidemic: A case study in the Guangzhou, China. *PLoS Negl Trop Dis.* 2019;13:e0007350. [PubMed](#) <https://doi.org/10.1371/journal.pntd.0007350>
30. Okano JT, Sharp K, Valdano E, Palk L, Blower S. HIV transmission and source-sink dynamics in sub-Saharan Africa. *Lancet HIV.* 2020;7:e209–14. [PubMed](#) [https://doi.org/10.1016/S2352-3018\(19\)30407-2](https://doi.org/10.1016/S2352-3018(19)30407-2)
31. Ecuadorian Ministry of Public Health. Weekly epidemiological gazette No 47. 2014 [cited 2022 Apr 13]. http://www.salud.gob.ec/wp-content/uploads/downloads/2014/12/Gaceta-N-47_opt.pdf
32. Ecuadorian Ministry of Public Health. Vector gazette N°52, 2019. 2019 [cited 2022 Apr 13]. <https://www.salud.gob.ec/wp-content/uploads/2020/02/GACETA-VECTORES-SE-52.pdf>
33. de Jesus JG, Dutra KR, Sales FCDS, Claro IM, Terzian AC, Candido DDS, et al. Genomic detection of a virus lineage replacement event of dengue virus serotype 2 in Brazil, 2019. *Mem Inst Oswaldo Cruz.* 2020;115:e190423–190423. [PubMed](#) <https://doi.org/10.1590/0074-02760190423>

34. Suzuki K, Phadungsombat J, Nakayama EE, Saito A, Egawa A, Sato T, et al. Genotype replacement of dengue virus type 3 and clade replacement of dengue virus type 2 genotype Cosmopolitan in Dhaka, Bangladesh in 2017. *Infect Genet Evol.* 2019;75:103977. [PubMed](#) <https://doi.org/10.1016/j.meegid.2019.103977>
35. Holmes EC, Twiddy SS. The origin, emergence and evolutionary genetics of dengue virus. *Infect Genet Evol.* 2003;3:19–28. [PubMed](#) [https://doi.org/10.1016/S1567-1348\(03\)00004-2](https://doi.org/10.1016/S1567-1348(03)00004-2)
36. Martinez DR, Yount B, Nivarthi U, Munt JE, Delacruz MJ, Whitehead SS, et al. Antigenic variation of the dengue virus 2 genotypes impacts the neutralization activity of human antibodies in vaccinees. *Cell Rep.* 2020;33:108226. [PubMed](#) <https://doi.org/10.1016/j.celrep.2020.108226>
37. Ko HY, Li YT, Chao DY, Chang YC, Li ZT, Wang M, et al. Inter- and intra-host sequence diversity reveal the emergence of viral variants during an overwintering epidemic caused by dengue virus serotype 2 in southern Taiwan. *PLoS Negl Trop Dis.* 2018;12:e0006827. [PubMed](#) <https://doi.org/10.1371/journal.pntd.0006827>
38. Maljkovic Berry I, Rutvisuttinunt W, Sippy R, Beltran-Ayala E, Figueroa K, Ryan S, et al. The origins of dengue and chikungunya viruses in Ecuador following increased migration from Venezuela and Colombia. *BMC Evol Biol.* 2020;20:31. [PubMed](#) <https://doi.org/10.1186/s12862-020-1596-8>
39. Campos TL, Durães-Carvalho R, Rezende AM, de Carvalho OV, Kohl A, Wallau GL, et al. Revisiting key entry routes of human epidemic arboviruses into the mainland Americas through large-scale phylogenomics. *Int J Genomics.* 2018;2018:6941735. [PubMed](#) <https://doi.org/10.1155/2018/6941735>

40. Blouin C. After the arrival: realities of Venezuelan migration. Lima: Pontifical Catholic University of Peru, Institute of Democracy and Human Rights (IDEHPUCP); 2019.
41. Carrillo-Hernandez MY, Ruiz-Saenz J, Jaimes-Villamizar L, Robledo-Restrepo SM, Martinez-Gutierrez M. Phylogenetic and evolutionary analysis of dengue virus serotypes circulating at the Colombian–Venezuelan border during 2015–2016 and 2018–2019. *PLoS One*. 2021;16:e0252379. [PubMed https://doi.org/10.1371/journal.pone.0252379](https://doi.org/10.1371/journal.pone.0252379)
42. Guo C, Zhou Z, Wen Z, Liu Y, Zeng C, Xiao D, et al. Global epidemiology of dengue outbreaks in 1990-2015: a systematic review and meta-analysis. *Front Cell Infect Microbiol*. 2017;7:317. [PubMed https://doi.org/10.3389/fcimb.2017.00317](https://doi.org/10.3389/fcimb.2017.00317)

CHAPTER 4

ASM Journal; Microbiology Resource Announcements . First published: 08 October 2020

DOI: <https://doi.org/10.1128/MRA.00996-20>

Metagenome of a Bronchoalveolar Lavage Fluid Sample from a Confirmed COVID-19 Case in Quito, Ecuador, Obtained Using Oxford Nanopore MinION Technology

Authors: Sully Márquez, Belén Prado-Vivar, Juan José Guadalupe, Bernardo Gutierrez, Mónica Becerra-Wong, Manuel Jibaja, Milton Tobar, Verónica Barragán, Patricio Rojas-Silva, Josefina Coloma, Gabriel Trueba, Michelle Grunauer, Paúl Cárdenas

ABSTRACT

We report the metagenome analysis of a bronchoalveolar lavage (BAL) fluid sample from a confirmed coronavirus disease 2019 (COVID-19) case in Quito, Ecuador. Sequencing was performed using MinION technology.

ANNOUNCEMENT

Metagenome analysis could be relevant in critically ill coronavirus disease 2019 (COVID-19) patients. These data can help identify coinfections and provide information for optimal treatment. We collected a sample of bronchoalveolar lavage (BAL) fluid from a confirmed COVID-19 case in Quito, Ecuador (HEE1). The patient, a tourist of Dutch origin in his late 50s, presented respiratory symptoms, including fever and cough, during a visit to Sucumbios Province in Ecuador's Amazon region. He was admitted with paroxysmal coughing to a public hospital in Lago Agrio, Ecuador, and an initial diagnosis of bacterial pneumonia was made. Diagnosis of

COVID-19 was confirmed by the Ecuadorian Ministry of Health on 7 March 2020. Because the patient's condition deteriorated, he was transferred to the Eugenio Espejo Hospital (HEE) intensive care unit (ICU) in Quito, Ecuador. On 11 March, a nonbronchoscopic protected BAL was performed using the double-catheter technique (the amount of aspirated fluid was 7 ml), and the sample was immediately transported for analysis. Sample positivity to severe acute respiratory syndrome coronavirus 2 (SARS-CoV-2) was confirmed with reverse transcription-quantitative PCR (RT-PCR) using the Veri-Q PCR 316 kit (MiCo BioMed, South Korea) that targets the ORF3a and N genes; the test came back positive for gene ORF3a with a quantification cycle (Cq) value of 32.59. The patient recovered after 1 month of hospitalization and returned to his native country on 10 April.

Metagenome sequencing of the BAL sample was carried out using Oxford Nanopore MinION technology. Total RNA was extracted from 250 μ l of the BAL sample using a QIAamp viral RNA extraction kit (Qiagen, Germany) following the manufacturer's instructions; no DNase digestion step was added. The sample was eluted in a final volume of 70 μ l. Extracted RNA was purified using the RNA Clean and Concentrator kit (Zymo Research, USA). Purified RNA (14 μ l) was used for retrotranscription of RNA to cDNA following the RNA Viral Metagenomics MinION one-pot sequencing protocol from the genomics department of Public Health England ([1](#), [2](#)). cDNA library preparation was performed using the rapid barcoding kit (SQK-RBK004; Oxford Nanopore Technologies [ONT], UK) following the manufacturer's instructions. The resulting library was loaded onto an Oxford MinION flow cell (FLO-MIN 106) and sequenced using MinKNOW version 4.05 for 24 h. Base calling and quality control analyses were performed using Guppy version 3.4.5 in high-accuracy mode and NanoPlot version 1.29.0, respectively ([3](#)). Adapters and

barcodes were removed from the reads using Porechop version 0.2.4 (<https://github.com/rrwick/Porechop>).

Taxonomic classification of the sequences was performed using the Kaiju platform (4). Metagenome analysis yielded a total of 206,111 DNA sequences with 43,603,091 bases and a read length N 50 value of 263 bp. Viral sequences represented 0.9% of the total metagenome, 4% of which corresponded to *Coronavirinae*. In this group, 83% represented nonassigned coronaviruses, and 17% were identified as SARS coronaviruses (Fig. 1A). Additionally, several bacterial and eukaryotic sequences related to the patient's respiratory microbiota were identified. The most relevant taxa found were *Streptococcus pneumoniae* (7%), *Chlamydia* spp. (5%), *Mycobacterium tuberculosis* (4%), and *Staphylococcus aureus* (3%). We did not identify any particular clinically relevant fungus.

A 3,173-bp SARS-CoV-2 consensus sequence was obtained by mapping reads against the reference strain Wuhan-Hu-1 (GenBank accession number [MN908947](https://www.ncbi.nlm.nih.gov/nuccore/MN908947)) using minimap2 version 2.14-r883 (5). Samtools version 1.9 (<http://samtools.github.io>) and Tablet alignment viewer version 1.19.09.3 (<https://ics.hutton.ac.uk/tablet>) were used to visualize the mapped sequence. A sequence similarity of 99.68% was found with ORF1AB, with 100% coverage. To confirm taxonomic classification, a phylogenetic tree (Fig. 1B) was inferred by using the maximum likelihood method and the Tamura-Nei model with MEGA X (6). The sequences used to build the phylogenetic tree included the ORF1AB gene sequence recovered from the metagenome analysis and the sequences of 7 SARS-CoV-2 strains and the closely related bat coronavirus strain RaTG13 (Fig. 1B) from GenBank NCBI (www.ncbi.nlm.nih.gov). All bioinformatic tools were run with default parameters.

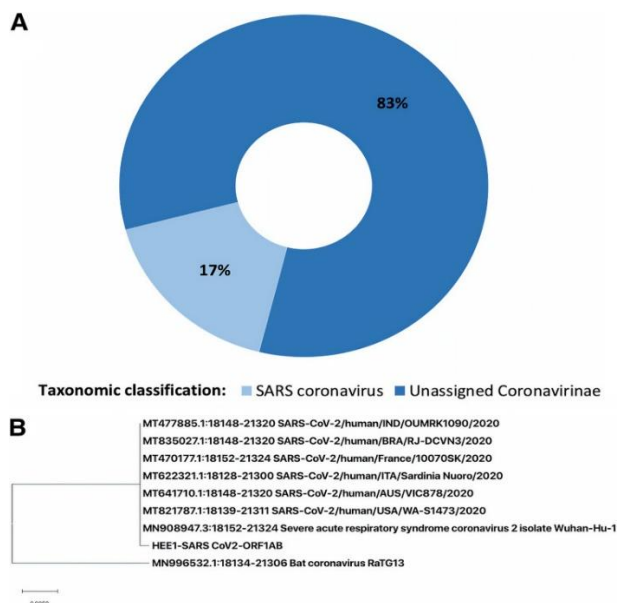


Figure 1. Taxonomic classification of viral sequences recovered from the bronchoalveolar lavage (BAL) fluid metagenome. (A) Krona chart showing the classification of sequences identified as *Coronavirinae*; 83% were unidentified coronaviruses, and 17% were SARS coronaviruses. (B) Phylogenetic characterization of SARS-CoV-2 *ORF1AB* sequence (HEE1) inferred by maximum likelihood. The sequence was aligned to other SARS-CoV-2 strains and the closely related bat coronavirus strain RaTG13 downloaded from GenBank NCBI (www.ncbi.nlm.nih.gov).

Ethical approval for using the sample was given by CEISH-USFQ (Comité de Ética de Investigación en Seres Humanos-USFQ) (IE-JP067-2020-CEISH-USFQ).

Data availability.

The metagenome sequences are publicly available at accession number [PRJNA613094](https://www.ncbi.nlm.nih.gov/submit/fastq-upload/?tab=submit&view=fastq) (Fastq for called reads, [SRR11341345](https://www.ncbi.nlm.nih.gov/submit/fastq-upload/?tab=submit&view=fastq); raw Fast5, [SRR12664395](https://www.ncbi.nlm.nih.gov/submit/fastq-upload/?tab=submit&view=fastq)).

ACKNOWLEDGMENTS

This work was funded by Universidad San Francisco de Quito and supported by the Centre for Arbovirus Discovery, Diagnostics, Genomics, and Epidemiology (CADDE)

(www.caddecentre.org/). P.C. is funded by NIH FIC D43TW010540 Global Health Equity

Scholars. B.G. is supported by the SENESCYT Scholarship Program (ARSEQ-BEC-003163-2017).

REFERENCES

1. Greninger AL, Naccache SN, Federman S, Yu G, Mbala P, Bres V, Stryke D, Bouquet J, Somasekar S, Linnen JM, Dodd R, Mulembakani P, Schneider BS, Muyembe-Tamfum JJ, Stramer SL, Chiu CY. 2015. Rapid metagenomic identification of viral pathogens in clinical samples by real-time nanopore sequencing analysis. *Genome Med* 7:1–13.
2. Kafetzopoulou LE, Efthymiadis K, Lewandowski K, Crook A, Carter D, Osborne J, Aarons E, Hewson R, Hiscox JA, Carroll MW, Vipond R, Pullan ST. 2018. Assessment of metagenomic Nanopore and Illumina sequencing for recovering whole genome sequences of chikungunya and dengue viruses directly from clinical samples. *Euro Surveill* 23:1800228.
3. De Coster W, D’Hert S, Schultz DT, Cruts M, Van Broeckhoven C. 2018. NanoPack: visualizing and processing long-read sequencing data. *Bioinformatics* 34:2666–2669.
4. Menzel P, Ng KL, Krogh A. 2016. Fast and sensitive taxonomic classification for metagenomics with Kaiju. *Nat Commun* 7:11257.
5. Li H. 2018. minimap2: pairwise alignment for nucleotide sequences. *Bioinformatics* 34:3094–3100.
6. Kumar S, Stecher G, Li M, Knyaz C, Tamura K. 2018. MEGA X: Molecular Evolutionary Genetics Analysis across Computing Platforms. *Mol Biol Evol* 35:1547–1549.

PUBLICATION AS CONTRIBUTING AUTHOR

Lancet Infect Dis . 2021 Jun;21(6):e142.

doi: 10.1016/S1473-3099(20)30910-5. Epub 2020 Nov 23.

A case of SARS-CoV-2 reinfection in Ecuador

Belén Prado-Vivar ¹, Mónica Becerra-Wong ², Juan José Guadalupe ³, Sully Márquez ², Bernardo Gutierrez ⁴, Patricio Rojas-Silva ², Michelle Grunauer ⁵, Gabriel Trueba ², Verónica Barragán ², _Paúl Cárdenas ⁶

Cases of severe acute respiratory syndrome coronavirus 2 (SARS-CoV-2) reinfection have been reported in Hong Kong, Belgium, the Netherlands, and the USA.^{1, 2, 3, 4} Here we report the first confirmed case of SARS-CoV-2 reinfection in Ecuador and South America. For full methodological details, see the [appendix \(pp 1, 2\)](#).

On May 12, 2020, a 46-year-old man presented in Quito, Ecuador, with 3 days of intense headache and drowsiness. On May 16, he took a rapid antibody test that was positive for IgM and negative for IgG. On May 20, the patient tested positive on RT-PCR (*ORF3a* gene, Cq=36.85). Subsequently, the patient's symptoms improved, and he tested negative on RT-PCR on June 3 ([appendix p 4](#)).

On July 20, the patient presented once again with symptoms suggestive of COVID-19. This time the symptoms were more severe and included odynophagia, nasal congestion, fever of 38.5°C, back pain, productive cough, and dyspnoea. He received an RT-PCR test on July 22, with a positive result (*N* gene, Cq=30.82). Despite having moderate symptoms and dyspnoea, the patient did not require hospitalisation, and his clinical status improved after several days. A fourth RT-PCR test was done on Aug 4, which was negative ([appendix p 4](#)). Finally, an ELISA quantitative antibody test was done on Aug 18, showing anti-SARS-CoV-2 IgG (34.1 NovaTec Units [NTU]) and IgM (54.2 NTU; both interpreted as positive).

SARS-CoV-2 genome sequencing was done using Oxford Nanopore Technologies' MinION, following the ARTIC Network protocols.⁵ Phylogenetic analysis revealed that the first infection variant belonged to clade 20A and lineage B1.p9, whereas the second infection variant belonged to clade 19B and lineage A.1.1 ([appendix p 4](#)). The mutation loci and amino acid changes are described in the [appendix \(p 5\)](#). No shared mutations were observed between the two sequences, further suggesting that both variants resulted from distinct evolutionary trajectories.

Although reinfections with coronaviruses that cause the common cold have been reported previously,⁶ the symptoms of reinfections are usually milder than those of the primary infections. It was therefore surprising that our patient showed more severe disease with the second infection than with the first, especially because the patient did not have any additional clinical conditions that could explain it. Increased severity of second SARS-CoV-2 infections has been reported previously: in a healthy man aged 25 years in Nevada, USA,² and in an immunocompromised woman aged 89 years in the Netherlands, which resulted in her death.⁴

The protective immune response to SARS-CoV-2 infection is not fully understood; however, protection against severe disease has been shown in animal models and inferred in humans infected with the virus.⁷ Interestingly, the antibody test performed during the first infection event showed the presence of specific anti-SARS-CoV-2 IgM and no IgG. However, it is not possible using conventional antibody tests to determine whether a protective immune response developed.

Acknowledgments

BP-V and MB-W contributed equally. We declare no competing interests.

REFERENCES

1. To KK-W, Hung IF-N, Ip JD, et al. COVID-19 re-infection by a phylogenetically distinct SARS-coronavirus-2 strain confirmed by whole genome sequencing. *Clin Infect Dis.* 2020 doi: 10.1093/cid/ciaa1275. published online Aug 25.
2. Tillett RL, Sevinsky JR, Hartley PD, et al. Genomic evidence for reinfection with SARS-CoV-2: a case study. *Lancet Infect Dis.* 2020 doi: 10.1016/S1473-3099(20)30764-7. published online Oct 12.
3. Iwasaki A. What reinfections mean for COVID-19. *Lancet Infect Dis.* 2020 doi: 10.1016/S1473-3099(20)30783-0. published online Oct 12.
4. Mulder M, van der Vegt DSJM, Oude Munnink BB, et al. Reinfection of SARS-CoV-2 in an immunocompromised patient: a case report. *Clin Infect Dis.* 2020 doi: 10.1093/cid/ciaa1538. published online Oct 9.
5. Quick J, Grubaugh ND, Pullan ST, et al. Multiplex PCR method for MinION and Illumina sequencing of Zika and other virus genomes directly from clinical samples. *Nat Protoc.* 2017;12:1261–1276.
6. Callow KA, Parry HF, Sergeant M, Tyrrell DAJ. The time course of the immune response to experimental coronavirus infection of man. *Epidemiol Infect.* 1990;105:435–446.]
7. Ladhani SN, Jeffery-Smith A, Patel M, et al. High prevalence of SARS-CoV-2 antibodies in care homes affected by COVID-19: prospective cohort study, England. *EClinicalMedicine.* 2020 doi: 10.1016/j.eclinm.2020.100597. published online Nov 5.

Appendix: COVID-19 re-infection by a phylogenetically distinct SARS-CoV-2 variant, first confirmed event in South America.

MATERIALS AND METHODS

Sample collection

Two oropharyngeal swabs were collected at two distinct time points corresponding to the period when the patient presented COVID-19-like symptoms. The samples were collected in 1.5 ml Eppendorf tubes with 1X DNA/RNA Shield (Zymo, USA), to preserve the contained genetic material and ensure viral inactivation. Sample positivity to COVID-19 was determined using the RT-PCR method, with the Veri-Q PCR 316 kit (Mico Biomed, South Korea), that target ORF3a and N genes. Both samples were stored in RNAsHield (Zymo, USA) at -80 °C after PCR analysis. The results were officially reported to the Ecuadorian Ministry of Public Health (MSP) and the National Institute of Public Health and Research (INSPI) following local protocols. RNA extraction RNA was extracted in a type II biosafety chamber with HEPA filters, at the Virology Laboratory of the IMUSFQ (Microbiology Institute of Universidad San Francisco de Quito). Quick-RNA™ Viral Kit (Zymo, USA) was used to extract the total RNA from each sample, following manufacturer instructions. Retrotranscription of RNA to cDNA was carried out using the ARTIC protocol (Quick, 2020).

Whole-genome sequencing

Target enrichment for further whole-genome sequencing was performed through the primer scheme approach developed by the ARTIC Network for nCoV-2019, using the V3 primer sets (Quick, 2020). The product of this reaction was purified by using AMPure XP magnetic beads

(Beckman Coulter, USA), following 2 manufacturer instructions; and it was quantified using QuBit (Thermo Fisher Scientific) with a Qubit RNA Assay Kit (Thermo Scientific, Invitrogen, USA). After normalization, cDNA library preparation was carried out by using the Rapid Barcoding kit (SQK-RBK004) (Oxford Nanopore Technologies), then, the library was loaded into the MinION flow cell (FLO-MIN 106). To monitor sequence in real-time, the RAMPART software (v1.0.5) from the ARTIC Network (<https://github.com/artic-network/rampart>) was used. After sequencing, Nanoplot (De Coster et al., 2018) and Porechop (version 0.2.4) (<https://github.com/rrwick/Porechop>) were used to determine sequence quality scores and to carried out demultiplexing and adapter removal, respectively. Then, the ARTIC Network bioinformatics pipeline was employed for variant calling (Quick, 2020). To generate consensus genomes, the reads were mapped against the reference strain Wuhan-Hu-1 (GenBank accession number MN908947). Tablet alignment viewer (version 1.19.09.03) (<https://ics.hutton.ac.uk/tablet>) was used to visualize the mapped sequence. The online tool NextClade (v0.4.0) (Hadfield et al., 2018) was used to assign the sequences to clades. Finally, the two genomes were uploaded to the CoV-GLUE online resource (Singer et al., 2018), for lineage classification and mutations determination. Immunological test A COVID-19 Qualitative antibody IgG/IgM Rapid Test (SAFECARE BIO-TECH, China) was performed by “AMC Laboratorio Clínico Pasteur”, a private laboratory in Quito during the first infection event. During the second event, an ELISA antibody test was performed by the medical clinic SIME (Sistemas Médicos Universidad San Francisco de Quito), using NovaLisa® SARS-CoV-2 IgG and NovaLisa® SARS-CoV-2 IgM (NovaTec Immundiagnostica GmbH, Germany).

Acknowledgments

This work was funded by Universidad San Francisco de Quito and supported by the Centre for

Arbovirus Discovery, Diagnostics, Genomics and Epidemiology – CADDE (www.caddecentre.org/). P.C. is funded by NIH FIC D43TW010540 Global Health Equity Scholars. BG is supported by SENESCYT Scholarship Program (ARSEQ-BEC-003163-2017). We would like to thank Rommel Guevara and Miguel Moncayo for all their help in keeping the patient database updated.

Availability of data: The sequences have been uploaded to GISAID under the accession numbers EPI_ISL_525430 (first infection) and EPI_ISL_516650 (second infection).

Ethical approval and consent to participate: The study protocol was approved by the Institutional Review Board of the Universidad San Francisco de Quito P2020-022IN (CEISH No. 1234) and by the Ecuadorian Ministry of Public Health MSP-CGDES-2020-0121-O. The patient provided written informed consent for sample analysis and publication.

FIGURES

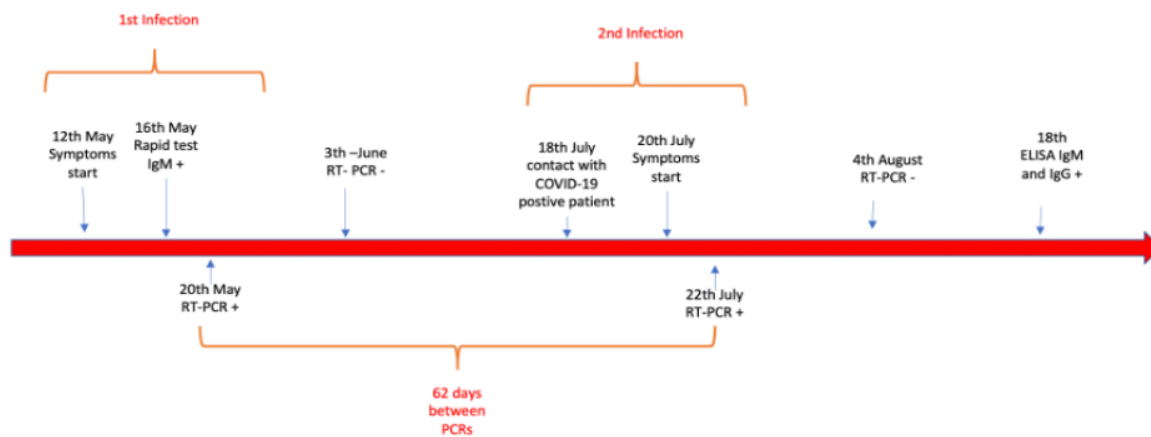


Figure 1. Timeline showing patients infection events and testing dates

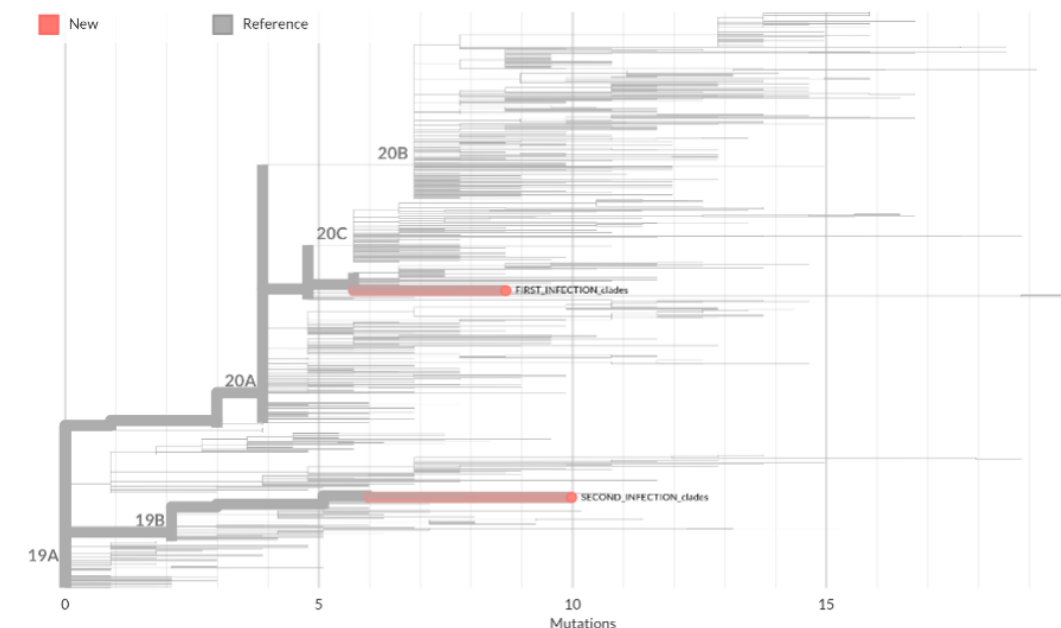


Figure 2. Phylogenetic assignment of two samples recovered from the same patient at different times. Sequences were aligned to a representation of the global SARS-CoV-2 genetic diversity using a banded Smith-Waterman algorithm with an affine gap-penalty. The genomes from the first and second infections are highlighted in red. The tree was obtained from NextClade v0.4.0.

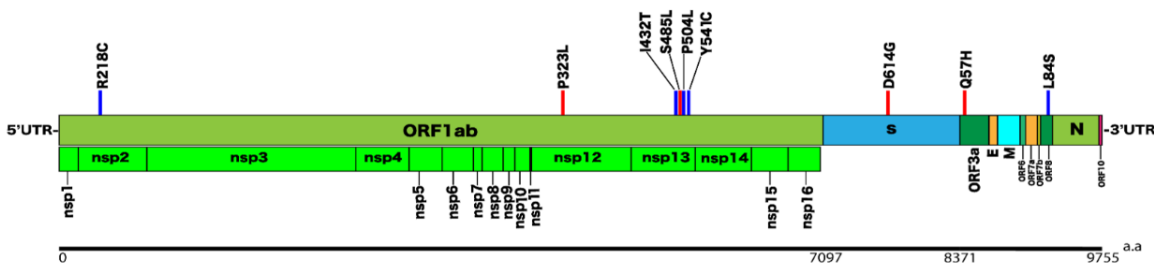


Figure 3. Genome annotation and amino acid changes were identified for each of the whole genome sequences obtained from the first and second infection events, compared to the Wuhan-Hu-1 (GenBank accession number MN908947) reference genome. In red: amino acid changes of the first genome sequence, In blue: amino acid changes of the second genome sequence. When compared to the Wuhan-Hu-1 reference genome, the sequence

from the first event has eight SNPs: C2113T, C3037T, C7765T, C14408T, C17690T, C18877T, A23403G, G25563T; these involve changes in four amino acids: P323L (in nsp12), S485L (in nsp13), D614G (in S) and Q57H (in ORF 3a). On the other hand, the genome from the second infection episode has ten SNPs: C1457T, C8782T, T9445C, T17531C, C17747T, A17858G, C18060T, G18756T, A24694T, T28144C; which determine five amino acid replacements: R218C (in nsp2), I432T, P504L, Y541C (in nsp13) and L84S (in ORF8).

OTHER PUBLICATIONS AS CONTRIBUTING AUTHOR

- Cadena, J. F., Muñoz, M., León, G. M., Armas-González, R., Márquez, D. A., Viteri, K. S., Consortium, P. C. & U.-C., Valiente-Echeverría, F., Rifo, R. S., & Molina, D. A. (2021). *Detection of the new SARS-CoV-2 variant B.1.526 with the Spike E484K mutation in South America* [Preprint]. In Review. <https://doi.org/10.21203/rs.3.rs-248965/v1>
- Carrasco-Montalvo, A., Armendáriz-Castillo, I., Tello, C. L., Morales, D., Armas-Gonzalez, R., Guizado-Herrera, D., León-Sosa, A., Ramos-Sarmiento, D., Fuertes, B., Cárdenas, P., Márquez, S., Prado-Vivar, B., Guadalupe, J. J., Gutiérrez, B., Wong, M. B., Grunauer, M., Trueba, G., Rojas-Silva, P., Barragán, V., & Patino, L. (2022). First detection of SARS-CoV-2 variant B.1.1.529 (Omicron) in Ecuador. *New Microbes and New Infections*, 45, 100951. <https://doi.org/10.1016/j.nmni.2022.100951>
- Egas, D., Guadalupe, J. J., Prado-Vivar, B., Becerra-Wong, M., Márquez, S., Castillo, S., Latta, J., Rodriguez, F., Escorza, G., Trueba, G., Grunauer, M., Barragán, V., Rojas-Silva, P., & Cárdenas, P. (2021). SARS-CoV-2 detection and sequencing in heart tissue associated with myocarditis and persistent arrhythmia: A case report. *IDCases*, 25, e01187. <https://doi.org/10.1016/j.idcr.2021.e01187>
- Emergence of lineage B.1.621 in Latin America and the Caribbean.* (2021, August 18). Virological. <https://virological.org/t/emergence-of-lineage-b-1-621-in-latin-america-and-the-caribbean/742>
- Fernandez-Cadena, J. C., Carvajal, M., Muñoz, E., Prado-Vivar, B., Marquez, S., Proaño, S., Bayas, R., Guadalupe, J. J., Becerra-Wong, M., Gutierrez, B., Morey-Leon, G., Trueba, G., Grunauer, M., Barragán, V., Rojas-Silva, P., Andrade-Molina, D., & Cárdenas, P. (2022). First case of within-host co-infection of different SARS-CoV-2 variants in Ecuador. *New Microbes and New Infections*, 48, 101001. <https://doi.org/10.1016/j.nmni.2022.101001>

- Guevara, R., Prado-Vivar, B., Márquez, S., Muñoz, E. B., Carvajal, M., Guadalupe, J. J., Becerra-Wong, M., Proaño, S., Bayas-Rea, R., Coloma, J., Grunauer, M., Trueba, G., Rojas-Silva, P., Barragán, V., & Cárdenas, P. (2022). Occurrence of SARS-CoV-2 reinfections at regular intervals in Ecuador. *Frontiers in Cellular and Infection Microbiology*, 12. <https://www.frontiersin.org/articles/10.3389/fcimb.2022.951383>
- Gutierrez, B., Márquez, S., Prado-Vivar, B., Becerra-Wong, M., Guadalupe, J. J., Candido, D. D. S., Fernandez-Cadena, J. C., Morey-Leon, G., Armas-Gonzalez, R., Andrade-Molina, D. M., Bruno, A., De Mora, D., Olmedo, M., Portugal, D., Gonzalez, M., Orlando, A., Drexler, J. F., Moreira-Soto, A., Sander, A.-L., ... Cárdenas, P. (2021). Genomic epidemiology of SARS-CoV-2 transmission lineages in Ecuador. *Virus Evolution*, 7(2), veab051. <https://doi.org/10.1093/ve/veab051>

CHAPTER 5

OVERALL PROTOCOLS AND METHODS USED IN THIS THESIS

5.1. ARBOVIRUS

5.1.1 Study site and sample collection

The study was conducted in Canton Eloy Alfaro located in Esmeraldas province in northwestern Ecuador. The serum samples were collected in six communities (Borbon, Timbiré, Colon Eloy, Maldonado, Santa María, Santo Domingo) from May 2019 until December 2021 during an active surveillance carried out in this site at individual level. A total of 1,460 households and 5,957 participants provided data for the active surveillance. The active surveillance was carried out as follows: Trained brigadistas conducted home visits weekly during the rainy season and biweekly during the dry season. During these visits the brigadistas applied a survey inquiring if house members had fever, red eyes or rash in the previous seven days, being fever the most important symptom. If a person was identified as symptomatic, the brigadista communicated directly with the auxiliar nurse who applied a questionnaire of 21 symptoms associated with suspected DENV and travel history. When a DENV-like illness was identified, the auxiliary collected a patient blood sample and a rapid test was performed. The study was approved by the Bioethics committee at the Universidad San Francisco de Quito, the University of Michigan, and the Ecuadorian Ministry of Health. The first screening was performed with a rapid test for dengue NS1, IgM and IgG in the field. Subsequently positive and negative samples were centrifuged, and the serum samples were divided into three aliquots and stored in liquid nitrogen. Then, these samples were transported in liquid nitrogen from the study site to the virology lab at Universidad

San Francisco. Here the samples were classified in the different serum aliquots from each sample. The second aliquot was used for the next steps.

5.1.2 RNA extraction

During the study period (dates 2019-2023) The RNA was extracted from 488 fever serum samples by using the QIAamp Viral RNA Mini Kit (250) Cat. No. 52906 (QIAGEN, <https://www.qiagen.com>, External Link), according to manufacturer's instructions. Briefly, 140 μ l of serum was added to 560 μ l of AVL buffer which contained 5.6 μ l of RNA carrier. The **AVL buffer** contains chaotropic salts and detergent which produce the lysis of the sample ensuring viral isolation and also is capable of inactivating RNAses. The **carrier RNA** is added to the AVL for two purposes, the first one is to enhance the binding of the RNA molecules to the membrane column and the second is to avoid degradation of isolated RNA molecules. The mixture was incubated for 10 minutes at room temperature, then 560 μ l of 100% ethanol was added. **Ethanol** is an important reagent since it is used to induce nucleic acid precipitation during the process. The **AVL buffer** and the **ethanol** inactivate the virus in the sample. Then a vortex for 15s was performed for the mixture and subsequently 630 μ l of the mixture were placed on the column in a 2ml tube. The mixture was centrifuged for 1 minute at 8000rpm. This step was performed two times. Subsequently, 500 μ l of **buffer AW1** were added to the column and centrifuged for 1 minute at 8000 rpm. **Buffer AW1** is supplied as a concentrate so before using for the first time, an amount of ethanol (96–100%) should be added as indicated on the bottle. In this case, an extraction kit for 250 reactions was used, so the volume added was 130ml of ethanol. This buffer contains a low concentration of Guanidinium Chloride leading to denaturation of proteins so these could pass through the filter. Then, 500 μ l of **buffer AW2** was added to the column and centrifuged for 3 minutes at 14,000 rpm. **Buffer AW2** is a Tris-based ethanol solution capable of removing salts,

allowing nucleic acid purification. The amount of ethanol 100% added to the buffer was 160ml according to manufacturer's instructions. Then, the columns were centrifuged once more for 1 minute at 14,000 rpm. This step is used to remove the excess of ethanol leading the column to dry. Then the column was placed in a new 1.5 ml tube and 60 µl of **AVE buffer** was added and incubated for 1 minute at room temperature. **AVE buffer** is RNase-free water that contains 0.04% sodium azide to avoid microbial growth and contamination with RNAses. The 60 µl of RNA was divided into 2 aliquots of 30 µl and stored at 80°C.

5.1.3 Real time PCR for the detection and differentiation of Zika virus, chikungunya virus, and dengue virus

The extracted RNA was used as a template to carried out the Real time PCR protocol “ZCD multiplex real time assay” (Waggoner et al, 2016) for DENV, ZIKV and CHIKV virus detection. The protocol was performed as follows:

Before performing the ZCD multiplex, all primers and probes were reconstituted at 100µM. Subsequently the ZCD mix was prepared according to the **Table 3** in which primer and probe mix formulations for ZCD preparation for 1000 µl are described:

Table 3. Primers used for ZCD Mix preparation for 1000 µl

Name	1000µl of Mix	
	µL of 100µM Stock	
Primer name	Volume (µl)	Primer Sequences
Den1-2-3 F-long	43.75	CAGATCTCTGATGAAC AACCAACG
Den1 5' New Down	37.50	TTTGAGAATCTCTTCG CCAAC
Den2 F-long C to T	43.75	CAGATCTCTGATGAAT AACCAACG
Den2 R2	43.75	AGTTGACACGCGGTTT CTCT
Den2 R2 A to G	43.75	AGTCGACACGCGGTTT CTCT
Den3 F-long C to T	37.50	CAGATTTCTGATGAAC AACCAACG
Den4 F1	56.25	GATCTCTGGAAAAATG AAC
Den4 R1	56.25	AGAATCTCTTCACCAA CC
RNAse P Forward	12.50	AGATTTGGACCTGCGA GCG
RNAse P Reverse	12.50	GAGCGGCTGTCTCCAC AAGT

Chik_D_F2Y	37.50	CATCTGCACYCAAGTG TACCA
Chik_D_R2	37.50	GCGCATTTTGCCTTCG TAATG
Zika_F1	37.50	CAGCTGGCATCATGAA GAAYC
Zika_R1_TC	37.50	CACTTGTCCCATCTTC TTCTCC
Zika_R1_CT	37.50	CACCTGTCCCATCTTT TTCTCC

Table 4. Probes used for ZCD Mix preparation for 1000 μ l

Name	Volume (μ l)	Probe sequences	Fluorophore
DENV1 BHQplus	12.50	CTCGCGCGTTTC AGCATAT	FAM
DENV2 BHQplus	12.50	CTCTCGCGTTTC AGCATAT	FAM
DENV2 Alt BHQplus	12.50	CTCTCACGTTTC AGCATATTG	FAM
DENV3 BHQplus	12.50	CTCACGCGTTTC AGCATAT	FAM

RNAse P	6.25	TTCTGACCTGAA GGCTCTGCGCG	Cal Fluor Orange 560
Chik_D_Probe2	12.50	GCGGTGTACACT GCCTGTGACYGC	Cal Fluor Red 610
Zika_Pr1	12.50	CACCTGTCCCAT CTTTTCTCC	Cal Gold
Sub-Total	656.25		
Water	343.75		
Total	1000		

A positive control for each target was included and as a negative control water was used. Samples and controls were thawed at 4°C and placed on ice while preparing the run. Then, a master mix was prepared using ZCD mix (**Table 4**) and 2x reaction mix and Taq polymerase from kit SuperScript® III Platinum® One-Step Quantitative RT-PCR System as follows (**Table 5**):

Table 5. Mastermix formulation for ZCD assay

ZCD Assay Master Mix	Volume - µl (1 rxn)
2X Mix/Buffer	12.50
ZCD Mix	2
SuperScript® III Platinum®	0.50
Water	5

Subtotal (μL)	20
Template (μL)	5
Total (μL)	25

Then the final reaction mixture was mixed with a low speed vortex and briefly centrifuge to remove fluid from the lid and load 20μL of master mix into each well and 5μl of the samples or controls were added.

The reactions were performed in a Biorad CFX96™ real-time PCR thermal cycler using the ZCD cycling conditions (**Table 6**). For result interpretation, the curves were visualized in log scale and if a signal is detected in blue, red or green with a $C_t > 38$ or if there is no signal is considered negative. If a signal is detected in blue, red or green with a $C_t < 38$ and considered as a “true” curve in log scale, the sample was considered as positive.

Table 6. ZCD qRT-PCR cycling conditions.

Step	Cycle	Temperature (°C)	Time (m/s)
Reverse transcription	1 cycle	52°C	15:00
Denature	1 cycle	94°C	2:00
Amplify	45 cycles	94°C	0:15
		55°C*	0:40
		68°C	0:20

	*Acquire in all channels at this step		
--	---------------------------------------	--	--

5.1.4 Conventional PCR

A conventional PCR for DENV serotyping (Harris et al, 1998) was performed with DENV positive serum samples. The primers and probes for each serotype are shown in **Table 7**.

Table 7. Primers for dengue serotype conventional RT-PCR

Pathogen (s)	Assay	Forward and reverse primers sequence (5'-3')	Reference
DENV serotypes 1-4	Conventional RT-PCR	D1: 5'-TCA ATA TGC TGA AAC GCG CGA GAA ACC G, TS1: 5'-CGT CTC AGT GAT CCG GGG G TS2: 5'-CGC CAC AAG GGC CAT GAA CAG TS3: 5'-TAA CAT CATCAT GAG ACA GAG C TS4: 5'-TGT TGT CTT AAA CAA GAG AGGTC	Harris et al, 1998 (23)

For the Master Mix Preparation, primers at 10 μ M and the 2x reaction mix (from SuperScript® III Platinum® one step system) were thawed at 4°C. The master mix was prepared as shown in

Table 8 as follows:

Table 8. Mastermix formulation for DENV serotype RT-PCR

Component	Volume - μ l (1 rxn)	Final concentration
Water	4.20	N/A
2x reaction mix	12.50	1.6mM
D1 (10 μ M)	0.50	200mM
TS1 (10 μ M)	0.50	200mM
TS2 (10 μ M)	0.50	200mM
TS3 (10 μ M)	0.50	200mM
DENV4 (10 μ M)	0.50	200mM
SuperScript® III Platinum®	0.80	4U/ μ l
Total	20 μ l	

Then the final reaction mixture was mixed with a low-speed vortex and briefly centrifuged to remove fluid from the lid and subsequently loaded 20 μ L of master mix into each 0.2 ml tube and then 5 μ l of the samples or controls were added.

The reactions were performed on a Biorad T100 conventional thermal cycler using the DENV-serotype cycling conditions described in **Table 7** as follows:

Table 9. DENV serotype RT-PCR cycling conditions.

Step name	Temp (°C)	Time (M:S)	#Cycles
Reverse Transcription	52	30:00	1
Incubation	94	02:00	1
Amplify	94	0:45	40
	55	1:00	
	72	1:00	
Final extension	72	05:00	1

5.1.4.1. Electrophoresis

An 1.5% agarose gel stained was prepared with 1µl of **Sybersafe**, which is a reagent that intercalates with DNA and fluoresces under UV light. The amplicons were separated using 110 volts for 30 minutes, run with a 100 bp DNA ladder and then visualized in the molecular Imager Gel Doc XR system and then visualized in the software Image lab. For each one of the serotypes the size of the products were as follows:

DENV-1 482 bp; DENV-2 119 bp; DENV-3 290 bp; DENV-4 389bp

For positives for CHIKV a conventional PCR was designed since we needed additional confirmation that these positives were CHIKV. (Marquez et al., 2022). The amplicons were sent for sequencing in Macrogen (South Korea). The primers and probes for CHIKV detection are shown in **Table 10**.

Table 10. CHIKV conventional RT-PCR assay primers

Pathogen (s)	Assay	Forward and reverse primers sequence (5'-3')	Probe sequence (5'-3')	Reference
CHIKV	Conventional RT-PCR	CHIK F 10011: 5'-CAA ATA GCA ACA AAC CCG-3' CHIK R 10396: 5'-GGC CGT CGA GAA AGA GAT-3'		Márquez et al (2022)

For the Master Mix Preparation, primers at 10 μ M and the 2x reaction mix (from SuperScript® III Platinum® one step system) were thawed at 4°C. The master mix was prepared as described in **Table 11**.

Table 11. Mastermix formulation for CHIKV RT-PCR.

Component	Volume - μ l (1 rxn)	Final concentration
Water	5.0	N/A
2x reaction mix	12.50	1.6mM
CHIKV F 10011 (10 μ M)	1.0	200mM
CHIKV R 10396 (10 μ M)	1.0	200mM

SuperScript® III Platinum®	0.80	80U/ul
----------------------------	------	--------

Then the final reaction mixture was mixed with a low-speed vortex and briefly centrifuged to remove fluid from the lid and subsequently loaded 20µL of master mix into each 0.2 ml tube and then 5µl of the samples or controls were added.

The reactions were performed on a Biorad T100 conventional thermal cycler using the DENV-serotype cycling conditions described in **Table 12** as follows:

Table 12. CHIKV RT-PCR cycling conditions.

Step name	Temp (°C)	Time (M:S)	#Cycles
Reverse Transcription	50	30:00	1
Incubation	95	15:00	1
Amplification	94	1:00	40
	52	1:00	
	72	1:00	
Final extension	72	10:00	1

5.1.4.2. Electrophoresis

An 1.5% agarose gel stained was prepared with 1µl of **Sybersafe**, which is a reagent that intercalates with DNA and fluoresces under UV light. The amplicons are separated using 110 volts for 30 minutes, run with a 100 bp DNA ladder and then visualized in the molecular Imager Gel Doc XR system and visualized in the software Image lab. The presence of a 385 bp product indicated a positive result for CHIKV.

5.1.5. Negative samples

Negative samples for DENV, ZIKV and CHIKV were further tested for other pathogens with Real time PCR protocols for MAYV, OROV and *Leptospira* as follows:

5.1.5.1. MAYV Real-time PCR

For MAYV detection in negative serum samples a real-time PCR assay was used with the following primers and probes described in **Table 13** (Powers et al., 2006).

Table 13. MAYV qRT-PCR assay primers and probes

Pathogen (s)	Assay	Forward and reverse primers sequence (5'-3')	Probe sequence (5'-3')	Reference
MAYV	qPCR	MAYARO 9666 F CATGGCCTACCTGTGGGATAAT A MAYARO 9797 R GCACTCCCGACGCTCACTG	MAYARO 9734(-) P FAM TCGGGCGCAACATGTAG TCAGGATAA BHQ1	Powers et al. 2006

For the Master Mix Preparation, primers at 10 μM and 2x reaction mix (from SuperScript® III Platinum® one step system) were thawed at 4°C. The master mix was prepared as shown in **Table 14**.

Table 14. Mastermix formulation for MAYV real-time PCR

Component	Volume - μl (1 rxn)
Water	3.44
2X Reaction mix	10
MAYARO 9666 (100 μM)	0.18
MAYARO 9797 (100 μM)	0.18
MAYARO 9734 FAM (10 μM)	0.4
SuperScript® III Platinum®	0.8

Then the final reaction mixture was mixed with a low-speed vortex and briefly centrifuge to remove fluid from the lid and subsequently loaded 20 μL of master mix into each well and then 5 μl of the samples or controls were added.

The reactions were performed on a Biorad CFX96™ real-time PCR thermal cycler using the MAYV cycling conditions (**Table 15**). For result interpretation, the curve visualization was in log scale and if a signal was detected in blue with a $C_t > 39$ or if there is no signal is considered negative. If a signal was detected in blue with a $C_t < 39$ and is considered as a “true” curve in log scale, the sample was considered positive.

Table 15. MAYV real-time PCR cycling conditions.

Step name	Temp (°C)	Time (M:S)	Cycles
Reverse Transcription	45	10:00	1
Denature	95	05:00	1
Amplify	95 57	0:05 0:35	45
Cooling	40	0:30	1

5.1.5.2 OROV Real-time PCR detection

For OROV detection in negative serum samples a real time PCR assay was used with the following primers and probes described in **Table 16** (Wise et al, 2020).

Table 16. OROV qRT-PCR assay primers and probes.

Pathogen (s)	Assay	Forward and reverse primers sequence (5'-3')	Probe sequence (5'-3')	Reference

OROV	qPCR	<p>OROV F</p> <p>CATTTGAAGCTAGATACGGACA</p> <p>A</p> <p>Ec2 R</p> <p>CATCTTTGGCCTTCTTTTRG</p>	<p>OROV P</p> <p>FAM-</p> <p>CAATGCTGGTGTGTTA</p> <p>G</p>	<p>Wise et al,</p> <p>2020</p>
------	------	---	--	--------------------------------

Before performing the assay, the primer/probe mix was prepared as follows:

1,114.5µl water + 54µl OROV F(100µM) + 54µl OROV Ec2 R (100µM) + 37.5µl OROV P (100µM). For the Master Mix Preparation, primer/probe mix at 10 µM and the 2x reaction mix (from SuperScript® III Platinum® one step system) were thawed at 4°C. The master mix was prepared as shown in **Table 17**.

Table 17. Mastermix formulation for OROV real-time PCR.

Component	Volume - µl (1 rxn)
Primer probe mix	4.2
2X Reaction mix	10.0
SuperScript® III Platinum®	0.8
Total	15

Then the final reaction mixture was mixed with a low speed vortex and briefly centrifuge to remove fluid from the lid and subsequently loaded of 15 μ L of master mix into each well followed by 5 μ l of the samples or controls.

The reactions were performed on a Biorad CFX96TM real-time PCR thermal cycler using the OROV cycling conditions (**Table 18**). For result interpretation, the curve visualization was in log scale and if a signal was detected in blue with a $C_t > 39$ or if there was no signal was considered negative. If a signal was detected in blue with a $C_t < 39$ and was considered as a “true” curve in log scale, the sample was considered as positive.

Table 18. OROV real-time PCR cycling conditions.

Step name	Temp (°C)	Time (M:S)	Cycles
RT	50	10:00	1
Denature	95	02:00	1
Amplify	95	0:10	45
	60	0:40	
Cooling	40	0:30	1

5.1.5.3. *Leptospira* Real-time PCR detection

For *Leptospira spp.* detection in negative serum samples, a real time PCR assay (Stoddard et al., 2009) was used with the following primers and probes described in **Table 19**.

Pathogen (s)	Assay	Forward and reverse primers sequence (5'-3')	Probe sequence (5'-3')	Reference
<i>Leptospira spp.</i>	qPCR	LipL32-45F 5'-AAG CAT TACCGC TTG TGG TG-3' LipL32-286R 5'-GAACTCCCA TTTCAGCGATT-3'	LipL32-189P FAM-5'- AAAGCCAGGACAAGCG CCG-3'-BHQ1	Stoddard et al, 2009 (26)

For the Master Mix Preparation, primers at 10 μ M and ABI taq man universal PCR (2X) were thawed at 4°C. The master mix was prepared as shown in **Table 20**:

Table 20. Mastermix formulation for *Leptospira* real-time PCR

Component	Volume - μ l (1 rxn)
Water	2.90
ABI taqman universal PCR (2X)	5
Lipl32 F (20 μ M)	0.45
Lipl32 R (20 μ M)	0.45
Lipl32 (20 μ M-FAM)	0.20

Then the final reaction mixture was mixed with a low speed vortex and briefly centrifuge to remove fluid from the lid and subsequently load 9 μ L of master mix into each well and then 1 μ l of the samples or controls were added.

The reactions were performed on a Biorad CFX96™ real-time PCR thermal cycler using the *Leptospira* cycling conditions (**Table 21**). For result interpretation, the curve visualization was in log scale and if a signal was detected in Blue with a $C_t > 39$ or if there was no signal was considered negative. If a signal is detected in Blue with a $C_t < 39$ and is considered as a “true” curve in log scale, the sample is considered positive.

Table 21. *Leptospira* spp. real-time PCR cycling conditions.

Step name	Temp (°C)	Time (M:S)	Cycles
UNG activation	50	02:00	1
Hot Start	95	10:00	1
Amplify	95	0:15	44
	58	01:00	

5.1.5.4. Metagenomic analysis

As ten samples remained negative for the previous screening, a metagenomic analysis was conducted in these samples since the main symptom was fever. The intention was to identify the pathogen and then generate whole genome sequences.

5.1.5.4.1 cDNA preparation

For cDNA preparation was performed with the Sequence-independent single-primer amplification (SISPA) as follows. The first strand was generated by mixing sol-primer A at a concentration of 40 μ M (5' GTT TCC CAC TGG AGG ATA NNN NNN NNN 3') and 4 μ l of the RNA template. This were incubated at 65°C for 5 minutes and subsequently at 21°C for 5 minutes. Then a reverse transcription reaction was performed using the total volume of the previous step and added 0.5 μ l of Superscript III RT Enzyme, 2 μ l of 5x first strand buffer, 1 μ l dNTPs (10 mM), 0.5 μ l of 0.1 DTT (0.1mM) and 1 μ l molecular grade water. This reaction was incubated at 42°C for 1 hour. Next, to synthesize the second strand, 10 μ l of the previously obtained first strand were mixed with 3.85 μ l of molecular grade water, 1 μ l of 5X Sequenase buffer and 0.15 μ l of Sequenase enzyme and incubated at 37°C for 8 minutes. Following the synthesis of the second strand, 15 μ l of the second strand was mixed with 0.45 μ l of Sequenase dilution buffer and 0.15 Sequenase enzyme. This reaction was incubated at 37°C for 8 minutes. After cDNA was synthesized, it was amplified by PCR, for which 5 μ l of cDNA was added and mixed with 35 μ l molecular grade water, 5 μ l of 10X Accutaq Reaction Mix, 1 μ l of Sol-Primer B at 100 μ M (5' GTT TCC CAC TGG AGG ATA 3'), 2.5 μ l of 10mM dNTPs and 0.5 μ l of Accutaq Enzyme. The cycling conditions for the PCR were: 98°C for 30 seconds, followed by 30 cycles at 94°C for 15 seconds, 50°C for 20 seconds, and 68°C for 5 minutes and a final extension at 68°C for 10 minutes (Kafetzopoulou LE et al., 2018).

5.1.5.4.2 Library preparation

Nanopore library preparation was performed using as template the SISPA PCR product following the manufacturer's instructions for sequencing protocols, Oxford Nanopore

Technologies Ligation kit protocol (SQK-LSK109; Oxford Nanopore Technologies, Oxford, United Kingdom) and Native barcoding kit (NB-114).

5.1.5.4.3. Library sequencing

This library was sequenced using MinKNOW version 4.05 for 24 hours. Base calling was performed using Guppy v. 3.4.5. Porechop v. 0.2.4 was performed for demultiplexing and to remove adapters and barcodes. The taxonomic profile of the sequences of each sample was classified with the Kaiju web server platform.²⁸ The database “NCBI Blast nr leuk” was selected (includes bacteria, archaea, fungi, viruses, and eukaryotes), the running method used was the MEM algorithm (maximum exact matches), and the rest of the parameters were kept by default. For the analysis of the taxonomic profiles, the number of assigned readings and the generated Krona charts were considered.

Another software used for taxonomic classification of metagenomes was Epi2me software. Among its main advantages is real-time analysis, as the fastq passes of the sequencing are generated. These are uploaded to the application and analyzed. The analysis in this case was Fastq WIMP. This analysis allowed us to identify viruses, bacteria, fungi and archaea from each sample. The next step was to select the analysis parameters. As these were human samples, “Yes” response was selected in both fields and the rest of the parameters were left by default. The data was uploaded to the program's server and after a few minutes information about the processed, classified and quality readings was generated. In addition to this, a report was generated in real time. This report was displayed in the browser and it showed a general classification of the microorganisms in the samples, the percentages of classified readings, genera and species. Another software for comparison of results was BugSeq which is a software

that works in the browser and also allowed the taxonomic assignment and assembly of metagenomes. This program is an Open-Source web-server and do not need installation (Go to <https://bugseq.com/academic>). The final results included a quality analysis of each sample, taxonomic assignment, and metagenome assembly in case there were enough reads. The results were available on the web for a maximum of 30 days. However, they could also be downloaded in "Download all as zip".

5.1.5.5. DNA extraction

The DNA was extracted from 10 serum samples, by using Pure® link DNA Kit (Thermo Fisher Scientific, California, USA) according to manufacturer's instructions. Briefly, 200µl of serum was added to 20 µl of proteinase K, 20 µl of RNase, A and 200 µl of lysis/binding. The mixture was incubated for 10 minutes at 55°C, then 200 µl of ethanol (96- 100%) was added. Then 640 µl were added to a spin column and centrifuged at 13,000 rpm for 1 minute. 500 µl of wash buffer 1 were added and centrifuged at 13,000 rpm for 1 minute. Then 500 µl of wash buffer 2 were added and then centrifuged at 13,000 rpm for 1 minute. The column was centrifuged at 14,000 rpm for 3 minutes at room temperature. Next, 70 µl of the elution buffer were added and incubated for 1 minute. Then the column was centrifuged at 14,000 rpm for 1 minute and the DNA was stored at -20°C.

5.1.5.6 Nested Conventional PCR for the detection and differentiation of *Plasmodium falciparum*

A conventional nested PCR for *Plasmodium falciparum* detection (Snounou et al, 1996) was performed for malaria confirmation with the following primers and probes described in **Table 22**. The protocol was provided by Fabián Saenz from Universidad Católica del Ecuador.

Table 22. *Plasmodium falciparum* conventional nested PCR assay primers (PCR 1 and PCR2)

Pathogen (s)	Assay	Forward and reverse primers sequence (5'-3')	Reference
<i>Plasmodium falciparum</i>	Conventional nested PCR	<p>PLU5</p> <p>5'-CCTGTTGCCTTAAACTTC-3'</p> <p>PLU 6</p> <p>5'-</p> <p>TTAAAATTGTTGCAGTTAAAAC</p> <p>G-3'</p> <p>FAL 1</p> <p>5'-</p> <p>TTAAACTGGTTTGGGAAAACCA</p> <p>AATATATT-3'</p> <p>FAL 2</p>	Snounou, 2002

		5'- ACACAATGAACTCAATCATCAT GACTACCCGTC-3'	
--	--	---	--

For the Master Mix Preparation **PCR 1**, primers at 10 μ M and *GoTaq® Green Master Mix* were thawed at 4°C. The master mix was prepared as described in **Table 23**.

Table 23. Mastermix formulation for *Plasmodium falciparum* PCR 1

Component	Volume - μ l (1 rxn)
Water	3
<i>GoTaq® Green Master Mix</i>	12.5
Primer F (Plu5) (10 μ M)	1
Primer R (Plu6) (10 μ M)	1
MgCl ₂ (25 μ M)	2.5

Then the final reaction mixture was mixed with a low-speed vortex and briefly centrifuged to remove fluid from the lid and subsequently load 20 μ L of master mix into each 0.2 ml tube and then 5 μ l of the samples or controls were added.

The reactions were performed on a Biorad T100 Thermal Cycler using the *Plasmodium* 1 cycling conditions described in **Table 24** as follows:

Table 24. *Plasmodium* PCR 1 cycling conditions

Step name	Temp (°C)	Time (M:S)	Cycles
Incubation	95	05:00	1
Amplify	58	02:00	25
	72	02:00	
	94	1:00	
Final extension	58	02:00	1
	72	05:00	1

For the Master Mix Preparation **PCR 2**, primers at 10 μ M and *GoTaq® Green Master Mix* were thawed at 4°C. The master mix was prepared as described in **Table 23**.

Table 25. Mastermix formulation for *Plasmodium falciparum* PCR 2

Component	Volume - μ l (1 rxn)
Water	3
<i>GoTaq® Green Master Mix</i>	12.50

Primer F (FAL1) (10 μ M)	1
Primer R (FAL2) (10 μ M)	1
MgCl ₂ (25 μ M)	2.50

Then the final reaction mixture was mixed with a low-speed vortex and briefly centrifuged to remove fluid from the lid and subsequently load 20 μ L of master mix into each 0.2 ml tube and then 5 μ l of the samples or controls were added.

The reactions were performed on a Biorad T100 Thermal Cycler using the *Plasmodium 2* cycling conditions described in **Table 26** as follows:

Table 26. *Plasmodium PCR 2* cycling conditions

Step name	Temp (°C)	Time (M:S)	Cycles
Incubation	95	05:00	1
Amplify	58	02:00	30
	72	02:00	
	94	1:00	
Final extension	58	02:00	1
	72	05:00	1

5.1.5.6.1. ELECTROPHORESIS:

To visualize amplified DNA by conventional PCRs, an 1.5% agarose gel stained was prepared with 1µl of **Sybersafe**, which is a reagent that intercalates with DNA and fluoresces under UV light. The amplicons were separated using 110 volts for 30 minutes, run with a 100 bp DNA ladder and then visualized in the molecular Imager Gel Doc XR system and the software Image lab. The presence of a 206 bp product indicated a positive result for *Plasmodium falciparum*.

5.1.6. DENGUE WHOLE GENOME SEQUENCING

From 121 positive serum samples for DENV from May 2019 to December 2021), 27 positive samples with the ZCD real-time PCR cycle threshold (Ct) value of <30 were optimal for sequencing. A 20µL aliquot of cDNA was obtained using the *SuperScript™ IV* Reverse Transcriptase. Briefly for the first master mix, 1 µL of random hexamers and 1 µL of 10mM dNTP mix were added. Then 11 µl of the RNA sample were added. Mix well and spin. The mix was incubated 65°C for 5 minutes and placed on ice for 1 minute. Next a second master mix was prepared as follows: 4µl of 5x SSIV buffer, 1µl of 100mM DTT, 1µl RNA out (inhibitor) and 1µl Superscript IV enzyme. This was followed by adding 7 µl of the second master mix to each sample from the previous reaction to complete a volume of 20 µl and then this reaction was incubated as follows: 23°C for 10 minutes, 50°C for 10 minutes and 80°C for 10 minutes.

Then a multiplex tiling PCR was performed using the primer scheme corresponding to each serotype, by adding 5 µL of 5X Q5 Reaction Buffer, 0.5 µL of 10 mM dNTPs, 0.25 µL of Q5 DNA polymerase, 15.25 µL nuclease-free water, and 1.5 µL primer pool A (10 µM) and primer pool B (10 µM). For DENV-1 and DENV-2, we added 1.5 µL primer pool B (10 µM). Then 2.5 µl of cDNA prepared above was added to each of the PCR reactions. The cycling conditions for the PCR were: 98°C for 30 seconds, followed by 45 cycles at 98°C for 15 seconds and 65°C for 5

minutes. Samples that showed a 900 bp band in pool A and pool B mix were selected for sequencing. Using 2.5 µl of PCR products from each pool diluted in 45 µl of PCR water, the library was prepared by using a native barcoding kit (NB-114) with a ligation sequencing kit (LSK-109) following manufacturers' instructions and loaded it into the MinION flow cell (FLO-MIN 106) (Oxford Nanopore Technologies, <https://nanoporetech.com>External Link). A demultiplexing and adaptor removal with Porechop version 0.2.3_seqan 2.1.1 (<https://github.com/rrwick/Porechop>External Link) and the sequencing reads were assembled with a de novo assembly approach using Spades version 3.13.0 (<http://cab.spbu.ru/files/release3.13.0/manual.html>External Link). Next, the reads were mapped in Minimap2 version 2.17-R941 (<https://github.com/lh3/minimap2>External Link) against reference genomes for DENV-1 (GenBank accession no. NC_001477.1) and DENV-2 (accession no. NC_001474.2). The consensus sequence was generated with Samtools version 1.7 (<http://www.htslib.org/doc/1.7/samtools.html>External Link) and the serotype was confirmed using Genome Detective Arbovirus Typing software Tool version 1.137 (*17*) and BLAST (<https://blast.ncbi.nlm.nih.gov/Blast.cgi>External Link).

5.1.7. Phylogenetic analysis

A total of 22 samples, comprising of 9 sequences of the DENV-1 virus and 13 sequences of the DENV-2 virus, from our field location were sequenced. These sequences were used for our phylogenetic study. Furthermore, we conducted sequencing on an additional 5 samples derived from the reference hospital in Esmeraldas, through the national surveillance system. Among these, 3 samples were identified as DENV-1 and 2 samples as DENV-2 (accession numbers SRR1593089–SRR15793115) confirming circulation of these two serotype in clinical cases. The

selection of these hospital samples was based on the patient clinical records, particularly focusing on those residing in Esmeraldas.

To enhance the diversity of the phylogenetic analysis, we integrated 22 sequences from GenBank. These comprised 21 sequences from El Oro Province, situated in the southern part of Ecuador, and 1 sample from Esmeraldas. In order to facilitate cross-border comparisons, we incorporated available GenBank sequences from various countries, including Argentina, Brazil, Peru, Nicaragua, Belize, Venezuela, and Colombia.

Before creating sequence alignments, we identified appropriate genomes from the NCBI. This was accomplished by a randomly selecting the results obtained from a BLAST search using our complete genome sequences for each serotype separately. Subsequently, we performed sequence alignments using MAFFT version 7.471 (<https://mafft.cbrc.jp/alignment/server>External Link), which were then carefully reviewed and adjusted using Aliview version 1.28 (<https://github.com/Aliview/Aliview>External Link).

The construction of maximum-likelihood phylogenetic trees for each serotype was done using RaxML-HPC Blackbox version 8.2.12 (<https://cme.h-its.org/exelixis/web/software/raxml>External Link). This was carried out under a general time-reversible substitution model (GTR) with 1,000 bootstrap replicates. The visual representation of these trees was accomplished using FigTree version 1.4.4 (<http://tree.bio.ed.ac.uk/software/figtree>External Link).

Temporal patterns within the datasets were explored by conducting root-to-tip genetic distance analysis using TempEst version 1.5.3 (18). Additionally, tree rooting was performed with R2 method. To explore the temporal dynamics of DENV dissemination, Bayesian time-calibrated

trees were constructed using BEAST version 1.10.4 under a Hasegawa-Kishino-Yano substitution model and an uncorrelated lognormal relaxed molecular clock (19). A Bayesian skyline tree prior was used (20) with 10 groups and piece-wise constant reconstruction. Then a Markov chain Monte Carlo chains over 100 million steps was used and recorded trees at intervals of 1,000 steps. The first 10% of trees were discarded as burn-in by using TreeAnnotator version 1.10.4 (<https://beast.community/treeannotator>). Convergence and mixing of model parameters were assessed, defined by effective sample of >200 in Tracer version 1.7.1 (21). Finally, maximum clade credibility (MCC) trees for each run using TreeAnnotator version 1.10.4, summarizing node ages as median heights.

5.2 SARS-CoV-2

5.2.1. Sample collection

Nasopharyngeal, oropharyngeal swabs, broncho-alveolar lavages, heart tissue were collected from symptomatic and asymptomatic patients in public third-level hospitals and clinics located in different provinces of Ecuador. Samples were stored in 1X DNA/RNA shield (Zymo, USA) for viral inactivation and preservation of nucleic acids. The samples were transported to Institute of microbiology at Universidad San Francisco de Quito in a sealed container following the biosafety and containment measures at room temperature. The study was approved by the Bioethics Committee of Universidad San Francisco de Quito (CEISH No. 1234) and was performed through a collaboration and authorization by the Ministry of Health.

5.2.2. RNA extraction

The RNA was extracted by using the Zymo Quick-RNA™ Viral Kit, according to manufacturer's instructions. Briefly, 200µl of the sample was added to 400 µl of Viral RNA buffer. The mixture was transferred into a spin column and centrifuged for 2 minutes at maximum speed. Then 500 µl of Viral Wash Buffer were added to the column and centrifuged for 30 seconds. The same step was repeated for a second time. Following this, 500 µl of ethanol 96% were added to the column and centrifuged for 1 minute to ensure complete removal of the wash buffer. For RNA elution, 15 µl of DNase/RNase-Free Water were added directly to the column matrix and centrifuged for 30 seconds. This RNA was stored at 80°C.

5.2.3 Real time RT-PCR for the detection of SARS-CoV-2 virus

The Luna® SARS-CoV-2 RT-qPCR Multiplex Assay Protocol (NEB #E3019) was used for SARS-Cov-2 detection, as it is a commercial kit, primers and probes are not known to the user.

For the Master Mix Preparation, Luna® probe one-step RT-qPCR 4X mix, SARS-CoV-2 primer mix (10x), positive control and nuclease-free water were thawed at room temperature. The master mix was prepared as shown in **Table 27**.

Table 27. Mastermix formulation for SARS-CoV-2 real time PCR

Component	Volume - µl (1 rxn)
Luna ® probe one-step RT-qPCR 4X mix	5
SARS-CoV-2 primer mix (10X)	2

Nuclease-free water	11
---------------------	----

Then the final reaction mixture was mixed with a low-speed vortex and briefly centrifuge to remove fluid from the lid and subsequently load 18 μ L of master mix into each well and then 2 μ l of the samples or controls.

The reactions were performed on a Biorad CFX96TM real-time PCR thermal cycler using the Mayaro cycling conditions (**Table 28**). For result interpretation, the Curve visualization is in log scale and if a signal is detected in Blue with a $C_t > 39$ or if there is no signal is considered negative. If a signal is detected in Blue with a $C_t < 39$ and is considered as a “true” curve in log scale, the sample is considered positive.

Table 28. SARS-CoV-2 real time PCR cycling conditions.

Step name	Temp (°C)	Time (M:S)	Cycles
Carryover prevention	25	0:30	1
Reverse transcription	55	10:00	
Initial Denature	95	01:00	
Amplification and Extension	95	0:10	45
	60	0:30	

Step name	Temp (°C)	Time (M:)	Cycles
Reverse Transcription	45	10:00	1
Denature	95	05:00	1
Amplification	95 57	0:05 0:35	45
Cooling	40	0:30	1

The fluorophores were assigned for each target as shown in **Table 27**.

Table 29. Targets and fluorophores for SARS-CoV-2 detection

Target	Fluorophore
2019-nCoV N1	HEX
2019-nCoV N2	FAM
Internal Control (RNase P)	Cy5

The amplification curves were analyzed and Ct values for each fluorophore and sample. Only positive samples were included in the sequencing protocol.

5.2.5 SARS-CoV-2 whole genome sequencing

5.2.5.1 Tiling PCR

The V3 pools have 110 primers in pool 1 and 108 primers in pool 2, so the requirement was ~ 4 µl of primer pool (10 micromolar (µM)) per 25 µl reaction. An aliquot of 10 µl of cDNA A 20µL aliquot of cDNA was obtained using the LunaScript® RT SuperMix Kit by mixing 2 µl of this reagent with 8 µl of RNA. The mix was incubated 25°C for 2 minutes, 55°C for 10 minutes and 95°C for 1 minute.

Then a multiplex tiling PCR was performed by adding 12.5 µL of Q5 Hot Start High-Fidelity 2X Master Mix, 3.6 µL of V3 primer pool A (10 µM) and V3 primer pool B (10 µM) and 5.4µL of nuclease-free water. Then 3.5 µl of cDNA were added to each of the PCR reactions. The cycling conditions for the PCR were: 98°C for 30 seconds, followed by 35 cycles at 98°C for 15 seconds and 65°C for 5 minutes. Samples that showed a 400 bp band in pool A and pool B mix were selected for sequencing.

5.2.5.2. Sequencing in Nanopore following the NCoV-2019 v3 Sequencing (Low Cost Protocol)

Using 2.5 µl of PCR products from each pool diluted in 45 µl of PCR water, the library was prepared by using a native barcoding kit (NB-114) with a ligation sequencing kit (LSK-109) following manufacturers' instructions and loaded it into the MinION flow cell (FLO-MIN 106) (Oxford Nanopore Technologies, <https://nanoporetech.com>External Link).

5.2.6. Bioinformatic pipeline for sequencing analysis (ARTIC PROTOCOL)

The wf-artic workflow implements a slightly modified ARTIC Field Bioinformatics workflow for the purpose of preparing consensus sequences from SARS-CoV-2 genomes that have been sequenced using a pooled tiling amplicon strategy. <https://github.com/epi2me-labs/wf-artic>. The workflow had a folder containing demultiplexed sequence reads done by either MinKNOW or Guppy. The workflow needed to know the primer scheme that has been used during genome amplification and library preparation in this case was ARTIC/V3. The sequences in FASTQ format were aggregated, filtered for sequence length and quality characteristics, and were mapped to the reference SARS-CoV-2 genome by using minimap2. A primer-scheme specific bed file was used to identify the regions of the mapped sequences that correspond to synthetic sequences (primers). These regions were trimmed to ensure that sequences are entirely of biological origin. The retained sequences were used to prepare a consensus sequence that was then polished using Medaka and variant calling is performed to produce a VCF file of genetic differences relative to the reference genome. The consensus sequence was annotated for virus clade information using NextClade and a strain assignment was performed using Pangolin. The completed analysis was summarized in an HTML format report that summarized key information that included number of reads, depth of coverage information per amplicon and both the Nextclade and Pangolin information.

CHAPTER 6

6.1. DISCUSSION

Current diagnostic tests such as PCR, ELISA, and RDTs are target-specific and require prior knowledge of the circulating pathogens. These tests are not very useful in tropical regions with a high incidence of unidentified febrile diseases. In this thesis, I used a combination of different approaches including molecular and serological assays to detect and confirm the presence of pathogens in clinical samples from patients suffering from unidentified febrile illnesses in tropical regions of Ecuador. In some cases, pathogens such as Oropouche virus (OROV), *Plasmodium* sp. and the SARS-CoV-2 virus were detected first using a metagenomic screening procedure (Wise *et al*, 2018, Marquez *et al*, 2022, Marquez *et al*, 2020) and subsequently confirmed by other specific protocols (Wise *et al*, 2020, Marquez *et al*, 2022). Another key element during my research was the use of active and passive surveillance to detect fevers. During the SARS-CoV-2 pandemic, my work pivoted to supporting the public health emergency through the implementation of validated QPCR diagnostics as well as conducting genomic surveillance of variants of Concern. Although COVID-19 is not specifically a tropical disease, my work in this area involved a range of innovative approaches to researching a novel virus.

The discovery of Oropouche virus (OROV) in Ecuador was done by metagenomic (MINION one-pot protocol) sequencing in a patient sample that was negative for Dengue virus (DENV), Chikungunya (CHIKV), Zika (ZIKV), Mayaro (MAYV) and Yellow fever (YFV) viruses as well as for *Plasmodium*, *Leptospira* and *Rickettsia* (Wise *et al*, 2018). After genetic confirmation, OROV was isolated from the serum sample (Wise *et al*, 2018). In our active surveillance study in Esmeraldas in 2019, 2 of 10 serum samples that were negative for the panel of febrile disease

agents (including DENV, ZIKV, CHIKV, OROV, MAYV and *Leptospira*) resulted positive for *Plasmodium* spp. using a metagenomic analysis (Accession ID: SAMN27568483, SAMN27568586) (Marquez et al, 2022). A nested PCR assay (Snounou, 1996). confirmed the presence of *Plasmodium falciparum*. During that year, the Ministry of Health reported the reintroduction and an outbreak of 146 cases of this pathogen in communities of Esmeraldas province. Based on this finding, metagenomic analysis was performed in the remaining 8 serum samples, identifying the presence of human Pegivirus (hepatitis G virus). Pegivirus has not been reported before in our study site. It is estimated that 750 million people are infected with this virus, known to be transmitted through sexual and parenteral routes. Although, the clinical significance of this finding is not clear, close to 25% of the positive cases develop persistent infection and may be associated with lymphomagenesis (Arroyave-Ospina et al., 2018).

In 2019, the Ecuadorian Ministry of Health reported 1,750 dengue cases and no Chikungunya cases Esmeraldas province. Officially, the Chikungunya epidemic that started in 2014 in Ecuador was over by 2018. The passive surveillance system of undifferentiated febrile diseases, carried out by the Ecuadorian Ministry of Health, mainly focuses on clinical diagnosis. In contrast, in our active surveillance study, using multiplex real-time PCR as a critical assay for arboviral screening of DENV, ZIKV and CHIKV, we showed that 61% of the febrile samples we processed contained CHIKV, 30% DENV, and 10% were coinfections of DENV/CHIKV. These results showed that Chikungunya was prevalent in 2019 on the northern Coast of Ecuador (Marquez et al, 2022) and that the outbreak went undetected by the public health system. Since the multiplex real-time PCR was not available for DENV serotyping, a multiplex conventional PCR that differentiates among the four serotypes was used (Harris et al, 1998). In this study, DENV-1 was found to be co-circulating with CHIKV during 2019 and April 2020 before the COVID-19 pandemic. Later in

January 2021, we reported the circulation of DENV-2 using the same PCR (Marquez et al, 2023). As mentioned in Chapter 1, real-time PCR presents several advantages over the conventional PCR due to its higher sensitivity, faster analysis, and the ability to be designed for simultaneous detection of co-circulating pathogens in endemic regions without the need for post-PCR electrophoresis.

During the pandemic of SARS-CoV-2 in 2020, the public health systems were overwhelmed in Latin America. Ecuador as most of its neighboring countries had limited capacity for COVID-19 diagnosis. For this reason, my research plans were pivoted to collaborations with other Ecuadorian universities and the Ministry of Health to carry out RT-PCR testing for the public as well as genomic surveillance activities including SARS-CoV-2 variant detection, and research on SARS-CoV-2. At the beginning of the pandemic in Ecuador, in March 2020, a Dutch tourist presented respiratory symptoms during a visit to Sucumbíos province in Ecuadorian Amazonia. The diagnosis of COVID-19 was confirmed by the Ecuadorian Ministry of Health. On March 11, the patient was transferred to the Eugenio Espejo Hospital in Quito to the intensive care unit. A 7 ml bronchoalveolar lavage sample was obtained using a non-bronchoscopic protected BAL.

A metagenomic analysis was performed, and 17% of the viral sequence was identified as SARS coronaviruses. Other bacterial and eukaryotic sequences were related to the patient's respiratory microbiota. By mapping the reads, a 3,173-bp SARS-CoV-2 consensus sequence was obtained (Marquez et al, 2020). Later on, as I continued to support research on COVID-19, one of the most important contributions was one of the first reports of SARS-CoV-2 reinfection worldwide and the first in Latin America (Prado-Vivar et al, 2021). On May 16th of 2020, a 46-year-old man tested positive for *ORF3a* gene with a Cq value of 36.85 for the first time. Subsequently, the patient's symptoms improved, and for confirmation, another RT-PCR was performed, testing negative on

June 3rd. One month later, the patient presented suggestive symptoms of SARS-CoV-2 once again and was tested with real-time PCR, giving a positive result (*N* gene, Cq=30.82) on July 22nd.

As his clinical status improved, a real-time PCR was performed, testing negative (Prado-Vivar et al 2020). Later, we detected additional reinfection cases in Ecuador reported by Guevara et al, (2022) in which different RT-PCR kits were used for diagnosis, such as VeriQ-PCR 316 kit, (MiCo BioMed, South Korea), the LightMix[®] SarbecoV E-gene kit (TIB Molbiol, Germany), or the Allplex[™] 2019-nCoV Assay (Seegene, South Korea). Further whole-genome sequencing was needed to confirm these reinfections as the performance of the PCR diagnostic kits and the cycle threshold value (CT) vary according to each manufacturer.

Another interesting finding by our group was the detection of SARS-CoV-2 in heart tissue in a 34-year-old patient with severe bradycardia (Egas et al, 2021). The patient worked closely with COVID-19 patients, and after one week, he developed fever, abdominal pain, vomiting, and anorexia. He was initially diagnosed and treated for gastroenteritis. However, after one week, the patient did not improve and was admitted to the hospital. An RT-PCR SARS-CoV-2 test of a nasal swab was performed at admission, and the patient tested positive to the virus. The next day the patient presented hypotension associated with bradycardia and was transferred to ICU. After 15 days, he tested negative for SARS-CoV-2.

As the pandemic was ongoing, in its early stages non-pharmaceutical interventions were established globally and in Ecuador to limit the spread of the virus (movement and social restrictions, school closures, remote study and work, mandatory masking etc). These interventions had a direct effect on disease transmission, leading to a decrease in the number of other respiratory illnesses such as influenza and rhinovirus cases, as well as DENV transmission. Once the

implementation of these measures was relaxed, infections with other respiratory viruses increased, surpassing pre-pandemic levels (Chow et al., 2023).

Even though metagenomics is a helpful tool for infectious disease detection, it also presents its limitations in relation to the library preparation method used for sequencing and its pricing. It is a tool better suited for research and not diagnosis. In 2019, negative by PCR (for the arbovirus panel) serum samples were processed using the ligation protocol, and Pegivirus reads were obtained. One of these serum samples (Pegivirus positive) was analyzed again using rapid ligation protocol, and the results were negative. The results differed significantly from the previous ones, as no Pegivirus reads were observed on the Kronachart. Some reads were likely lost due to the transposase activity of the barcode transposome complex used during library preparation, which randomly cleaves the template during library preparation. This analysis assigned most reads to bacterial genera; no virus or eukaryotic classifications were obtained. This experience shows the need of careful interpretation of metagenomic results, considering the sample metadata, the protocol used and the sample itself.

Another limitation of performing RNA metagenomic analysis in fever serum samples with unknown etiology is that, despite PCR amplification of cDNA, quantifications are low (6ng/μl o to 10 ng/μl), limiting the amount of reads or depth of sequence obtained. Nevertheless, metagenomic analysis using RNA viral metagenomics one pot sequencing protocol with ligation library preparation is recommended for any sample, demonstrating that metagenomics is a promising diagnostic tool capable of detecting a broad range of pathogens.

Furthermore, the implementation of the novel whole genome sequencing (WGS) using Nanopore technology (Oxford, UK) has been an essential step towards understanding both the dynamics of DENV transmission and that of the SARS-CoV-2 variants in Ecuador. We were able

to generate 27 whole genome sequences of DENV from serum samples of our study site, 12 for DENV-1 and 15 for DENV-2. These samples included community and hospital samples collected from May 2019 to December 2021. Subsequently, these sequences were used in a phylogenetic analysis applying a Bayesian model. The dengue phylogenetic analysis from 2019 to 2021 suggested that Esmeraldas province serves as the entry point for DENV in Northern Ecuador, with the virus arriving from Colombia and circulating locally before further dissemination (Marquez, et al 2021).

Moreover, this analysis showed that rural and remote areas in northern Ecuador has sustained virus transmission that is evolving independently of external introductions. DENV is largely considered an urban disease, but we obtained our samples from smaller rural sectors in Esmeraldas. We do observe however, through phylogenetic analysis of DENV-1 sequences within Esmeraldas province, that larger population centers are the sources of viruses circulating in smaller communities, these acting as sinks of virus once herd immunity is achieved. However, the phylogenetic analysis for DENV-2 suggests that the virus also moves from remote communities to larger, commercial centers. Although the dataset was limited, complete genomes and posterior probabilities in the nodes of the phylogenetic tree suggested that small population centers play an essential role in DENV transmission dynamics. The analysis also showed that the virus is likely spreading from Esmeraldas to other provinces of Ecuador (Marquez et al, 2023). Further sequencing is needed in Esmeraldas province and other provinces to better understand Ecuador's DENV transmission dynamics.

The implementation of Nanopore sequencing was necessary during SARS-CoV-2 pandemic to understand the genomic epidemiology of the transmission lineages in Ecuador during the first year of the pandemic. Through our analysis, we identified multiple introduction events (82) and

local circulation of virus variants were identified. Human mobility and air travel introductions played a determinant role in the spread of SARS-CoV-2. Furthermore, the province of Guayas played a vital role in viral sourcing and spread (especially at the beginning of the pandemic) throughout Ecuador. This study also suggested that high connectivity between provinces was determinant for local transmission of the SARS-CoV-2 virus (Gutierrez et al, 2021).

Moreover, two SARS-CoV-2 viral genomes (HGSQ-USFQ-007 and HGSQ-USFQ-010) showed a distinct mutation implicated in the increase of virulence by inhibiting the interferon response (Konno et al, 2020). Subsequently, the first reinfection case in Ecuador was reported, and sequencing revealed that the first infection variant belonged to clade 20A and lineage B.1.p9 while the second infection variant belonged to clade 19B and lineage A.1.1. These variants had different evolutionary trajectories. Later, with the introduction of Omicron to Ecuador, the frequency of reinfections increased 10-fold, and phylogenetic analysis confirmed that these variants do not share the same common ancestor (Guevara et al, 2022). Another important finding was the detection of lineage B.1.621 in Latin America and the Caribbean, which was widely identified in Colombia and rapidly disseminated throughout Latin America. This lineage was classified as a variant of interest named Mu in 2021 by the World Health Organization (Virological report, 2021). Due to our team's genomic surveillance, the circulation of different VOCs was reported in Ecuador, Alpha (January 2021), Gamma (March 2021), Delta (June 2021), and Omicron (December 2021). Although Delta was the predominant variant at the end of 2021, the dynamics changed with the introduction of the first Omicron lineage (B.1.1.529), which became the most prevalent and widely diverged. The Omicron lineages that have circulated in the first six months of 2023 reported by our laboratory are BQ.1.1.13, XBB.1, and XBB.1.5 (unpublished data).

Genomic surveillance has contributed to genotyping, serotyping, lineage assignment, identifying national and international transmission routes, detection of variants of concern, and identifying critical mutations for the development of treatments, diagnostic tests, and vaccines ((Lo & Jamrozy, 2020). It highlights the importance of its implementation and its direct impact on the surveillance, policymaking, and establishment of control and prevention measures for emerging infectious diseases.

The implementation of Oxford Nanopore Sequencing began through a collaboration between USFQ and Public Health England in 2019, a few months before the COVID-19 pandemic. The collaboration involved qRT-PCR and metagenomic sequencing training, where protocols for real-time PCR detection of arboviruses (MAYV, OROV, ZIKV, CHIKV, DENV) and *Leptospira*, and RNA metagenomic sequencing in serum samples were shared. With the guidance of Public Health England, primers, probes, and sequencing reagents were purchased, enabling the performance of the first assays for arboviral sequencing could be performed at the USFQ laboratory. However, in 2020 the pandemic reached Ecuador, leading to a shift in sequencing goals from febrile diseases to SARS-CoV-2. All efforts were redirected toward this new infection, and the metagenomic protocol was adapted for SARS-CoV-2 with the first sample, a bronchioalveolar lavage sample obtained from a patient that was diagnosed with COVID-19.

Subsequently, the Primer Scheme (V1 and V3) developed by the ARTIC network for nCoV-2019 became available, and the laboratory needed to implement and standardize the sequencing protocol. Collaborators from Oxford University provided the primer scheme V1 (approximately 250 primers) and the instructions for primer reconstitution and pooling. Initially, the sequencing did not work appropriately due to inaccurate sample normalization. After several attempts, the

ARTIC protocol worked, and the sequencing pipeline was successfully established. The laboratory obtained the first ten whole genomes and performed the first lineage classifications.

As the protocol continued to work, the sequencing group became part of the A2CARES consortium (Asian-American Center for Arbovirus Research and Enhanced Surveillance, part of CREID, the Centers for Research in Emerging Infectious Diseases of the US National Institutes of Health). The principal aim of this consortium was to develop interconnected networks of laboratories from different sites (Ecuador, Nicaragua, Sri Lanka, and the United States of America), run parallel arbovirus cohorts, develop, and implement molecular and serological tests and contribute to research capacity building in the country. Thus, Oxford Nanopore sequencing for SARS-Cov-2 became a vital approach to be shared with partners from Ecuador and other countries. As the USFQ laboratory had already implemented the ARTIC sequencing protocol, both consortium leaders requested USFQ to prepare an online workshop for partners in Nicaragua and Paraguay. For the first part of the workshop, the USFQ team prepared a step-by-step procedure for sequencing in a video for their laboratories. The workshop was conducted through Zoom live on April 20-21, 2021, and the video was made available and translated so other labs could benefit from the training. The second part of the workshop focused on the bioinformatics pipeline and the phylogenetic analysis conducted, which was also recorded. The A2CARES consortium organized another workshop on April 28th, 29th & 30th, 2021, related explicitly to the phylogenetic analysis of DENV, which included a practical component, supported by Dr Shannon Bennett from the California Academy of Sciences and Dr Bernardo Gutierrez from Oxford University. We learned and subsequently performed the Bayesian analysis with our Dengue Ecuadorian sequences (Marquez et al, 2023). During those months, we provided support to our Nicaraguan colleagues in implementing the ARTIC protocol in their laboratory.

As the ECODESS and A2CARES surveillance study was reactivated after pandemic restrictions, we needed to generate complete DENV genomes from serum samples of our study site. Our colleagues from Oxford University shared the primer schemes for Dengue and Chikungunya, enabling the implementation of the protocol. With prior experience with SARS-CoV-2, I was able to generate 27 complete DENV genomes (DENV-1 and DENV-2). With the dengue virus sequencing protocol successfully working, an on-site sequencing training session was prepared for our Nicaraguan partners from July 10 to July 23, 2022. Myself and a technician/student from our group also traveled to the Centro Nacional de Salud y Referencia (MINSAL CENDR) and Instituto de Ciencias Sostenibles/Sustainable Sciences Institute (ICS/SSI) in Managua to assist in the training activities. During the training, the lab technicians from ICS shared their knowledge and expertise in antigen preparation, SARS-CoV-2 ELISA protocol, and sample management and organization in the biorepository (Biobank). As a result of this training, our Nicaraguan colleagues are now sequencing the four DENV serotypes and conducting their own *in situ* phylogenetic analysis. In addition, during our training in Nicaragua, we supported our partners in Sri Lanka with Nanopore DENV sequencing protocol through Zoom meetings. Currently, they are implementing the protocol in their laboratory.

Furthermore, we shared the DENV and CHIKV sequencing protocols with colleagues in Paraguay, which proved very useful in the recent Chikungunya outbreak in 2023. Recently, in collaboration with our Paraguayan colleagues, we performed a phylogenetic analysis using the Bayesian model, revealing a new clade of the ECSA genotype circulating in Paraguay. Also, mutation analysis in structural and non-structural proteins was performed by them and published in the virological blog (Virological, 2023).

6.2. GENERAL CONCLUSION

In conclusion, these experiences underscore the importance of strengthening the laboratory capacity and fostering scientific collaborations at local and international levels to respond to new outbreaks effectively. The role of the USFQ during the COVID-19 pandemic and in several international research collaborations has been invaluable in supporting the development of a new generation of scientific researchers and leaders in our country and the region. In addition, these experiences reinforce the importance of an integrated approach through cross-sector collaborations for the improvement and investment in national diagnostic capacity and genomic surveillance for timely identification of novel pathogens and to monitor the evolution and transmission of infectious diseases. Given that climate pattern changes result in the emergence and reemergence of climate-sensitive diseases as DENV, it is important that Ministry of Health and academia join forces for prevention, management and control of infectious diseases to ensure the country's preparedness for future outbreaks.

As future research possibilities, it is important to continue with genomic surveillance at national level to track DENV movement throughout the country and to sequence other genotypes which are probably displacing the pre-existing genotypes as DENV-2 Asian-American genotype. It is important to carry out cross-border surveillance studies with Perú and Colombia for early warning of potential outbreaks, to monitor and control diseases more effectively and to understand other factors such as human mobility that might be directly affecting viral transmission. Moreover, it is important to test the hypothesis of arboviral movement from rural to urban sites in Esmeraldas communities by conducting more sequencing from rural sites as they might be sources of

arboviruses and other pathogens as *Leptospira* and *Plasmodium*. It might also be interesting to understand the reemergence of serotypes and determine the role of asymptomatic transmission of DENV by evaluating mutation rates in different viral genes from year to year. Also, more studies are needed at vector level as characterization of *Aedes* microbiome since microbiota interactions modulate vector competence. Similarly, the study of the diversity of *Aedes* virome is highly important since insect-specific viruses might affect transmission of arboviruses.